

Distribution Agreement

In presenting this thesis or dissertation as a partial fulfillment of the requirements for an advanced degree from Emory University, I hereby grant to Emory University and its agents the non-exclusive license to archive, make accessible, and display my thesis or dissertation in whole or in part in all forms of media, now or hereafter known, including display on the world wide web. I understand that I may select some access restrictions as part of the online submission of this thesis or dissertation. I retain all ownership rights to the copyright of the thesis or dissertation. I also retain the right to use in future works (such as articles or books) all or part of this thesis or dissertation.

Signature:

Brian S. Robinson

Date

Identification and Characterization of Novel Regulators of Salvador-Warts-Hippo Signaling
in *Drosophila*

By

Brian S. Robinson

Doctor of Philosophy

Graduate Division of Biological and Biomedical Sciences
Biochemistry, Cell and Developmental Biology

Kenneth Moberg
Advisor

Andy Kowalczyk, Ph.D.
Committee Member

Asma Nusrat, M.D.
Committee Member

Subhabrata Sanyal, Ph.D.
Committee Member

Barry Yedvobnick, Ph.D.
Committee Member

Accepted:

Lisa A. Tedesco, Ph.D. Dean of the James T. Laney School of Graduate Studies

Date

Identification and Characterization of Novel Regulators of Salvador-Warts-Hippo Signaling
in *Drosophila*

By

Brian S. Robinson
B.S., University of California, Davis, 2004

Advisor: Kenneth H. Moberg, Ph.D.

An abstract of
A dissertation submitted to the Faculty of the James T. Laney School of Graduate Studies of
Emory University
in partial fulfillment of the requirements for the degree of Doctor of Philosophy in the
Graduate Division of Biological and Biomedical Sciences
Biochemistry, Cell and Developmental Biology Program
2011

Abstract

Identification and Characterization of Novel Regulators of Salvador-Warts-Hippo Signaling in *Drosophila*

By Brian S. Robinson

Patterned growth is fundamental to proper metazoan development, and deregulated growth is implicated in human diseases including cancer. We use the fruit fly *Drosophila melanogaster* as a model system to identify growth regulatory mechanisms in developing epithelia. In an effort to understand how defects in apicobasal polarity of epithelial cells influences cellular proliferation, we performed a genetic screen against an overgrowth phenotype elicited by the transmembrane protein Crumbs (Crb), a protein known for its role in apicobasal polarity formation. Interestingly, we find that Crb-driven wing overgrowth is sensitive to the genetic dose of the Salvador-Warts-Hippo (SWH)-pathway, a conserved growth regulatory network that function across metazoans to control organ size. Although the SWH is active in all types of metazoan epithelia yet examined, large gaps remain in understanding the physiologic inputs to this pathway in developing tissues. We show that in *Drosophila* epithelia, Crb controls the levels and localization of the cytoskeleton-associated FERM-domain protein Expanded (Ex), a protein that regulates SWH-activity in cells. Moreover, we show that Crb integrates these effects through a domain that is distinct from those required for apicobasal polarity regulation, allowing for Crb to integrate junctional polarity signals with growth signals. In an effort to define whether SWH-activation also exists in mutants that are defective in Crb turnover and hyper-accumulate Crb, we analyzed SWH-activity in mutants on

the endolysosomal pathway. We find that, like those tissues in which Crb is overexpressed, endolysosomal mutants display ectopic activation of Yki in cells and altered levels of Ex. In the final part of my thesis work I have focused on analyzing the role of *taiman* (*tai*) in regulating SWH-activity. *taiman* is the *Drosophila* ortholog of human AIB1 (Amplified In Breast cancer-1), which potentiates nuclear steroid signaling and is amplified in several human cancers. We identified *tai* as a genetic modifier of Crb-driven overgrowth and find that like Crb, Tai can activate SWH-signaling in cells. Moreover, we show that Tai and Yorkie (Yki), the transcriptional effector of the SWH-pathway, shows a mutual reliance on each other in their effects on cells: Tai cannot fully activate SWH-signaling without Yki, while reciprocally, Yki cannot drive overgrowth in the absence of Tai. In summary, these studies highlight three novel inputs into SWH-signaling in *Drosophila* and further delineate factors and mechanisms that control SWH signaling in cells.

Identification and Characterization of Novel Regulators of Salvador-Warts-Hippo Signaling
in *Drosophila*

By

Brian S. Robinson
B.S., University of California, Davis, 2004

Advisor: Kenneth H. Moberg, Ph.D.

A dissertation submitted to the Faculty of the
James T. Laney School of Graduate Studies of Emory University
in partial fulfillment of the requirements for the degree of Doctor of Philosophy in the
Graduate Division of Biological and Biomedical Sciences
Biochemistry, Cell and Developmental Biology Program
2011

Acknowledgements

Over the course of the four-plus years and countless hours it took to produce the data presented in this dissertation, I learned one of sciences great secrets: behind every discovery is a little bit of luck. And while I certainly received my share of good fortune behind the microscope, I contend that my true fortune remains in those people who surrounded me during my graduate school training. Everyone at Emory, from the janitorial staff to the Departmental Chairs, has been extremely supportive in my development as a young scientist and I cannot imagine training in a better environment. I especially want to thank everyone in the Cell Biology Department, who made my “home away from away” not only a fun and comfortable place to work, but also an intellectually engaging place to work. I would also like to thank everyone in my lab, both old and new, who, through their active involvement not only into my experiments but also my intellectual development have taught me that research truly operates best when approached as a ‘team sport.’

In addition I would like to thank my advisor Ken, whose guidance has been requisite to this completion of this work. Besides being extremely patient and selfless with his time, Ken has been actively involved in my development as a young scientist, constantly questioning my reasoning and distilling my thoughts to a testable question. It is through Ken that I believe I truly learned the process of how to *think* like a scientist. In addition, Ken has instilled in me another valuable lesson regarding a career in science: that happiness in the lab generally follows a balanced life at home. And it is this latter lesson that, though sometimes hard to achieve, I now hold as one of my central tenets.

I would also like to thank my friends and family for their love and support these past four years. Research, for the most part, is an extremely grueling process often requiring physical and/or mental retreats. Whether through long runs in Chandler Park, trips to the ball-yard, long cross-continental phone calls, or weekend barbeques, my friends and family have always been there for me providing a constant outlet for the stress and anxieties that emanate from the requirements of graduate school training. I especially want to thank Karl and Deb, who have provided not only a physical but also an emotional “home away from home” over the last 6-years. I also would like to acknowledge my parents, Ellyn and Pablo, to whom I dedicate this work. They are the foundation from which I derive my values, and serve as a constant source of inspiration in their enthusiasm and resilience.

Lastly, I would like to thank my wife, Tamar. Her love and patience are unmatched, and without her in my life this work would not be possible.

Table of Contents

Chapter 1: An Introduction	1
Growth Control as a Biological Question	2
<i>Drosophila</i> as a model organism to understand organ size-control	4
Features of <i>Drosophila</i>	4
Genetic Manipulation in <i>Drosophila</i>	5
GAL4-UAS system.....	5
FLP-FRT system	6
Genetic Analysis in <i>Drosophila</i>	7
Epithelia in <i>Drosophila</i>	11
Polarity Control in <i>Drosophila</i> Imaginal Disc Epithelia.....	13
The ‘apical membrane determinant’ <i>crumbs</i>	15
Growth Control in <i>Drosophila</i>	21
Cell Division	22
Cell Growth.....	24
Cell Death (Apoptosis)	25
Pathways implicated in growth control in <i>Drosophila</i>	29
The MAP Kinase Pathways	29
The Salvador-Warts-Hippo (SWH) Pathway	32
The JAK-STAT Pathway.....	34
The Notch Pathway	35
The Ecdysone Pathway	37
Neoplastic growth in <i>Drosophila</i>	38
Scope and Significance.....	46
Chapter 2: Dominant-Modifiers of Crumbs-driven Overgrowth	47
Introduction	48
Results	50
Overexpression of <i>crbⁱ</i> drives overgrowth of the <i>Drosophila</i> wing.....	50
A candidate-based approach reveals dominant modifiers of <i>crbⁱ</i> -driven overgrowth ..	53
A discovery-based screen reveals genetic loci that reproducibly modify <i>crbⁱ</i> -driven overgrowth.....	57
Discussion	61
Experimental Procedures.....	65
Chapter 3: The apical membrane determinant Crumbs acts via the FERM-domain protein Expanded to control SWH signaling in <i>Drosophila</i>	67
Introduction	68
Results	70
The intracellular domain of <i>crb</i> requires <i>yki</i> to drive tissue growth	70
<i>crbⁱ</i> expression elevates Yki activity in developing epithelia	73
<i>crbⁱ</i> downregulates Ex protein levels in wing disc cells.....	77
The juxtamembrane domain of Crb regulates Ex <i>in vivo</i>	86
Effects of <i>crb</i> loss on Ex protein and Yki activity	93
Modification by Crb-interacting factors	98
Effect of <i>crb</i> loss on Yki activity	101
Discussion	104
Experimental Procedures.....	108
Chapter 4: Blockade of the Endolysosomal Pathway Affects SWH-signaling via the c-Jun N-Terminal MAP Kinase Pathway in <i>Drosophila</i>	110
Introduction	111

Results	114
<i>ept</i> mutant cells display altered <i>yki</i> -activity	114
Loss of both early and late endocytic nTSG elevates <i>yki</i> -activity <i>in vivo</i>	117
Endocytic neoplastic tumor suppressor genes require <i>yki</i> to overgrow	121
Endocytic neoplastic tumor suppressor genes elevate JNK activity <i>in vivo</i>	123
Discussion	128
Experimental Procedures.....	131
Chapter 5: The Nuclear Receptor Co-Activator Taiman promotes a Yorkie-	
dependent growth program in <i>Drosophila</i>	132
Introduction	133
Results	135
<i>taiman</i> regulates imaginal disc growth.....	135
Excess <i>tai</i> elevates <i>yki</i> -activity.....	142
Loss of <i>tai</i> reduces <i>yki</i> -activity	145
<i>yki</i> is required for <i>tai</i> to elevate <i>ex-lacZ</i> and drive imaginal discs growth	147
<i>tai</i> growth phenotypes occur independently of the β -HLH and <i>ecdysone</i> signaling	149
<i>tai</i> functions genetically downstream of core pathway components to control organ	
size	154
Discussion	158
Experimental Procedures.....	161
Chapter 6: Future Directions	163
Future Directions	164
The Crb ⁱ Dominant-Modifier Screen.....	166
The Crb-Ex Regulatory Network.....	169
Endocytic Regulation of SWH-signaling	172
Taiman	175
Concluding Remarks.....	178
References	181

Index of Figures

1.1 The GAL4-UAS System.....	17
1.2 The 'Actin-FLP-Out' System	18
1.3 Clonal Analysis in <i>Drosophila</i>	19
1.4 Polarity Control in <i>Drosophila</i>	20
1.5 Growth phenotypes in <i>Drosophila</i>	27
1.6 Inputs into Organ Size in <i>Drosophila</i>	28
1.7 MAP Kinase Signaling in <i>Drosophila</i>	41
1.8 The Salvador-Warts-Hippo Pathway in <i>Drosophila</i>	42
1.9 The JAK-STAT Pathway in <i>Drosophila</i>	43
1.10 The Notch Pathway in <i>Drosophila</i>	44
1.11 Ecdysone Signaling in <i>Drosophila</i>	45
2.1 Growth phenotypes in <i>en>crbⁱ</i> animals.....	52
2.2 Model of potential regulation of Notch activity by Crb	64
3.1 Overgrowth driven by the <i>crbⁱ</i> transgene is sensitive to the dose of SWH pathway genes.....	72
3.2 <i>crbⁱ</i> elevates Yki-activity	75
3.3 <i>crbⁱ</i> does not effect Notch activity and localization	76
3.4 <i>crbⁱ</i> does not effect the levels and localization of Mer and Fat	79
3.5 Excess Crb does not alter or require Fat pathway activity.....	80
3.6 <i>crbⁱ</i> downregulates Ex levels	81
3.7 Arm protein is not altered in <i>en>crbⁱ</i> wing discs	83
3.8 Expression of <i>crbⁱ</i> phenocopies loss of <i>ex</i>	84
3.9 The Crb-JM controls Ex levels and Yki activity	88
3.10 Tissue architecture of Crb-JM and Crb-PBM wings discs	90
3.11 Crb ⁱ -driven loss of Ex is sensitive to the activity of the proteasome.....	91
3.12 Loss of Ex following expression of Crb ⁱ is not accompanied by routing of Ex:GFP into a chloroquine-sensitive lysosomal compartment	92
3.13 Effect of <i>crb</i> loss on Ex in disc cells	95
3.14 Dlg, Arm and Mer protein expression is unaffected in <i>crb^{11A22}</i> clones	97
3.15 Functional interactions with putative Crb interactors.....	100
3.16 Growth phenotypes associated with loss of Crb	102
3.17 <i>crb</i> alleles interact with <i>ex</i> and elevate DIAP1 expression posterior to the furrow	103
4.1 <i>ept</i> elevates Yki-activity	116
4.2 Multiple blocks in the endolysosomal pathway elevate Yki-activity	119
4.3 <i>avl^{IR}</i> elevates the <i>th-lacZ</i> Yki-reporter	120
4.4 endolysosomal growth phenotypes are sensitive to the dose of Yki	122
4.5 Ex Expression is altered in endolysosomal mutants.....	125
4.6 Loss of <i>ept</i> elevates JNK-activity	126
4.7 Loss AP2 σ , Syx7, and Vps25 elevate JNK-activity	127
5.1 Mapping of the <i>crbⁱ</i> modifier Df(2L)N22-14	138
5.2 <i>tai</i> controls larval imaginal wing disc growth.....	139

5.3 <i>tai</i> controls the growth of multiple <i>Drosophila</i> epithelia	140
5.4 <i>tai^{IR}</i> and <i>tai^{61G1}</i> clones have reduced levels of <i>tai</i>	141
5.5 <i>tai</i> elevates Yki-activity	144
5.6 <i>tai</i> is required for basal Yki-target gene expression	146
5.7 <i>yki</i> is required for <i>tai</i> -driven overgrowth	148
5.8 The <i>tai</i> β -HLH domain is not required for <i>tai</i> -driven overgrowth	151
5.9 <i>Tai</i> elevates MMP-1 expression.....	152
5.10 The <i>tai</i> β -HLH domain is not required for <i>tai</i> -driven overgrowth.....	153
5.11 <i>tai</i> modifies Yki ^{S168A} -driven overgrowth	156
5.12 <i>tai</i> does not activate the 32bp-HRE	157
5.13 Models of <i>tai</i> -dependent regulation of SWH-signaling	160
6.1 Elaboration of the SWH-signaling network	165
6.2 Model of the Crb-Ex regulatory network	171
6.3 Model of SWH-control by endocytic regulators	174
6.4 Model of SWH-control by <i>taiman</i>	177

Index of Tables

2.1 Effect of established growth-regulators on Crb ⁱ -driven wing growth.....	56
2.2 Results from the deficiency-modifier screen	59
2.3 Analysis of selected alleles from the deficiency-modifier screen.....	60

Chapter 1: An Introduction

Growth Control as a Biological Question

How an organism gains its particular size and form is an incredibly complex question that has been scrutinized by nearly every society in human history. However, the general acceptance of the 'cell' theory has led to the understanding that organism size and shape is largely the product of molecular signaling cascades that modulate three basic cell biological phenomena: cell growth (i.e. mass accumulation), cell division, and cellular apoptosis. Together, these three processes represent the main inputs into organ size and shape, and defects in their regulation contribute to many developmental anomalies and disease states including cancer.

The distinction between cell *growth* and *division* as determinants of organ size can first be attributed to Rudolf Virchow, a pathologist who coined the terms 'hypertrophy' to define tissue enlargement by the accumulation of cell mass (i.e., cell growth) and 'hyperplasia' to define tissue enlargement by the accumulation of cell numbers (i.e., cell division) [1]. Though Virchow's definitions appear long before the general acceptance of the cell theory, these concepts laid the groundwork for the molecular and genetic dissection into the components required for hypertrophy and hyperplasia, and it is now generally accepted that the molecular mechanisms that control *cell growth* and *cell division* (i.e., progression through the cell division cycle) are distinct. Similarly, although the contribution of apoptosis to organ size control took somewhat longer to appreciate, it is now widely accepted that distinct signaling modalities impinge on apoptotic mechanisms to control tissue form.

Although the terminal endpoints of pathways that control cell division, growth, and survival are distinct, a considerable body of work has shown that these

pathways do not necessarily operate independently of one another. In fact, certain signaling pathways can simultaneously regulate cellular growth, division, and apoptosis to control organ size. Moreover, the signals that function to initiate these processes are not always intrinsic to a cell. Cells can activate internal signals and *autonomously* modulate their own survival or proliferation, but can also initiate signals that modulate the survival and proliferation of neighboring cells via *non-autonomous* mechanisms. These latter pathways are important for coordinating signals among groups of cells in the same developing organ and may also play important roles in homeostatic mechanisms like regenerative growth and wound healing. Many elements of these types of regulatory mechanisms remain poorly understood, including the identification and characterization of yet unidentified growth regulators that control organ size, and the determining how defects in basic cellular processes known to affect organ size (e.g. endocytosis, apicobasal polarity, etc.) actually alter the molecular properties of established survival and proliferation pathways.

In this dissertation, I will examine genes and cellular programs required for organ size control in the model organism *Drosophila melanogaster*. In particular, I will focus my efforts on defining the role of Crumbs, a protein known for its role in apical-basal polarity formation, in regulating the growth of the *Drosophila* imaginal disc epithelia. In so doing, I show that Crumbs and its regulators are components of the Salvador-Warts-Hippo pathway, an emerging tumor suppressor network that was discovered in flies and functions across metazoans to regulate organ size. What follows is an introduction to the terms and concepts used in these studies.

***DROSOPHILA* AS A MODEL ORGANISM TO UNDERSTAND ORGAN SIZE-CONTROL**

Features of *Drosophila*

Drosophila melanogaster is an excellent experimental system with an attractive array of features that has provided insight into nearly every cellular and molecular process in metazoans since its initial utilization in the early 20th century [2]. These features include, but are not limited to, the following:

- A short life-cycle and robust fecundity, permitting high-throughput genetic analysis.
- Relatively low maintenance cost, allowing for inexpensive analysis.
- Reproducible and visually apparent phenotypes, allowing for the observation of subtle genetic modifications and the ability to perform epistatic analysis
- Conservation with human genes; estimates suggest that ~75% of the disease causing genes in humans have orthologs in *Drosophila* [3], permitting the examination of clinically relevant biological problems.
- A sequenced genome with vast databases [4], allowing for the quick isolation of a genetic loci responsible for an observed phenotype, the identification of its potential orthologs in other species, the determination of all known genetic and proteins interactions associated with that locus, and the inspection of all previous studies associated with its characterization.
- An expansive genetic tool-kit, allowing for the genetic manipulation (i.e., overexpression and/or removal) of any gene or DNA-sequence in any tissue, at anytime (see detailed discussion below)

Genetic Manipulation in *Drosophila*

The ability to manipulate gene expression in *Drosophila* is one of its greatest attributes. Though new technologies are emerging everyday to manipulate gene expression in *Drosophila*, including the ability to ‘knock-in’ sequence specific genes within an endogenous locus [5], the studies performed herein rely heavily on two systems mobilized from *Saccharomyces cerevisiae*, including the GAL4-UAS system [6] and the FLP-FRT system [7]. What follows is an introduction into their background and modality.

The GAL4-UAS System: The GAL4-UAS system is a binary expression system that allows for the expression of a distinct DNA-sequence in a specific spatiotemporal pattern. At its core, this system relies on two components derived from yeast that are otherwise absent in *Drosophila*: the DNA-binding/DNA-activating protein GAL4 and its enhancer element UAS (Upstream Activating Sequence) [6]. Briefly, tissue specific and/or cell specific promoters are fused with the GAL4 coding sequence to generate a transgenic fly (termed the ‘driver’) that expresses GAL4 in a temporally and spatially defined pattern. This fly is the crossed to another transgenic fly, in which a sequence of choice (protein coding sequence or RNAi cassette) has been placed downstream of UAS enhancer elements. Thus, when these two transgenic lines are crossed, they produce F1 offspring that express the chosen sequence in the pattern of the GAL4 driver (Figure 1.1). For example, in this dissertation I sought to examine the effects of ectopic expression of a protein called Crumbs (Crb) on the growth of the *Drosophila* wing. For these studies, I crossed flies that contained the

wing driver *engrailed-GAL4* to flies that contained *UAS-crumbs* sequences, and analyzed the growth of the wing in their offspring that had both *engrailed-GAL4* and *UAS-crumbs* together (N.B., typical nomenclature denotes these animals as *engrailed>crumbs*, which can be shortened to *en>crb*, to indicate the expression of *crumbs* by the driver *engrailed*).

The power of the GAL4-UAS system cannot be overstated, as it allows for the manipulation of nearly any gene in any tissue at any developmental stage. Hundreds of Gal4 drivers have been generated and are freely available. Reciprocally, several different public stock centers maintain large collections of randomly inserted UAS elements (such as the Rørth EP collection [8]). These *UAS* elements have a particular affinity for inserting into promoter-rich regions, allowing for the overexpression of downstream components. Recently, groups at Harvard and Vienna complimented these EP collections by generating collections of transgenic lines that harbor *UAS*-elements linked to sequences encoding short-hairpin RNAs (aka inverted-repeats, or IR) directed at nearly every gene in the entire genome [9, 10]. Once processed into micro RNAs by the Drosha/Dicer pathway, these RNAs bind to the 3'-UTR of endogenous transcripts and reduce the expression of target genes in cells. Together, these EP- and IR-based collections allow for the overexpression or removal of nearly every gene in the *Drosophila* genome.

The FLP-FRT system: Another technique that allows for spatiotemporal regulation of gene expression is called the 'FLP-FRT' (or 'flip-frit') system. This system utilizes a protein called Flippase (FLP) to induce recombination between two FRT sites (e.g.,

Flippase Recognition Target), which are placed either *cis* or *trans* to one another [7]. When *cis* to one another, as is the case in with the Actin 'flip-out' technique [11], the FLP-FRT system can be used to remove genetic material between the two flanking FRT sites (Figure 1.2). When FRT sites are present in *trans* to one another at the same location on homologous chromosomes, the FLP-FRT system can also be used to induce mitotic recombination at FRT sites allowing for the exchange of all genetic material distal to the FRT site (Figure 1.3). This latter situation is especially useful because it allows for tissue specific mitotic recombination (when FLP is expressed using a tissue specific promoters) to produce patches (or clones) of cells that are homozygous for a mutation of interest. This system thus bypasses the embryonic lethality associated with many interesting mutations and allows for phenotypic analysis in later stages of development, such as growth and patterning of larval organs and appendages [12].

Genetic Analysis in *Drosophila*

Above all, *Drosophila* is associated with genetic interaction studies (i.e., genetic screens), likely due to the ease with which they can be performed. In general, genetic screens have at their core two fundamental components. The first is a reproducible and visually robust phenotype produced by loss or overexpression of the gene of interest. The second component, a collection of candidate modifier alleles, is then introduced into this background in an effort to identify those rare alleles that alter (ie 'modify') the baseline phenotype. Historically, *Drosophila* biologists have used genotoxic agents like ethyl methanesulfonate (EMS) or high

energy X-rays to produce a pool of new genetic variants that can be screened for modifying activity; however, the advent of more modern techniques such as GAL4/UAS system and FLP/FRT has allowed these techniques to be used in genetic screens as well.

'Enhancer/suppressor' screens are among the most commonly used classes of genetic interaction studies (reviewed in [13]). These screens come in many flavors and styles, the description of which is beyond the scope of this dissertation. However, one type of enhancer/suppressor genetic screen that will be discussed here is the 'dominant modifier' screen (mainly because of its central role in this work). Dominant modification is based on the simple hypothesis that a phenotype produced by an allele of interest (e.g. overexpression of gene A) is dependent on the diploid dose of genes encoding factors that act downstream of this allele, and that heterozygosity for these factors will therefore 'modify' original phenotype. Typically, these studies involve introducing a single loss-of-function allele into a genetic background that has a phenotype (e.g., a mutant with a large eye, etc.) and assessing the ability of that allele to modify (i.e., enhance or suppress) the original phenotype. If modification is observed, and it is determined that that allele does not produce a phenotype on its own, the phenotype is deemed 'dominantly-modified' by the allele and a genetic interaction is noted. At its core, dominant modification assumes that in order to produce a phenotype, a protein must 'hijack' endogenous signaling components to elicit a phenotype and thus becomes highly sensitive to loss of these factors. However, since halving the dose of a protein is generally not enough to impair its function in cells (i.e., the vast majority of null mutations are recessive),

the absence of dominant modification in a genetic assay *does not* rule out a role for that protein in the pathway of interest.

Dominant modification screens have been utilized to define roles of uncharacterized proteins, but also to define novel components within known cellular networks. For example, in this dissertation I determined which of the known growth regulatory programs are downstream of deregulated polarity programs by testing the ability of alleles from known growth regulatory programs to dominantly modify a wing overgrowth phenotype produced by overexpression of the polarity factor Crumbs. In later studies, in order to define novel components within this Crumbs/growth pathway, I utilized a collection of genomic deficiencies that removed large chunks of the *Drosophila* genome and tested their ability to dominantly modify Crumbs-driven overgrowth. These deficiencies highlighted several loci, which were narrowed to specific genes that appear to act downstream of Crumbs in growth control pathways.

Another form of genetic analysis that deserves a brief introduction, simply for its role in defining an array a novel growth regulating pathways in recent years, are those that have combined EMS-dependent mutagenesis with the FLP-FRT system (i.e., FLP-FRT screens, reviewed in [13]). Central to these studies is the analysis of mosaic tissue that contains clones of mutant cells and their adjacent wildtype twin-spot clones. These studies are initiated with mutagenesis of wildtype FRT chromosomes to produce an animal that is heterozygous at a locus, and crossing this animal into the background of an animal that has a source of FLP and a wildtype FRT chromosome. Typically, the FLP is placed under a promoter such that

its expression is tissue specific (e.g., under the *eyeless* promoter such that clones are produced in the eye). Moreover, FRT chromosomes in these stocks are often marked with a dominant marker (e.g., with the *mini-white* pigment gene such that wild-type tissue is pigmented red). Thus, when FLP is expressed it produces two types of clones in a tissue of choice, one that is homozygous mutant at a locus, and another that is homozygous wild-type and denoted by some marker (i.e., eye color, GFP, etc.)

FLP-FRT screens have been used to identify novel regulators of a variety of cellular processes, and now are a mainstay in *Drosophila* biology. Over the last decade, several labs have used this technique to identify novel regulators of growth in the *Drosophila* eye, by comparing the clonal overgrowth of mutant tissue with that of wild-type clones [14-17]. These studies centered on the comparison of the amount of mutant tissue (identified by the lack of pigment in the eye, as homozygous mutant tissue was absent for the pigment-producing *white* gene) to that of the ‘wild-type’ tissue (identified by the presence of pigment, as homozygous wild-type tissue contained the *white* gene) in animals in which eye-specific mitotic recombination had been produced (Figure 1.3). The power of these studies is that, unlike traditional mutagenesis screens studies looking for growth phenotypes in zygotic mutant animals, they allowed for the observation of homozygous phenotypes that might otherwise be lost to developmental lethality. Such was the case for a *salvador*, *warts*, and *hippo*—three genes that form a core kinase cassette of a major tumor suppressor pathway in flies and humans—originally linked to growth suppression by their ability to promote clonal overgrowth when analyzed in the *Drosophila* eye [14, 15, 17].

This is not to suggest that these studies are limited to the eye; in fact, mosaic screens have been performed in a variety of tissues for a variety of purposes. These include studies seeking to identify regulators of wing hair orientation (a marker of planar cell polarity) [18], photoreceptor development [19], genes required to restrict cell invasion and metastasis in the follicular epithelium [20], as well, as in the nervous system to unearth genes required for axonal branching [21]. Moreover, this analysis is limited to mosaic tissue alone. In fact, *Drosophila* geneticists have utilized the FLP-FRT system to generate epithelia that are composed of mutant tissue alone. In these systems, mutant FRT chromosomes are recombined with FRT chromosomes that have recessive cell-lethal mutations in their background, such that when clones are generated, the non-mutant clones can no longer survive. This powerful technique allows for the identification and characterization of genes that might otherwise be lost in mosaic fashion, like those involved in *Drosophila* neoplasia where mutant clones are killed by their neighbors via a yet ill-defined mechanism [22].

Epithelia in *Drosophila*

In metazoans, epithelia are the tissues that line organs and provide several critical functions including forming a protective barrier from the environment, the absorption of nutrients, the secretion of various substances, the transcellular transport of macromolecules, and the initial perception of the outside world (i.e., sensation). To provide these functions, epithelia maintain a distinct architecture where lipids and macromolecules are subdivided into distinct domains, including

apical (i.e., those closest to the lumen or outside world) and basolateral domains (i.e., those closest to the underlying basement membrane). In *Drosophila*, the distinction between those domains occurs at a structure termed the *adherens junctions* (or zonula adherens), a cell-cell junction where adhesive proteins like E-cadherin and other protein complexes coalesce and form a network that links the plasma membrane to the underlying cytoskeleton (Figure 1.4; reviewed in [23]. This is slightly different than vertebrate systems, where the distinction between apical and basolateral domains occurs at a cell-cell junction known as the tight junction, though the proteins and processes required to form these structures are the same as those in *Drosophila*.

Given the wide-array of tissues that exist throughout embryonic, larval, and adult development, it is not surprising that *Drosophila* maintain several different types of epithelia that all vary slightly in their architecture in order to optimize certain functions. The studies in this dissertation focus on a particular type of epithelia, the imaginal disc epithelia, which are found in larvae and are the precursors for all the external epithelia structures observed in adult animals (i.e., the eye, wing, legs, abdomen, genitalia, etc; reviewed in [24]). The development of each of the various types of imaginal discs (e.g. leg disc, eye disc, etc.) begins during embryogenesis, with the specification of a patch of 20-30 cells as the organ primordium. These 20-30 cells eventually form a small epithelial sac during the first stage of larval development, when then undergoes expansive growth and development during the three successive stages of larval development to reach a final size of 20-50,000 cells during pupal metamorphosis.

Imaginal discs have several features that make them optimal for genetic analysis of growth regulatory pathways. First, as mentioned above, they undergo extensive growth during their development, and are thus amenable to identifying and analyzing genes required for this effect. Imaginal discs are also easy to manipulate and dissect, allowing for complex biochemical and molecular analysis. In addition, imaginal disc development is extremely well characterized, allowing for the quick and fairly reliable placement of mutants into cellular pathways or processes based on readily observable traits. Finally, the biology of these structures is extremely well conserved with that of vertebrates, including those genes required for morphogen-driven patterning, epithelial growth control, apical-basal polarity control, and endolysosomal turnover of membrane, and membrane-associated proteins. This last trait is especially important for this dissertation, as studies will focus on understanding how apical-basal polarity programs and endolysosomal programs function to regulate the growth of *Drosophila* imaginal disc epithelia.

Polarity Control in *Drosophila* Imaginal Disc Epithelia

Epithelial cell polarization is defined by the compartmentalization of cellular lipids and proteins into distinct domains, including the apical (or adluminal) and basolateral surfaces (Figure 1.4). The distinction between these domains in *Drosophila* occurs at the *adherens junction* (A), also called the *zonula adherens* (ZA), an adhesive cell-cell junction that is physically linked to a concentrated ring of actin that underlies the plasma membrane at the apical surface. The development of a polarized epithelium is thought to be controlled by functional interactions between

a small number of membrane-associated protein complexes that line the apical and basolateral surface (reviewed in [25]). These include two apical complexes, Par6/Par3/aPKC and Crumbs/Patj/Pals1, and a basolateral complex composed of the proteins Discs Large (Dlg) and Scribble (Scrib). The recruitment and stabilization of these complexes to their respective domains is absolutely required for proper AJ formation and cell polarization; without them cells cannot form complete AJs and instead linger with incomplete structures called the 'spot AJ' [26-28]. It is not yet known how these complexes are recruited to their respective domains, and in what order, and currently these questions are an active source of investigation.

Studies in the embryonic ectoderm and in imaginal disc epithelia have led to a model whereby the Par/aPKC, Crb and Dlg/Scrib polarity modules antagonize one another to maintain a polarized epithelium as shown in Figure 1.4 [29, 30]. Recruitment of the Dlg/Scrib complex to the basolateral cell membrane is initially needed to functionally antagonize the apical Par/aPKC complex. To combat this, the Par/aPKC complex subsequently recruits and activates the Crumbs complex, which in turn represses activity of the Scrib complex. Mutations in *Dlg*, *scrib* or a third factor required for Dlg/Scrib function, *lethal giant larva (lgl)*, thus lead to membrane 'apicalization' in which the Crb complex spreads ectopically into the basolateral membrane. Significantly, overexpression of Crb in imaginal disc epithelia leads to spreading of the protein into the basolateral domain and produces phenotypes overtly similar to those produced by loss of *Dlg*, *scrib*, or *lgl* [31, 32]. Thus, it is the delicate balance of these three complexes that maintains the proper cell polarization

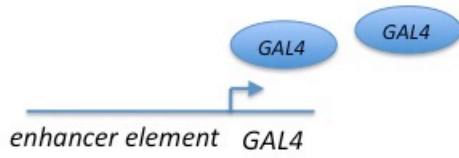
required for epithelial homeostasis. Just how these complexes exert their effects on one another is not known, however, it is thought that their ability to serve as membrane-associated protein scaffolds likely promotes a network of interactions that ultimately contribute to mutual repression.

The ‘apical membrane determinant’ *crumbs*: Many studies performed in this thesis center around the transmembrane protein Crumbs (Crb). *crb* was the first gene identified in *Drosophila* to regulate epithelial polarization [33]. In *crb* mutants, the ZA does not form in the embryonic ectoderm and instead ectodermal tissue undergoes extensive apoptosis and excretes cuticle inwardly making mutant embryos appear as if they are filled with ‘crumbs’ [26]. Crb is known as the ‘apical membrane determinant’ because (1) *crb* mutants fail to localize proteins properly to the apical membrane and (2) expression of Crb can confer apical properties to non-apical domains [26, 32].

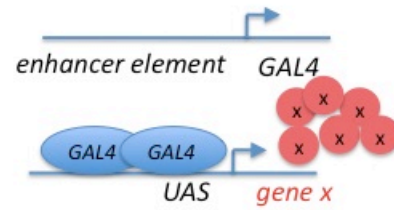
Crb ‘activity’ appears to converge on the Crb intracellular tail, as expression of a membrane-tethered version of the intracellular tail can rescue most *crb*-mutant phenotypes [32]. The 37 amino acid intracellular tail of Crb contains two functional motifs that are conserved across Crb proteins in multiple species: (i) the 15-amino acid juxtamembrane FERM-binding motif (JM), which mediates a direct interaction with the FERM-domain protein Yurt, and indirectly interacts with DMOesin (DMoe) and β_H -spectrin to link Crb to the underlying actin/spectrin cytoskeleton, and (ii) the C-terminal PDZ-binding motif (PBM), which is composed of the last 4 residues of

the Crb tail (ERLI) and directs interactions with Sdt and Patj to form a polarity regulatory module commonly referred to as the Crb complex (reviewed in [34]).

P1 male.



X →



F1 offspring

P1 female.



Figure 1.1. The GAL4-UAS System. Schematic representation of the GAL4-UAS system as described in the text. Briefly, transgenic flies containing GAL4-sequence placed downstream of enhancer elements are crossed to transgenic flies containing UAS-elements upstream of “gene x.” This allows for the tissue specific expression of “gene x” in their progeny.

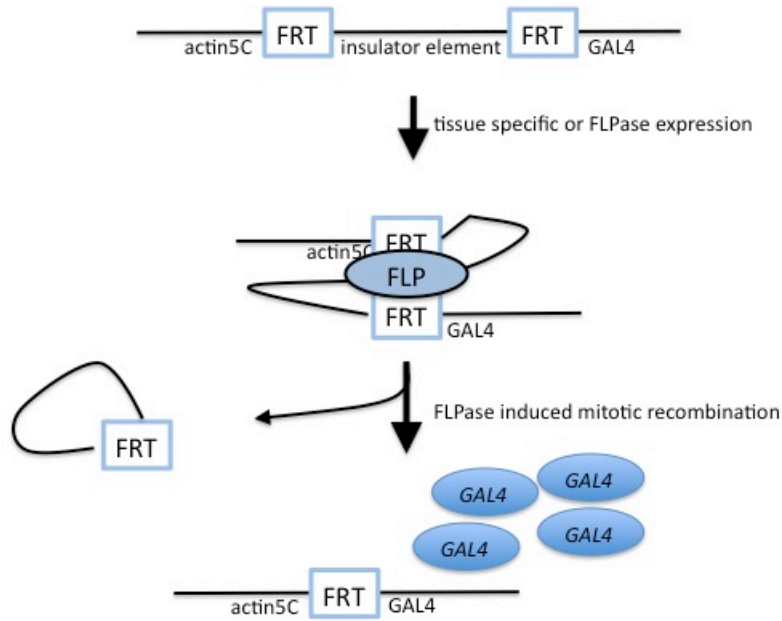


Figure 1.2. The 'Actin-FLP-Out' System. Schematic representation of the 'Actin-FLP-out' system as described in the text. Briefly, FLPase acts on *cis* FRT sites to remove DNA-insulators, thereby bringing the *actin5C* promoter in close proximity to GAL4 coding sequence allowing for robust expression of sequences placed downstream of UAS elements. (Adapted from [35]).

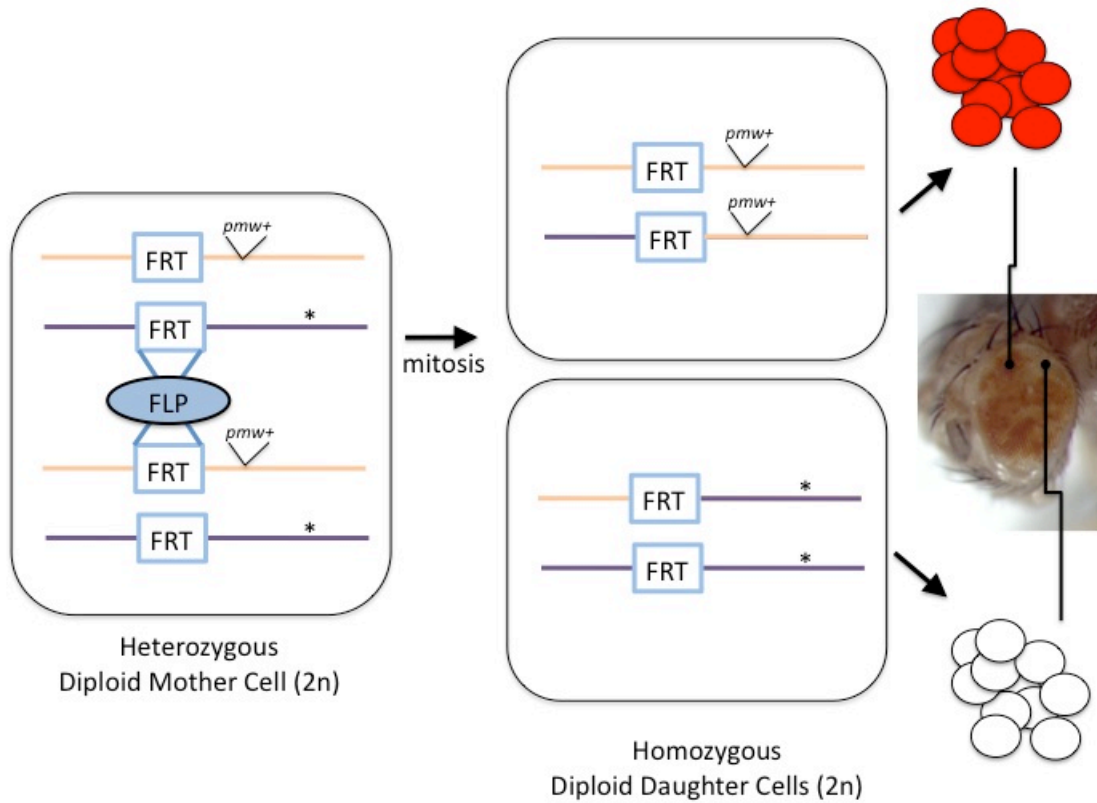


Figure 1.3. Clonal Analysis in *Drosophila*. Schematic representation of clonal analysis using FLP-FRT system in the eye. Briefly, FLP recombinase acts on *trans* FRT sites to promote mitotic recombination between chromosomes, creating two clones of cells that are homozygous for downstream elements (Adapted from [13]).

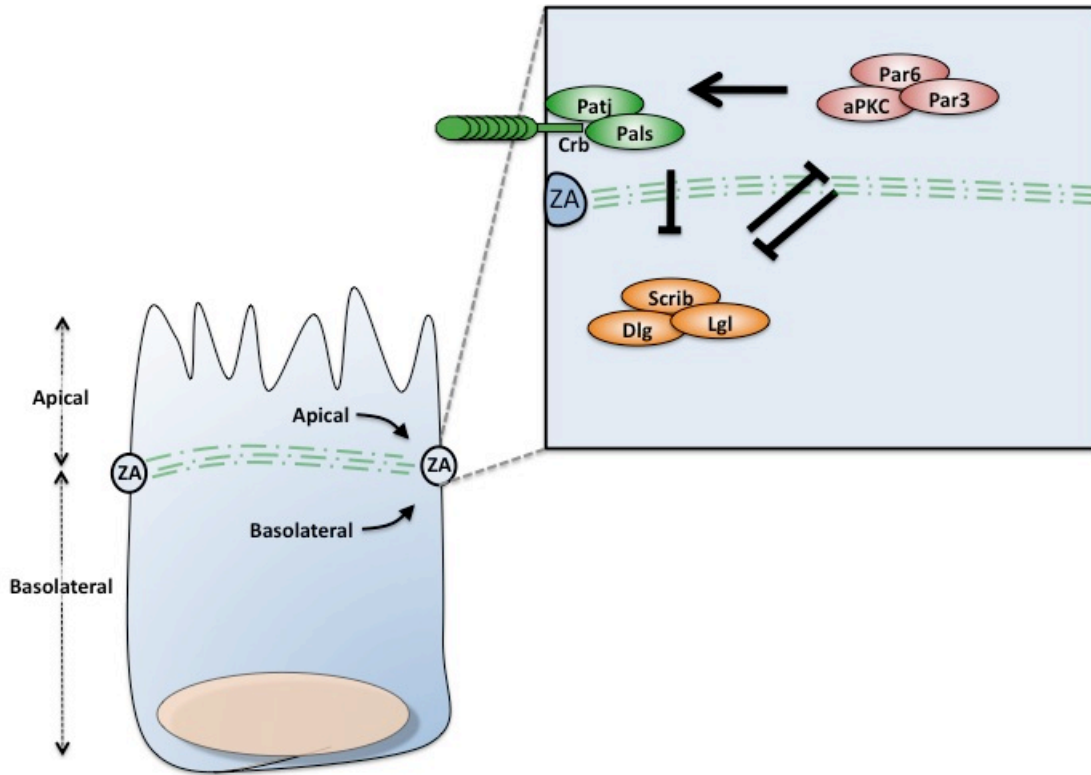


Figure 1.4. Polarity Control in *Drosophila*. Genetic interaction studies from the embryonic ectoderm and imaginal disc epithelia reveal antagonistic interactions from the basolateral Scrib/Dlg/Lgl complex and the apical aPKC/Par and Crb complexes required for the establishment of apical and basolateral membranes in cells.

GROWTH CONTROL IN *DROSOPHILA*

At first glance, using *Drosophila* to examine growth regulatory pathways that are common to all metazoans may seem far-fetched, given their distant evolutionary relationship to vertebrates. However, studies dating back as far as 1916 show analysis of melanotic tumors in *Drosophila*, making it one of the oldest model organisms in cancer research [36]. Since then, *Drosophila* has provided a wealth of information regarding genes responsible for human tumor formation, and remains an active source for characterizing and mapping human cancer pathways. These findings include the elucidation of the Ras proto-oncogene pathway (the most commonly mutated pathway in human cancers) [37], and the identification of several novel tumor suppressor pathways that are mutated in human cancers [16, 38-40]. Moreover, as the reactivation of developmental signaling cascades continues to be linked to oncogenesis [41, 42], studies that examine how these developmental growth-regulatory programs modulate cell growth, division and survival are increasingly more imperative.

In *Drosophila*, growth phenotypes are generally grouped by their effect on organismal patterning (reviewed in [43]). Hyperplastic growth (i.e., patterned overgrowth) is an increase in organ size that is generally not accompanied with an alteration in patterning such that with the affected organ is enlarged but morphologically normal (Figure 1.5A). Pathways linked to hyperplastic growth in *Drosophila* include the Tsc/*tor* pathway, the IGF/PI3K pathway, the Salvador-Warts-Hippo pathway, and those pathways linked to regulating the expression of Myc (i.e., the *archipelago* tumor suppressor pathway) or Cyclin D. Similar to hyperplastic

growth, there are pathways that promote hyperplastic-like growth phenotypes but also promote subtle defects in cell fate specification such that affected organ is often mis-patterned. Pathways linked to this type of growth include the Ras/MAP kinase pathway, the Notch pathway, and the JAK/STAT pathway. Finally, there is neoplastic growth (i.e., unpatterned overgrowth). In this situation, cells grow without deference to their neighbors, and fail to respond to developmental cues that control cell fates, and thus produce organs that often lack patterning and are highly disorganized (Figure 1.5B). Genes associated with neoplastic growth tend to disrupt key cellular processes (i.e., membrane compartmentalization, endocytosis, transcription, etc.) that are often linked to many pathways.

Before presenting a detailed discussion of organ size control pathways, I will first briefly discuss the three processes that operate to control organ size (i.e., cell division, cell growth, and cell apoptosis).

Cell Division

Cell division is a term describing the process whereby a parental cell divides and produces two daughter cells with the same genetic composition. This process is termed the cell division cycle, whereby DNA is replicated, divided into two portions, and then partitioned into the two daughter before cell fission (i.e., telophase).

Critical to step-wise progression of the cell cycle is the presence of several cyclically expressed proteins known as cyclins, which bind to cyclin-dependent kinases (CDK) and together produce the effects required for each of the transitions of the cell cycle. Given their role in the initiation and proper execution of the cell

division, it is not surprising that many pathways control cell proliferation via regulation of key cyclins (Figure 1.5). One cyclin that appears to be a particular focal point of developmental control of cell division is Cyclin E (CycE), which together with its binding partner Cdk2 mediates the transition between the first growth phase (G1) and the DNA synthesis phase (S-phase) of the cell cycle [44-46]. CycE promotes S-phase in part by promoting activity of the E2F family of transcription factors, which in *Drosophila* consists of dE2f1 and dE2f2. dE2f1 primarily acts as a transcriptional activator, while dE2f2 acts primarily as a repressor [47]. dE2f1 is inactive when bound to its repressor Rbf1, which is the invertebrate orthologue of the Rb tumor suppressor protein; however, upon phosphorylation of Rbf1 by CycE-Cdk2, Rbf1 dissociates from dE2f1, allowing 'free' dE2f1 to drive the expression of S-phase promoting genes. Several growth regulatory pathways, including the Ras-MAP kinase pathway and the Salvador-Warts-Hippo (SWH) pathway regulate cell number and organ size (in part) through regulating the expression of CycE and promoting the G1/S transition [48, 49]. Consistent with this concept are a myriad of studies highlighting CycE as a positive prognostic indicator of poor clinical outcome in cancer [50].

Because patterns of cell division in developing *Drosophila* organs are stereotyped and exceedingly well characterized, they have proven to be very amenable to genetic dissection. For instance, in the larval eye disc, morphogens - including the TGF- β ortholog Dpp, Hedgehog, and the Wnt ortholog Wg - promote formation of an indentation in the disc called the 'morphogenetic furrow' (MF), which sweeps from posterior-to-anterior across the eye field [51]. As the MF moves

anteriorly across the eye, cells within it synchronously enter a G1 arrest, and then undergo a single synchronous division in its immediate wake. Thus, to assay whether a particular gene affects a step in the cell division cycle, one can simply perform clonal analysis and see if mutant cells show a defect in any of these preprogrammed cell cycle regulatory events. Moreover, because tissues are highly accessible, easy to stain, and reagents exist to analyze multiple phases of the cell cycle, this type of analysis can be performed with relative ease.

Cell Growth

The regulation of cell growth is not as well-studied or understood as the regulation of cell division, but work by many labs has provided a basic framework to understand how signaling pathways can promote the accumulation of cell mass. In general, mechanisms that modulate cell growth do so by altering rates of protein biosynthesis, mainly via control of ribosome biogenesis and activity (Figure 1.6). Moreover, increasing evidence indicates that signaling pathways can also control macromolecular degradative processes such as autophagy to control cell size [52]. One focal point of biosynthetic control is the transcription factor Myc (dMyc in *Drosophila*), which binds to the promoters of ribosomal proteins and rRNA to control their expression [53, 54]. Perhaps as a result of its potent pro-growth effects, Myc is a major proto-oncogene and is upregulated in a myriad of human cancers (reviewed in [55]). Another focal point of growth control is the translation factor S6 kinase, which phosphorylates ribosomal protein S6 to control its activity in cells [56]. Similarly, many pathways also regulate translation elongation factor

eIF4E by relieving suppression imposed the inhibitory binding protein eIF4E-BP [57].

As with cell cycle analysis, cell growth can be easily visualized and assayed in *Drosophila*. Classically, assessments of cell size were determined by counting the number of wing hairs in a fixed area of the wing; as each wing hair cell makes a single hair, this was a convenient and simple way to estimate cell size. If fewer wing hairs occupied a given area when compared to control animals, it was assumed that each cell was larger. If, on the other-hand, more wing hairs occupied in a given area, it was assumed that each cell was smaller. These techniques are still in use today but are supported by more modern techniques to assess cell size include the assessment of forward scatter via FACS (fluorescent-analysis and cell sorting) analysis and direct visualization of cell dimensions via immunohistochemical analysis.

Cell Death

The regulation of cell death is another means with which cellular pathways operate to control organ size (Figure 1.6). Central to programmed cell death (i.e., apoptosis) is the regulation of a family of proteases called caspases which, when activated, act on a number of substrates to produce apoptotic phenotypes (i.e., nuclear lamins, PARP, ICAD, etc; reviewed in [58]). The mechanisms controlling cell death differ slightly between vertebrates and *Drosophila*, thus what follows is a schema of cell death regulation in *Drosophila* (Figure 1.6; reviewed in [59]). In *Drosophila*, apoptosis is primarily regulated by DIAP1 (Drosophila Inhibitor of Apoptosis-1), which binds to and inactivates the caspases the DRONC and DRICE. DIAP1 is a focal

point of regulation by cellular pathways and is regulated by any number of means, including at the transcriptional and post-translational level, the latter process mediated by three proteins known as Reaper, Grim, and Hid. Reaper, Grim and Hid form a complex and promote the turnover in DIAP1 and disrupt DIAP1-dependent interactions, thereby promoting DRONC and DRICE activation in cells. It is worth noting that cells are eliminated by others means besides apoptosis, in fact caspase-independent cell death (CICD) pathways have been described across metazoans though how CICD pathways operate to control organ size remains less clear (reviewed in [60]).

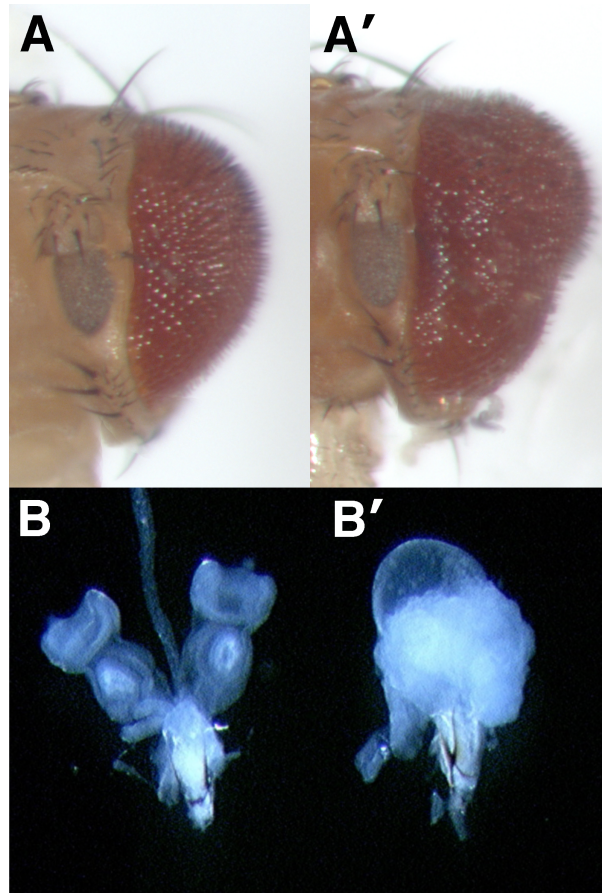


Figure 1.5. Growth phenotypes in *Drosophila*. Images of adult eyes (A) and larval imaginal eye discs from control (A,B) and mutant (A',B') animals. With hyperplastic growth (A), growth is patterned such that animals eclose with large irregular eyes. With neoplastic growth (B), animals do not eclose in instead produce large disorganized imaginal disc structures.

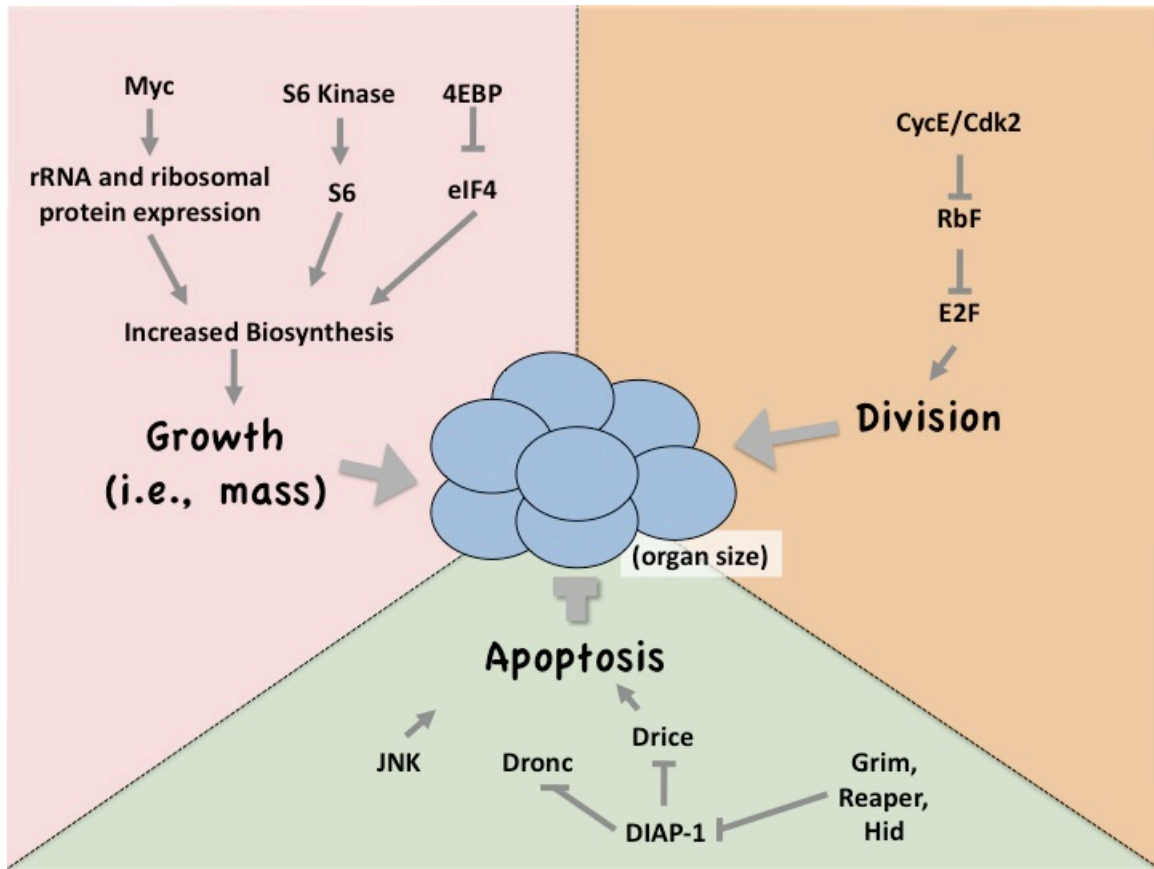


Figure 1.6. Inputs into Organ Size in *Drosophila*. Schematic representation of the major regulatory components of the inputs (cell growth, division, and apoptosis) into organ size *Drosophila* as described in the text. In general, pathways act on any number of these elements to control organ size.

PATHWAYS IMPLICATED IN GROWTH CONTROL IN *DROSOPHILA*

As noted above, genes associated with hyperplastic and mis-patterned growth are often linked to cellular pathways that alter cell division, cell growth, and cell death. What follows is an introduction to several of these pathways and their genetic components. Note, that discussions of several key pathways, including the Insulin/Tor and IGF-1/PI3-Kinase pathways, are absent as they are beyond the scope of this dissertation.

The MAP Kinase Pathway

The MAP (mitogen-activated protein) kinases are a family of kinases known for their ability to respond to intracellular and extracellular cues and control differentiation, proliferation, or survival (reviewed in [61]). MAPKs were first identified as components of receptor tyrosine kinase (RTK) cascades in the 1980's [62]. Analysis in yeast identified two proteins, Kss1p and Fus3p, as the primary targets of receptor tyrosine kinase phosphorylation in response to pheromones and other extracellular cues [63-65]. Subsequent analysis in vertebrates resulted in the cloning and characterization of yeast MAPK mammalian orthologs, ERK1, ERK2, and ERK3 (extracellular-signal regulated kinase), and the birth of a field centered on defining their activation and function in cells [66, 67]. Central to these were genetic interaction studies performed in *Drosophila* and *C. elegans*, which ordered these biochemically defined components into a linear pathway that functioned from the membrane to the nucleus [37, 68]. In current models, intrinsic and extrinsic cues lead to the activation of a series of at least three protein kinases, the last of which is

the multifunctional terminal MAP kinase (MAPK) which acts on several targets to modulate its biological effect (Figure 1.7).

In reality, the term 'MAP kinase pathway' is a broad term that refers to a family of kinase modules that signal through a series of kinases and impinge on a terminal MAPK protein. Thus, since multiple terminal MAPK proteins exist in cells, each with a distinct regulation and functionality, multiple MAPK *pathways* are present in cells. In general these pathways are named according to the terminal MAPK they operate through: these include ERK, JNK (c-Jun N-terminal kinase), and p38. These pathways respond to different stimuli. For instance, the ERK MAPK pathway is activated by ligand binding to RTKs and can, depending on context, drive differentiation or promote increased cell survival and proliferation [69]. Conversely, the JNK MAPK pathway is thought to be activated via cellular stress signals and promote primarily an apoptotic response [70, 71].

In *Drosophila*, ERK MAPK signaling begins with the activation one of five receptor tyrosine kinases (RTK), including the *Drosophila* Epidermal Growth Factor Receptor (DER), Torso, Breathless, Heartless and the eye-specific RTK Sevenless [72-74]. RTK activation promotes the membrane recruitment and activation of the small GTPase Ras1, which when activated recruits and stimulates the serine/threonine kinase Raf1 [74]. Raf1 is MAP kinase kinase kinase (MAPKKK), which acts on the MAP kinase kinase (MAPKK) Dsor1 (Downstream of Ras1) to promote Dsor1-dependent activation of the serine/threonine kinase Rolled, the terminal MAPK of the ERK MAPK pathway in *Drosophila* [75]. Activation of Rolled, in turn, leads to phosphorylation of cytoplasmic targets and subsequent translocation

into the nucleus and phosphorylation of several well-characterized transcription factors, including *pointed*, *yan*, *jun-related antigen* (D-Jun), and *seven in absentia* (*sina*) which act on an array of transcriptional programs involved in a variety of developmental processes [37]. These developmental programs include patterning photoreceptors in the eye, vein formation in the wing, the dorsal-ventral axis in the embryo, and several others (reviewed in [76]). Importantly, Ras1 and Rolled-dependent signaling also plays a critical role in the growth and division of several organs during *Drosophila* development, including those of imaginal disc epithelia by up-regulating targets like Myc and Cyclin E [69].

The other MAP kinase pathway associated with organ-size control in *Drosophila* is the JNK MAP kinase pathway. As with the ERK MAP kinase pathway, several RTK's act upstream of JNK activation in *Drosophila*, including Wengen, and PVR (PDGF/VEGF receptor) (reviewed in [77]). These RTKs stimulate the activation of several MAPKKK-activators including the small GTPases Rac1 and Cdc42 [78], the sterile20-like kinase Misshapen, and the tumor necrosis receptor associated factors dTRAF1 and dTRAF2. Their activation stimulates different JNK MAPKKKs, including dTAK1, DASK1, Slipper, and dMEKK1 which activate the MAPKK Hemipterious (Hep). Hep, in turn, phosphorylates Basket (Bsk or D-JNK), the terminal MAP kinase of the JNK pathway, which acts on the transcription factors D-Jun and Fos (or Kayak), as well as several cytosolic targets. Typically Bsk-activation promotes apoptosis via a variety of mechanisms including the transcriptional upregulation of the pro-apoptotic factor Reaper. However, recent studies have shown that JNK-pathway activation in cells in which apoptosis is blocked, or in cells with excess Ras

signaling, can drive dramatic overgrowth phenotypes in imaginal discs [79-81]. The mechanism underlying this effect is very poorly defined, but it suggests that JNK growth outputs are extremely context-dependent.

The Salvador-Warts-Hippo (SWH) Pathway

The SWH pathway, or Hippo/Mst-2 tumor suppressor pathway as it is also called, is a conserved developmental pathway that functions across metazoans to regulate organ-size (reviewed in [82]). Its history dates to the early 1990s, when the gene *warts* was identified in an FLP-FRT screen trying to identify genes that restrict epithelial growth in *Drosophila* [39, 40]. Since then, many additional SWH components have been identified and placed into an emerging molecular pathway (Figure 1.8). Moreover, studies in vertebrates have shown that the fly SWH pathway is well conserved and also controls the growth of mammalian tissues. Indeed, delineation of the vertebrate SWH pathway has linked several well recognized, yet seemingly disconnected, tumor suppressors into a single linear pathway that suppresses tumorigenesis (see [83]).

The first identified member of the SWH pathway, *warts* (*wts*), is a serine/threonine NDR (Nuclear DBf-2-related) kinase. At the time of its discovery, Wts had no known function beyond a potent overgrowth phenotype associated with *wts* mutant epithelia [39, 40]. Subsequent studies revealed similar overgrowth phenotypes occurred upon loss of the scaffolding proteins Salvador (Sav) and Mob-As-Tumor-Suppressor (Mats), and the kinase Hippo (Hpo), leading to the eventual discovery that Hpo, Sav, Mats and Wts proteins complex together as a core kinase

cassette to control proliferative programs (Figure 1.8; [15, 17, 48, 84]). Hpo, aided by interaction with Sav, phosphorylates Wts, which when activated forms a stable complex with Mats. Phospho-Wts in-turn phosphorylates the transcriptional co-factor Yorkie (Yki), which results in the Yki cytosolic sequestration [85]. When in the nucleus, Yki can bind to one of several DNA-binding factors, including Scalloped, Teashirt, and Homothorax, to drive the transcription of several pro-proliferative and anti-apoptotic genes that control organ size [86-89]. These genes include *dmyc*, *cyclin E*, *diap1*, the microRNA *bantam*, and the FERM-domain containing protein *expanded*. Several factors act upstream of the core kinase cassette to regulate Wts activity, including the transmembrane protein Fat, the cytosolic FERM-domain containing proteins Expanded and Merlin, and the WW-domain containing protein Kibra (reviewed in [90]). Precisely how each of these factors feed in to regulate Hpo-Sav-Wts activity is unclear. Similarly, what factors are required by Yki to promote transcriptional activation is unclear. Thus, these questions, as well as how other developmental programs feed into augment SWH-activity, are likely to be the center of intense focus in the coming years.

Studies in vertebrates have confirmed that SWH-signaling is conserved across metazoans and functions to regulate organ size. These include studies in the mice examining the role of Mst1/2, WW45, and Lats1/2, the *Drosophila* orthologs of Hpo, Sav, and Wts respectively, in controlling the phosphorylation state and subcellular localization of YAP, the *Drosophila* ortholog of Yki [85]. Moreover, studies have highlighted a developmental role for this pathway in regulating processes like contact inhibition and stem/progenitor cell proliferation in

vertebrate systems [91, 92]. Additionally, studies have also revealed a role for SWH-pathway members in tumorigenesis, further highlighting their role in organ size control. These include studies demonstrating that loss of Lats1 and/or the amplification of YAP can promote tumor formation in mice and that mutations and/or alterations in Lats1/2, WW45, and YAP are found not only in human and mouse cancer cell lines, but in tumor samples as well [48, 93-95]. Moreover, examination of NF2, the vertebrate ortholog of Mer and Ex, has shown a conserved role in controlling vertebrate SWH-activity, giving a potential pathophysiologic mechanism to the Neurofibromatosis-2 cancer syndrome [96].

The JAK-STAT Pathway

The Janus-kinase (JAK)-signal transducer and activator of transcription (STAT) pathway is a major signaling pathway in metazoans, originally identified for its intracellular role in mediating cytokine signaling in vertebrates (reviewed in [97]). Orthologs in *Drosophila* were identified shortly thereafter in studies examining genes involved in embryonic segmentation, and since then *Drosophila* has provided insight into the developmental roles of this pathway. Importantly studies in *Drosophila* have been especially insightful due to the lack of genetic redundancy, as the *Drosophila* genome contains both a single JAK tyrosine kinase and STAT transcription factor, while vertebrates display four and seven orthologs, respectively.

In *Drosophila*, JAK-STAT signaling begins with the binding of the extracellular ligand, Unpaired (upd), to the transmembrane receptor Domeless (Dome). Binding

of Upd promotes Dome dimerization, which in turn promotes the recruitment of the JAK tyrosine kinase to the membrane. JAK's phosphorylate many targets including themselves and the Dome receptor. This produces docking sites for the intracellular transcription factor STAT92E, which then becomes an additional target of JAK tyrosine kinase activity, leading to STAT92E dimerization and translocation into the nucleus where it activates the expression of target genes (Figure 1.9).

In the nucleus, STAT92E drives the activation wide-variety of processes, including the induction of growth programs in epithelia (ref: Bach 2003). Targets identified to date include the G1/S regulator *cyclin D*, the G2/M regulator *cyclin B*, the golgi kinase *Four-Jointed*, and the anti-apoptotic gene *diap1* [98-101]. Emerging data has also provided evidence of a non-canonical mechanism in which STAT92E regulates global gene expression via binding to chromatin regulatory factors like Heterochromatin Protein 1 (HP1) [102]. When un-phosphorylated, STAT remains stably bound to HP1 on DNA; upon phosphorylation by JAK or other tyrosine kinases, STAT dissociates from HP1, promoting HP-1 destabilization and loss of heterochromatic regions (Figure 1.9).

The Notch Pathway

The history of the Notch pathway dates to 1916, when members of the Morgan lab first identified a mutant strain of flies that had a notch on the edge of their wing blade (reviewed in [103]). The genetic basis of this phenotype remained unexplored until the recognition of that the *Notch* alleles (as they had come to be named) produced a rare 'neurogenic' phenotype, where cells destined to become the

epidermis instead switched cell fates and developed as neural tissue. Cloning of the *Notch* gene in the mid-1980's, coupled with genetic interaction studies performed shortly thereafter, led to the elucidation of the Notch signaling pathway and allowed for more thorough analysis of its role in *Drosophila* development. Since then, the Notch pathway has been the subject of intense scrutiny, and identified as a major player in developmental disorders and disease states in humans, including cancer. (reviewed in [104])

Classically, Notch signaling is thought to begin at the cell surface where Notch, a large single-pass transmembrane protein, engages transmembrane ligands expressed on the surface of neighboring cells (Figure 1.10; reviewed in [103]). Binding of Notch to one of these ligands, Delta or Serrate, results in cleavage of the Notch intracellular domain (NICD) by the presenilin γ -secretase, freeing the NICD to translocate to the nucleus where it participates in transcriptional regulation of target genes. Recent work showing that the NICD is cleaved in the internal lumen of endocytic vesicles has led to a reexamination of the cellular location of NICD cleavage [105]. However, what remains clear is that once free, the NICD translocates into the nucleus and interacts with Suppressor of Hairless and recruits factors like Mastermind to drive the expression of cell fate and proliferative programs.

One intriguing aspect of Notch biology is that its effect on proliferative programs appears to be extremely context dependent. Studies examining the control of the role of Notch-signaling in *Drosophila* follicle cells have demonstrated a requirement for Notch in controlling follicle cell endocycling, a process where cells increase their ploidy by reiteratively entering S-phase without entering mitosis

[106]. Here, Notch is thought to promote S-phase entry by down-regulating the CycE inhibitor *dacapo* and upregulating the Anaphase Promoting Complex (APC) *fizzy-related/Cdh1*, which promotes degradation of mitotic cyclins [107]. Conversely, in the eye and wing Notch has been shown to have an anti-proliferative role, primarily by repressing CycE levels as tissues undergo developmental patterning [108]. Our laboratory recently showed that Notch restricts CycE protein levels in the eye via induction of the ubiquitin ligase component *archipelago (ago)* [109], which encodes a protein that binds CycE and stimulates its proteolytic destruction [16]. These context-dependent roles for Notch in proliferative control is not restricted to *Drosophila* alone; in fact, studies in vertebrates have also shown that Notch can act as an oncogene or a tumor suppressor depending on the tumor being examined (reviewed in [110]).

The Ecdysone Pathway

Insects undergo a series of developmental stages associated with dramatic tissue morphogenesis and alterations in organ size. These transitions are often coordinated by humoral factors, including steroids. In *Drosophila*, the key factor that initiates postembryonic transitions in development is the steroid hormone 20-hydroxyecdysone (20E or ecdysone). Ecdysone operates in a system analogous to vertebrates that utilize estrogen and progesterone to mediate juvenile development in humans (reviewed in [111]). Thus, *Drosophila* has served as a platform to understand the molecular basis of steroid-mediated postembryonic developmental transitions in metazoans. Furthermore, as studies have demonstrated a role for

steroidal pathways in regulating the autonomous growth of cells (see discussion below), the ecdysone pathway has been utilized to understand the molecular basis by which steroids promote diseases of altered organ size, like cancer.

Ecdysone, like other steroid hormones, is a lipophilic molecule that circulates in the blood (or hemolymph in *Drosophila*) and freely diffuses into and out of cells. Upon entry into the cell, ecdysone encounters its receptor, the ecdysone receptor, which is a heterodimeric complex composed of two nuclear receptors, Ultraspiracle (Usp) and Ecdysone Receptor (EcR). Binding of ecdysone to the ecdysone receptor complex leads to its activation and subsequent translocation into the nucleus, where it binds to DNA and drives the expression of genes. Many of the targets of EcR activity have been identified and include transcription factors required for the proliferation and death of cells, including *dMyc* [112]. To mediate these effects, EcR is thought to activate and recruit several additional factors, including the transcriptional co-activator *taiman* (*tai*; [113, 114]). *Tai* is the *Drosophila* ortholog of human Nuclear Receptor Coactivator-3 (aka Amplified in Breast Cancer-1 or AIB1), a protein heavily implicated in oncogenesis [115]. Important to this dissertation, Chapter 5 describes an analysis of the growth regulatory properties of *tai*, and presents evidence that *Tai* may also act within the SWH pathway.

Neoplastic growth in *Drosophila*

As mentioned previously, neoplastic growth refers to a unique growth phenotype in which tissue overgrowth is disorganized and lacks patterning (Figure 1.5B). Neoplastic growth is characterized by several common features, including

altered apical-basal polarity, a loss of contact inhibition and/or excessive proliferation, altered tissue architecture, increased invasiveness, and an inability to differentiate properly (reviewed in [43, 116]). Additionally, these cells have decreased survival when surrounded by 'wild-type' neighbors. Thus, neoplasia has only been observed when (1) either an entire epithelium is mutant for genes associated with these phenotypes or (2) cell death has been eliminated in mutant clones. It is worth noting that the definition of neoplasia used by *Drosophila* biologists is subtly different than that used by pathologist; whereas the clinical definition of neoplasia refers to *any* abnormal growth, whether differentiated or not, *Drosophila* neoplasia is limited to growth of undifferentiated cells only.

Genes that act to restrict neoplasia in *Drosophila* typically fall into one of three general classes based on their biologic function in cells [116, 117]. These include those involved in the formation and maintenance of apical-basal polarity programs (e.g., *l(2)gl*, *dlg*, and *scrib*), those involved in regulating endocytosis and endolysosomal degradation (e.g., *shi*, *AP2 σ* , *rab-5*, *rabx-5*, *syx7/avl*, *vps45*, *vps23/tsg101*, *vps25*, *vps28*, *vps4*), and those involved in epigenetic regulation (e.g. *Psc-Su(z)2*, *ph*, *Pc* and *Sce*). To date, no unifying theory exists merging these three classes of genes into a model whereby their neoplastic phenotype can be explained. An interesting model that has been proposed, yet remains unproven, is that perhaps these processes deregulate a common factor needed to restrain neoplastic transformation. One such candidate is the polarity factor Crumbs (*crb*), which genetically interacts with *lgl*, *dlg*, and *scrib*. To date, Crb is the only molecule that when overexpressed is *sufficient* to drive neoplasia [31]. Moreover, Crb accumulates

in the cells lacking anti-neoplastic endocytic genes such as *tsg101/vps23* and *vps25* [31, 118-120]. Furthermore, both endocytic and epigenetic neoplastic tumor suppressor genes have been shown to regulate JAK/Stat signaling, which in turn controls tissue architecture and cell polarity via direct transcriptional control of *crb* [121].

To date, no study has shown evidence that removing *crb* from neoplastic backgrounds restores epithelia architecture and patterning. Moreover, studies have shown that *crb* loss can alter cell architecture and growth programs, arguing that if *crb* is the primary driver of neoplasia, it is either a neomorphic consequence of too much *crb*, or that cells require some basal steady-state levels for survival [122]. A more likely explanation, is that instead of operating through a single factor, genes that restrict neoplasia control cell biological processes that impinge on several cell signaling cascades and gene expression programs at once, permitting for the simultaneous misregulation of polarity, differentiation, adhesion, and proliferation programs in cells. In fact, studies examining single *Drosophila* neoplasia mutants have show altered MAP kinase, JAK/Stat, and Notch signaling in mutant cells [79, 118, 120, 123]. From these pathways alone, we can begin to see the web of phenotypes that could emerge, as MAP kinase signaling as been connected to proliferation and altered tissue architecture, JAK/Stat signaling to proliferation, cell polarity and architecture, and Notch signaling to polarity, proliferation and differentiation programs.

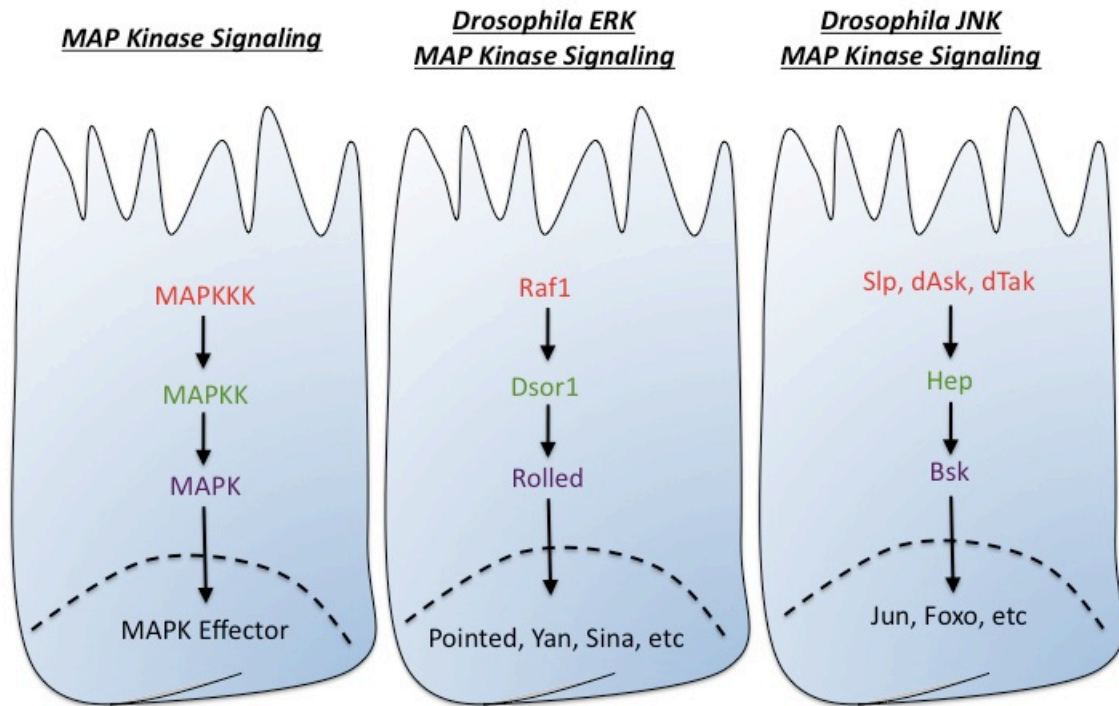


Figure 1.7. MAP Kinase Signaling in *Drosophila*. Depiction of general MAP kinase signaling (left), ERK MAP kinase (middle) and JNK MAP kinase (right) signaling, as described in the text. (Adapted from [61]).

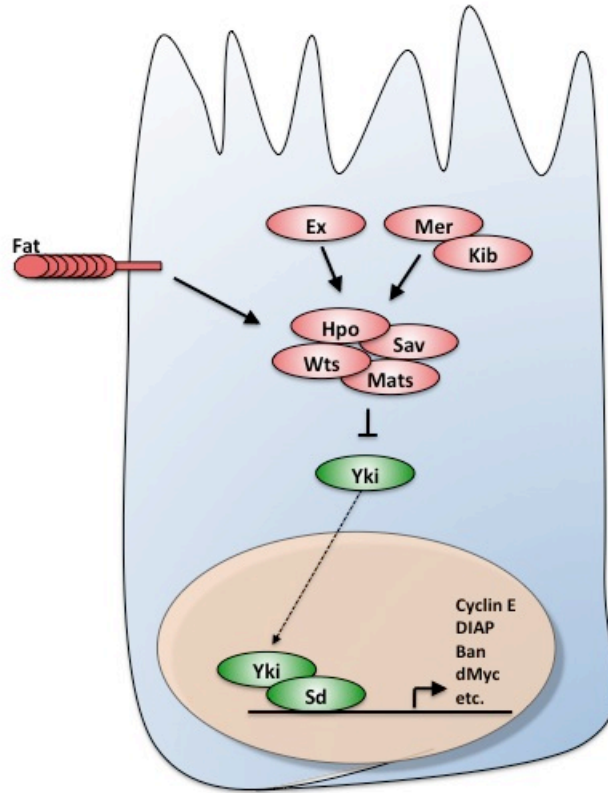


Figure 1.8. The Salvador-Warts-Hippo Pathway in *Drosophila*. Depiction of Salvador-Warts-Hippo Signaling in *Drosophila* as described in the text. Briefly, the core kinase-cassette, composed of Hpo, Sav, Wts, and Mats, act to restrict growth via controlling the localization of the pro-growth transcription co-activator Yki. Fat, Ex, Mer, and Kibra act upstream of Hippo to control Yki-activity, while Sd acts in the nucleus to properly localize Yki to target promoters.

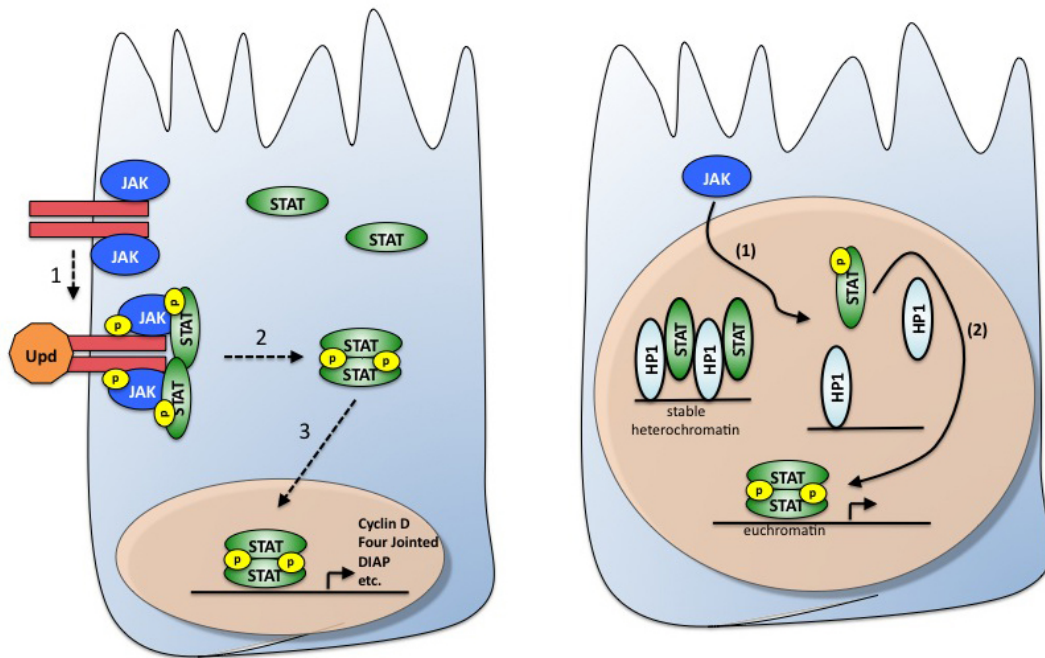


Figure 1.9. The JAK-STAT Pathway in *Drosophila*. Depiction of JAK-STAT Signaling in *Drosophila*, as described in the text. Canonical signaling (left) involves binding of the morphogen Upd to the transmembrane receptor Dome (red), which promotes Dome activation and recruitment of JAK (1). This leads to the phosphorylation and dimerization of the STAT transcription factor (2), which translocates into the nucleus and activates growth and patterning programs (3). With non-canonical JAK-STAT signaling (right), heterochromatin formation is controlled through binding of STAT to the chromatin regulator HP1. Upon phosphorylation by JAK (1), STAT-based inhibition of HP1 is relieved, and STAT-target promoters are revealed (2). (Adapted from [97]).

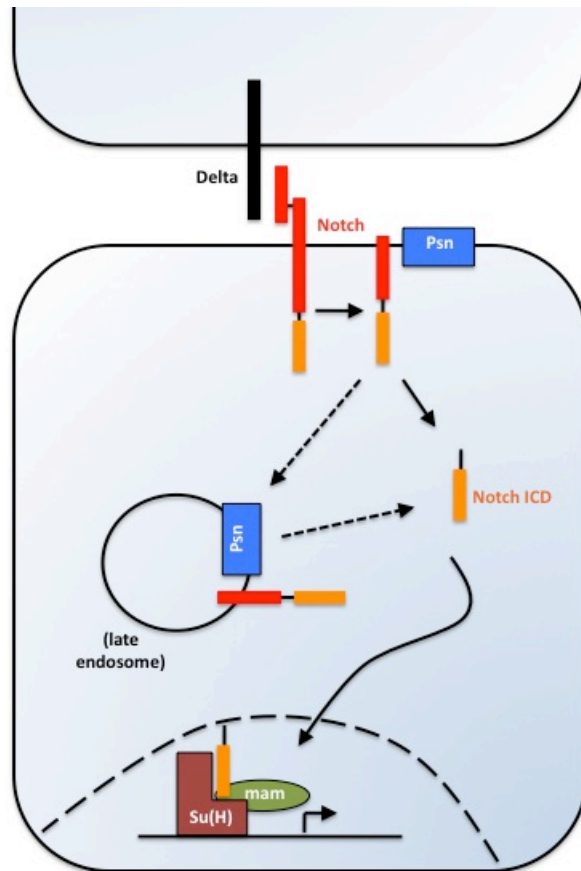


Figure 1.10. The Notch Pathway in *Drosophila*. Depiction of Notch Signaling in *Drosophila*, as described in the text. Binding of Notch to its ligand Delta promotes its cleavage and subsequent interaction with Psn, either at the cell surface or at endosomal (dotted lines) membranes. Psn further cleaves Notch, releasing the Notch intracellular domain (ICD) into the cytosol, which translocates into the nucleus and drives the expression of target genes.

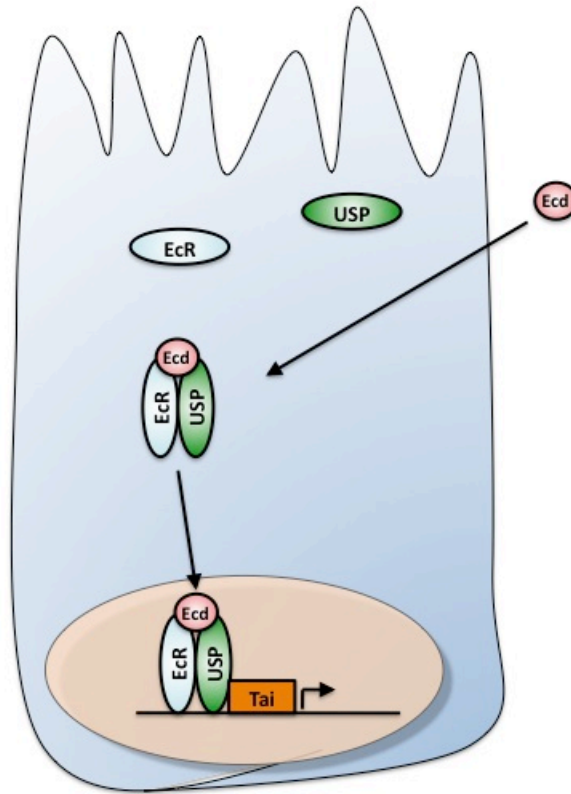


Figure 1.11. Ecdysone Signaling in *Drosophila*. Depiction of Ecdysone Signaling in *Drosophila*, as described in the text. Ecdysone (Ecd) binds to the Ecdysone Receptor, which is composed of EcR and USP. Binding of Ecd to the Ecdysone Receptor promotes its nuclear localization and activation of transcriptional programs. Many factors aid in ecdysone-dependent transcriptional activation, including with the transcriptional co-activator Taiman (Tai).

SCOPE AND SIGNIFICANCE

At present, there are many questions outstanding regarding developmental control of organ size. These include: What is the identity of apparently novel genes that act to control organ size? How does crosstalk between known growth-regulatory pathways occur? How do defects in basic cell biological processes (i.e., endocytosis, tissue polarization, etc.) deregulate known organ size control programs?

One cellular process known to influence organ size is that of apicobasal polarity. To date, no comprehensive model exists detailing how altered expression of apicobasal polarity factors promotes proliferation in cells. In this dissertation, I sought to understand this link further by examining the requirements of a growth phenotype driven by overexpression of the polarity factor Crumbs (Crb). I found that Crb-driven overgrowth is reliant on the activity of the SWH-pathway. Moreover, I characterized a new growth regulator, *taiman*, which is also required for Crb-dependent overgrowth. Lastly, in order to better understand the generalizability of these effects, I examine the role of SWH-signaling in endocytic-mutants that have similar phenotypes as excess Crb and maintain altered expression of Crb. In summary, these studies highlight a novel signaling network whereby the apical-basal polarity factor Crb and endocytic mutants can signal to growth programs in the nucleus, and lend insight into their tumor promoting properties in vertebrates.

Chapter 2: Dominant-Modifiers of Crumbs-driven Overgrowth

INTRODUCTION

The execution of reproducible organismal form and shape requires the proper spatiotemporal regulation and coordination of three fundamental cellular processes: cell growth, cell division, and cell death. These three processes form the collective input into organismal/organ size, and are central to developmental anomalies and disease states in which organ size is altered, like cancer. Thus, uncovering the signals that serve as inputs into these processes and function to regulate the eventual nuclear programs that impinge on these processes is vital to understanding the cellular basis of these disorders.

One biological program that has been shown to augment organ-size control is apical-basal cell polarity. Mutations in genes required for the formation and maintenance of apical-basal polarity, *lethal (2) giant larvae (lgl)*, *discs large (dlg)*, and *scribble (scrib)*, were first identified by their ability to induce neoplasia in *Drosophila* epithelia, a phenotype whose characteristics include a loss of contact inhibition and excess proliferation [124-126]. Subsequent studies revealed a role for these proteins in tumor formation in vertebrates [127], providing a molecular basis for the well-established observation that loss of apical-basal polarity correlates with the ability of tumors to undergo malignant progression in the prostate, colon, and breast [128, 129].

In *Drosophila*, the polarization of epithelial cells is controlled by functional interactions between a small number of membrane-associated protein complexes that line the apical and basolateral surface (reviewed in [25]). The *Drosophila* Dlg and Scrib proteins form a complex that localizes to the basolateral cell membrane

and functionally antagonizes the apical membrane complex Par6/Par3/aPKC. This Par6/Par3/aPKC complex subsequently recruits and activates a second apically localized complex, composed of the Crumbs (Crb), Patj and Pals1/Stardust proteins, that in turn indirectly represses activity of the Scrib complex. Mutations in *Dlg*, *lgl* or *scrib* thus lead to membrane 'apicalization' in which the Crb complex spreads ectopically into the basolateral membrane [29, 30]. Significantly, overexpression of Crb in imaginal disc epithelia leads to spreading of the protein into the basolateral domain and produces neoplastic growth in a manner overtly similar to that produced by loss of *Dlg*, *scrib*, or *lgl* [31, 32].

In order to better understand the mechanisms whereby apical-basal polarity program functions to regulate cellular growth programs, we performed a genetic screen against a growth phenotype driven by excess Crb in the *Drosophila* wing. We find that several components of well-established signaling pathways, as well as, several novel genetic loci dominantly modify the ability of Crb to drive growth in the *Drosophila* wing. Thus, these studies highlight connections between apicobasal polarity programs and known cellular growth programs, and potentially articulate novel means by which apicobasal polarity programs and growth programs signal between one another.

RESULTS

Overexpression of *crbⁱ* drives overgrowth of the *Drosophila* wing

To model the effects of excess *crb*, we utilized the posterior wing driver *engrailed-Gal4* (*en-Gal4*) to drive the expression of a transgene that contains the transmembrane and intracellular domains of *crb* (e.g., *UAS-crbi*). We tested the effects of a wild-type *crb* transgene, however, in light of significant embryonic lethality observed in *en>crb^{wt}* animals, and the observations that demonstrating that the *crbi* transgene can not only recapitulate neoplastic phenotypes but also rescue *crb*-null phenotypes [31, 32], opted instead to examine *en>crbi* animals.

Expression of a *UAS-GFP* transgene using the *en-GAL4* wing driver clearly demarcates the *en-Gal4* expression domain in the posterior domain of the larval imaginal wing discs (Figure 2.1A). As prior studies have noted expansion of this domain upon introduction of the *crbi* transgene [31], we first sought to examine whether this effect was accompanied with excess proliferation, as proliferative phenotypes have been observed with alteration in other polarity mutants [130]. BrdU-labeling in the background of *crbi* reveals a clear elevation in the number of cells entering S-phase in the posterior domain relative to the control anterior side, a phenotype which was not observed in control animals (Figure 2.1B, personal communication BSR).

Finally, we sought to determine whether these effects observed in larval wing discs correlated with an alteration in organ size in adult *en>crbi* animals. We attempted to obtain animals reared at 25°, the temperature in which the larval

experiments were performed, however were unsuccessful and found that many of these animals died as pharate adults trapped in their pupal cases. However, when *en>crbⁱ* animals are reared at 20°, which reduces GAL4 protein activity in cells and thus tempers *en>crbⁱ*-driven phenotypes, we found a significant rescue of this lethality and observed that *en>crbⁱ* animals eclose with wings significantly larger than their control counterparts (Figure 2.1C'-C'').

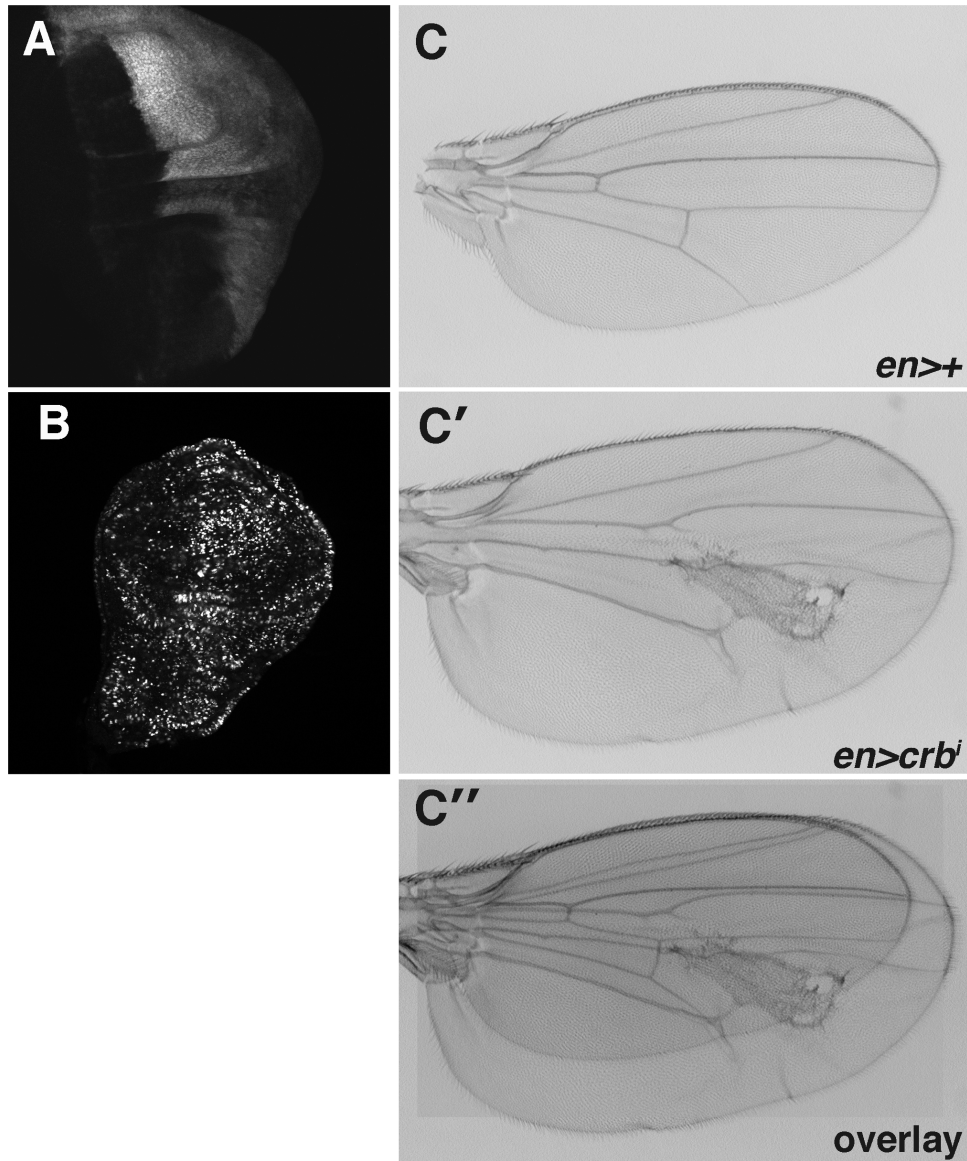


Figure 2.1. Growth phenotypes in *en>crbi* animals. (A) Confocal images of GFP expression in *en>GFP* animals. (B) Pattern of BrdU-incorporation in *en>crbi* animals; posterior is to the right. (C) Light microscopic images of adult wings of (C) *en* and (C') *en>crbi* animals, and (C'') their comparison when superimposed.

A candidate-based approach reveals dominant modifiers of *crbⁱ*-driven overgrowth

Having established that the *crbⁱ* transgene elicits a potent growth phenotype when driven by *en-GAL4*, we next sought to determine if we could utilize this phenotype to screen for genetic components downstream of altered polarity programs. First, we measured *en>crbⁱ* wing size in order to determine whether effects driven by excess Crbⁱ are quantifiable. We reasoned that comparison of the size of the posterior compartment relative to the whole wing, a measure we term ‘posterior compartment ratio’ (PCR), would be highly specific for *en>crbⁱ* phenotypes since (1) this is the region where *crbⁱ* transgene was being expressed by *en-GAL4* and (2) this analysis would control for variance in organ size that might occur due nutrient availability, etc. Analysis of *en* and *en>crbⁱ* animals reveals a statistically significant increase in the PCR of *en>crbⁱ* animals, consistent with a model where Crbⁱ drives growth in this region of the *Drosophila* wing (Table 2.1).

Next, we utilized the wing growth observed in *en>crbⁱ* animals to test whether we could determine which of the major growth regulatory pathways remain downstream of excess *crbⁱ*. We surmised that phenotypes driven by excess *crbⁱ* would be sensitive to the genetic dose of factors required to elicit those phenotypes, as these phenotypes relied heavily on their activity. Thus, we took selected alleles of known growth regulators—including alleles from Salvador-Warts-Hippo (SWH) pathway, the ERK/MAPK pathway, the JAK-STAT pathway, the Wingless (Wg) pathway, the Notch pathway and core cell cycle/cell growth

members—and tested their ability to dominantly modify the ability of *Crbⁱ*-driven overgrowth in the posterior compartment of the *Drosophila* wing.

This analysis yielded several promising results, including the observation that *crbⁱ*-driven overgrowth is genetically sensitive to the dose of SWH and Notch pathway components (Table 2.1). Alleles of the transcription factors *yorkie* (*yki*) and *scalloped*, which bind together and form a complex to activate SWH-pathway gene expression [86, 88, 89], dominantly suppress the ability of *Crbⁱ* to drive overgrowth in the wing (Table 2.1). Similar effects were observed with an allele of *bantam*, a pro-growth miRNA that is the target of Yki activity [131, 132]. Slight suppression is also observed with the transcription factors Myc and E2F1, two proteins that have been shown to collaborate with Yki to drive hyperplastic phenotypes [133, 134]. Lastly, nearly complete suppression is observed with co-expression of Salvador, a scaffolding protein that inhibits Yki activity in cells [17, 48].

To a lesser extent, similar results were obtained with Notch pathway members, where alleles of *presenilin* (*psn*) and *mastermind* (*mam*), two proteins required for Notch activation [135-138], dominantly suppress *crbⁱ*-driven overgrowth (Table 2.1). These results, though statistically significant, were neither as robust nor reproducible as those components in the SWH-pathway. Effects were not observed in the background of loss-of-function alleles of *rolled*, *STAT92E*, and *Tor*— pro-growth members of the ERK/MAPK, JAK/STAT, and TSC/Tor pathways respectively—arguing that these pathways may not be involved in *Crbⁱ* overgrowth (Table 2.1).

Finally we sought to explore the role of atypical Protein Kinase C (aPKC) in promoting *crbi*-driven overgrowth. Previous studies have demonstrated that a *DN-aPKC* transgene can suppress *crbi*-driven phenotypes [31]. We find that a loss-of-function allele of aPKC dominantly enhances the ability of *crbi* to drive overgrowth (Table 2.1). Moreover, we find that an allele of aPKC that contains a 'EY-element,' which harbors UAS sites allowing for overexpression, dominantly suppresses the ability of *crbi* to drive overgrowth (Table 2.1). Together, these results suggest that aPKC is required to restrict Crb-growth regulatory activity.

Genotype	BL #	PCR	p-value
<i>en>+ (w1118)</i>	-	0.61	-
<i>en>crbⁱ</i>	-	0.70	1.3E-10
<i>en>crbⁱ, yki^{B5}</i>	-	0.66	6.4E-12
<i>en>crbⁱ, bantam^{A1}</i>	-	0.68	9.0E-06
<i>en>crbⁱ, sd^{ETX4}</i>	-	0.68	3.2E-03
<i>en>crbⁱ, UAS-Sav</i>	-	0.60	2.8E-17
<i>en>crbⁱ, tor^{D9}</i>	-	0.70	2.4E-02
<i>en>crbⁱ, cdk4³</i>	-	0.70	1.3E-01
<i>en>crbⁱ, myc¹</i>	-	0.71	1.7E-02
<i>en>crbⁱ, dmyc^{PL35}</i>	-	0.68	1.8E-04
<i>en>crbⁱ, stat92E</i>	-	0.69	1.8E-02
<i>en>crbⁱ, rl¹⁰</i>	-	0.70	2.1E-02
<i>en>crbⁱ, aPKC^{k06403}</i>	10622	0.72	2.3E-03
<i>en>crbⁱ, aPKC^{EY22946}</i>	23116	0.68	2.4E-03
<i>en>crbⁱ, wg^{I-17}</i>	2980	0.67	4.5E-04
<i>en>crbⁱ, Df(2L)DE</i>	6653	0.70	6.8E-01
<i>en>crbⁱ, Pi4KIIa^{c02099}</i>	10833	0.68	4.9E-03
<i>en>crbⁱ, slif^{KG02761}</i>	13492	0.67	2.1E-03
<i>en>crbⁱ, mam⁸</i>	-	0.67	3.3E-03
<i>en>crbⁱ, psn²²⁷</i>	-	0.67	2.2E-02
<i>en>crbⁱ, cycE^{JP}</i>	-	0.69	4.7E-01
<i>en>crbⁱ; e2f^{m729}/+</i>	-	0.68	3.1E-08

Table 2.1. Effect of established growth-regulators on Crbⁱ-driven wing growth.

Posterior compartment ratios (PCR) in indicated genotypes heterozygous for specified alleles. Values are indicative of experiments from multiple animals. p-value measurements were obtained by a Student t-test when compared to *en>crbⁱ* animals, except for the p-value indicated in *en>crbⁱ* animals which was obtained by comparison to *en* animals. BL #: Bloomington Stock Number. Green shade indicates ≤ 0.68 ; red shade indicates ≥ 0.71 . Blue text indicates ≤ 0.05 and ≥ 0.0005 ; red text indicates ≤ 0.0005 .

A discovery-based screen reveals genetic loci that reproducibly modify *crbⁱ*-driven overgrowth

Given the ability of known genes to dominantly modify *crbⁱ*-driven overgrowth, we next asked whether this approach could be used to identify novel components of a Crb-regulatory growth network. Thus, we tested the ability of a collection deficiency, each containing a deletion for different regions covering the 2nd and 3rd chromosomes that equates to roughly two-thirds of *Drosophila* genome, to dominantly modify the ability of *crbⁱ* to drive overgrowth. Hits were initially culled by their ability to modify *crbⁱ*-driven overgrowth with a p-value ≤ 0.05 when compared to control animals; these hits were then reassessed using a greater number of samples ensure accuracy and reproducibility. Those deficiencies that reproducibly dominantly modified *crbⁱ*-driven wing growth are shown in Table 2.2. In all ten deficiency modifiers were uncovered on chromosome 2, and twelve on chromosome 3.

Next we sought to determine sought to determine the genetic basis for the observed suppression. Subsequent to our analysis, we noted that the stock used to test *Df(2L)Prl* had a allele of *nubbin* in its background which produces a dominant phenotype in the wing [139], and thus excluded it from further analysis. Similarly, *Df(2R)robl-c* removed only a single gene, *roadblock (robl)*, arguing strongly for *robl* as the causative factor. Also, we choose not to follow-up *Df(3L)Ar14-8* as it removed a region uncovering *ban*, which we found in our candidate approach could suppress *crbⁱ*-driven overgrowth (Table 2.1). For most other deficiency modifiers, we utilized several smaller overlapping deficiencies that remove region within the original

modifying deficiency, and determined the shortest region of overlap. The results of this analysis are summarized in Appendix Tables A.1-A.17.

For several of the original deficiency-modifiers we were able to narrow the modifying effect to a relatively small span of the genome. In these circumstances, we next ordered selected alleles from genes within that region and assessed the ability of those deficiencies to recapitulate the original phenotype observed (Table 2.3). Alleles to be tested were selected on the basis of (1) their availability and (2) their biologic plausibility (i.e., associated with growth control, etc.). From this analysis, we observe reproducible effects with alleles of *taiman* (*tai*), *rho1*, *CTP:phosphocholine cytidyltransferase 1* (*cct1*), *rpt1*, *TNF-receptor associated factor-4* (*traf4*), *ventral veins lacking* (*vvl*), and *target of wingless* (*tow*).

Chromosome 2 Hits						
Genomic Information from Hits			Primary Result		Repeat Performance	
Deficiency	Deleted Region	BL #	PCR	p-value	PCR	p-value
Df(2L)ast2	21D1-2;22B2-3	3084	0.71	1.1E-02	0.73	1.0E-04
Df(2L)sc19-8	24C2-8;25C8-9, 24D4;25F2	693	0.67	3.4E-03	0.67	1.7E-05
Df(2L)Dwee1-W05	27C2-3;27C4-5	5420	0.72	4.9E-03	0.72	3.4E-03
Df(2L)N22-14	29C1-2;30C8-9	2892	0.65	8.7E-04	0.67	2.9E-07
Df(2R)ST1	42B3-5;43E15-18	1888	0.66	1.5E-04	0.67	6.0E-10
Df(2R)H3C1	43F;44D3-8	198	0.67	1.9E-02	0.67	2.5E-05
Df(2R)vg-B	49D3-49D4;50A2	752	0.66	1.1E-03	0.69	1.1E-05
Df(2R)Jp1	51D3-8;52F5-9	3518	0.67	3.1E-03	0.65	3.2E-10
Df(2R)robl-c	54B17-C4;54C1-4	5680	0.68	4.3E-02	0.68	1.2E-05
Df(2R)AA21	56F9-17;57D11-12	3467	0.66	2.8E-03	0.68	2.8E-05
Chromosome 3 Hits						
Genomic Information from Hits			Primary Result		Repeat Performance	
Deficiency	Deleted Region	BL #	PCR	p-value	PCR	p-value
Df(3L)Ar14-8	61C5-8;62A8	439	0.68	4.3E-03	0.67	5.4E-05
Df(3L)Exel6087	62A2;62A6	7566	0.71	4.5E-04	0.72	2.6E-05
Df(3L)XDI98	65A2;65E1	4393	0.67	4.4E-04	0.68	4.5E-04
Df(3L)fz-GF3b	70C1-2;70D4-5	3124	0.67	2.8E-07	0.67	2.5E-07
Df(3L)BSC21	79E5-F1;80A2-3	6649	0.67	2.8E-05	0.67	4.8E-08
Df(3R)ME15	81F3-6;82F5-7	1518	0.67	4.6E-07	0.67	6.5E-07
Df(3R)p712	84D4-6;85B6	1968	0.68	1.7E-03	0.67	3.5E-08
Df(3R)by10	85D8-12;85E7-F1	1931	-	lethal	0.72	4.7E-06
Df(3R)ea	88E7-13;89A1	383	0.66	1.9E-07	0.68	1.8E-03
Df(3R)BSC56	94E1-2;94F1-2	8583	0.71	1.8E-02	0.72	2.0E-05
Df(3R)BSC140	96F1;96F10	9500	0.72	2.8E-06	0.74	4.9E-09
Df(3R)3450	98E03;99A6-8	430	0.67	3.9E-06	0.67	1.2E-08

Table 2.2. Results from the deficiency-modifier screen. Posterior compartment ratios (PCR) of *en>crbi* animals heterozygous for specified genomic deficiencies. p-value measurements were obtained from a Student's t-test when compared to *en>crbi* animals. BL #: Bloomington Stock Number. Green shade indicates ≤ 0.68 ; red shade indicates ≥ 0.71 .

Gene	Original Modifying Df (BL #)	Stock Test	BL #	PCR	p-value
<i>traf4</i>	693	<i>traf4</i> ^{EP578}	17285	0.66	2.2E-04
<i>traf4</i>	693	<i>traf4</i> ^{EY09771}	17600	0.70	1.1E-01
<i>rpt1</i>	1888	<i>rpt1</i> ^{K11110}	10437	0.68	6.4E-02
<i>rpt1</i>	1888	<i>rpt1</i> ^{O5643}	11448	0.67	4.9E-02
<i>tor</i>	1888	<i>tor</i> ^{E00150}	17818	0.71	2.8E-03
<i>aPS4</i>	3518	<i>aPS4</i> ^{MB02574}	23578	0.70	1.5E-02
<i>aPS4</i>	3518	<i>aPS4-IR</i>	28535	0.71	3.7E-03
<i>fs</i>	3518	<i>Fs</i> ^{I00897}	18386	0.69	9.3E-01
<i>fs</i>	3518	<i>Fs</i> ^{MB12011}	29272	0.71	1.3E-03
<i>scb</i>	3518	<i>scb</i> ^{O1288}	11035	0.68	2.8E-01
<i>rho1</i>	3518	<i>Rho1</i> ^{1B}	9477	0.64	2.21E-09
<i>rho1</i>	3518	<i>Rho1</i> ^{E3.1}	3176	0.64	2.87E-11
<i>vvl</i>	4393	<i>vvl</i> ^{M638}	4387	0.67	1.8E-03
<i>vvl</i>	4393	<i>vvl-IR</i>	26228	0.70	1.8E-01
<i>tow</i>	4393	<i>tow</i> ^{LA00200}	22222	0.65	8.5E-04
<i>cct1</i>	7566	<i>Cct1</i> ^{EP3346}	17268	0.69	4.3E-01
<i>cct1</i>	7566	<i>Cct1</i> ^{DG23712}	20484	0.69	9.7E-01
<i>cct1</i>	7566	<i>Cct1</i> ^{HP35812}	22123	0.70	4.3E-02
<i>cct1</i>	7566	<i>Cct1</i> ^{I6919}	7319	0.69	7.1E-01
<i>tai</i>	2892	<i>tai</i> ^{K05809}		0.69	1.3E-03
<i>tai</i>	2892	<i>tai</i> ^{6TG1}		0.69	5.7E-02
<i>tai</i>	2892	<i>tai</i> ^{O1351}		0.68	7.0E-10
<i>tai</i>	2892	<i>tai</i> ^{K15101}		0.70	1.4E-02

Table 2.3. Analysis of selected alleles from the deficiency-modifier screen.

Posterior compartment ratios (PCR) of *en>crbi* animals heterozygous for specified alleles. p-value measurements were obtained from a Student t-test when compared to *en>crbi* animals. BL #: Bloomington Stock Number. Green shade indicates ≤ 0.68 ; red shade indicates ≥ 0.71 . Blue text indicates ≤ 0.05 and ≥ 0.0005 ; red text indicates ≤ 0.0005 .

Discussion:

The ability of apical-basal polarity programs to control organ size and promote tumorigenesis is well established. Here we utilize an overgrowth phenotype produced by the overexpression of the apical polarity factor Crumbs (Crb) to identify mechanisms whereby polarity factors signal to the nucleus to control proliferative programs in cells. We find that Crb-driven overgrowth is sensitive to the genetic dosage of two well-conserved growth regulatory pathways, the Notch and Salvador-Warts-Hippo (SWH) pathways. Moreover, using a discovery-based approach we identify several genes and genetic loci that reproducibly modify Crb-driven overgrowth and could potentially define additional signaling nodes between polarity and proliferative programs.

The ability of Notch and SWH-pathway components to modify Crb-driven overgrowth suggests that these pathways may function downstream of Crb to control organ size. Indeed, connections between Crb and Notch signaling are well documented, albeit in a polarity independent manner [140, 141]. Crb is a target of Notch signaling in the dorsal-ventral margin of the wing, where it is thought to feedback and negatively regulate Notch activation through controlling γ -secretase activity [141, 142]. Similarly, in the *Drosophila* eye, loss of Crb elicits a Notch-dependent overgrowth phenotype that is accompanied with altered localization of Notch and its ligand Delta [140]. Given the recent findings demonstrating that cleavage of Notch by presenilin occurs on internal luminal structures [105], it is intriguing to speculate that these findings may be unified via a model whereby Crb controls Notch internalization, thereby regulating its access to γ -secretase

enzymatic activity (Figure 2.2). However, as these phenotypes occur in the *absence* of defective polarization it is likely that these mechanisms do not contribute greatly to the excess growth seen with defective polarization.

The observation that SWH-signaling may operate downstream of excess Crb is especially intriguing given the numerous studies highlighting the role of the SWH-pathway in controlling epithelial differentiation, proliferation, and tumorigenesis in vertebrates (reviewed in [82]). In Chapter 3 of this dissertation, I examine the link between Crb and SWH-signaling in detail and define a direct connection between Crb and the SWH-regulator *expanded (ex)*. These studies highlight not only a novel relationship between polarity programs and the SWH-pathway, a link that was subsequently confirmed by several other labs [143-145], but may also explain the defective Notch internalization observed in *crb*-deficient cells. Studies examining *ex* and *merlin*, a protein functionally redundant to *ex*, show that *ex* can control Notch turnover at the cell surface [146]. Moreover, studies in the *Drosophila* oocyte show that ectopic activation of SWH-signaling can control Notch activation through regulating apical endocytosis, though these studies did not explore whether *ex* was required for this effect [147].

Future studies stemming from this analysis should also focus on determining the mechanisms underlying the suppression observed by those uncovered from our deficiency modifier screen. Confirmation of *roadblock (robl)* as a modifier is enticing, given *robl* is a dynein-light chain subunit required for efficient cell division [148]. *rho1* and *traf4* also should be explored, as they may represent connections between Crb and JNK-signaling. This is notable, as JNK-signaling has been linked to

in multiple contexts Yki-activation in *Drosophila* [80, 149-151]. *rho1* was recently been placed upstream of JNK in overgrowth phenotype produced by altered expression of the polarity protein *cdc42* [152]. *traf4* has been linked to JNK-signaling, though whether this acts to promote or restrict growth remains unresolved [153, 154]. We found that expression of an EP placed in front of *traf4* suppressed Crb-dependent overgrowth, but had no effect on the basal expression of the SWH-reporter *ex-lacZ* (BSR, personal communication), arguing that either *traf4* exerts its effects in an SWH-independent manner or acts only to suppress ectopic Yki-activity in cells. *tai* and *vvl*, two well-characterized transcriptional regulators, appear to represent nuclear inputs into Crb-dependent overgrowth. This is especially intriguing given the unresolved questions regarding how *yki* functions within the nucleus to drive proliferative programs. In Chapter 5 of this dissertation, I examine the role of *tai* in controlling growth and SWH-signaling of imaginal disc epithelia.

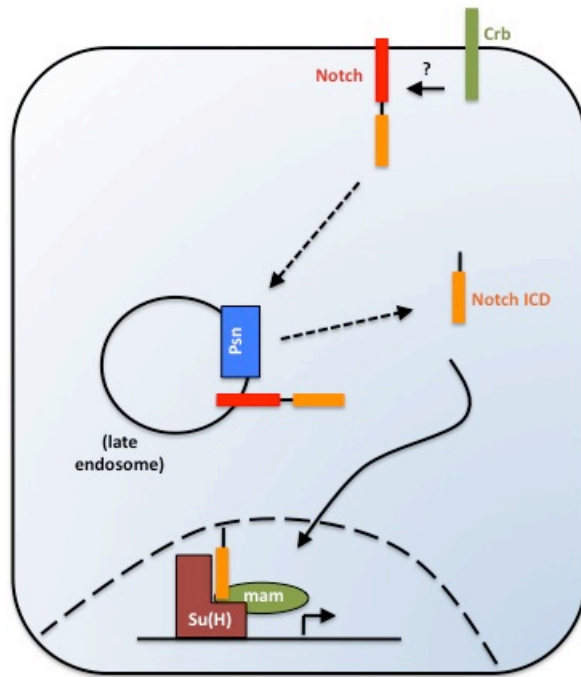


Figure 2.2. Model of potential regulation of Notch activity by Crb. As described in text, subtle modification by Notch signaling components may represent Crb-dependent regulation of Notch internalization, limiting access of Notch to endocytic compartments required for efficient activation in cells.

EXPERIMENTAL PROCEDURES

Genetics

Crosses performed at 25°C unless noted. Larval wing discs were harvested from animals kept at 20°C during embryogenesis. Animals were maintained at 20°C for adult wing analysis. Alleles used besides those indicated in text include: *en-GAL4*, *UAS-myc-crb^{intra}*; *UAS-GFP*. Stocks used for the deficiency modifier screen were obtained from the Bloomington stock center and include those contained in the Bloomington Deficiency Kit as of January 2008.

Wing Analysis

Wings were imaged on a Leica DFC500 CCD camera and quantified with Adobe Photoshop. Briefly, quantification involved measurement of the total number of pixels for both the entire wing and posterior compartment of the wing for ~10 wings per genotype. Posterior compartment ratio (PCR) = posterior compartment size/total wing size.

BrdU incorporation Assay

Briefly, wing discs were dissected in Schneiders media and transferred into 500 ul of Schneider's containing 10mM BrdU for 30' incubation. Discs were then washed 2X in PBS, pH 7.4 and fixed overnight at 4° in 1.5% formaldehyde/0.01% Tween-20 in PBS. Following overnight incubation, discs were then washed 5X with PBS and treated with DNase for 45' at 37°C (RQ1 DNAase Promega). Discs were then washed 3X with PBS/0.3% Triton X-100 and incubated with anti-BrdU (1:100) in 10%

normal goat serum and PBS/0.1% Triton X-100. Following at least a 2-hour incubation in primary antibody, discs were then washed and incubated with goat-anti-mouse-cy3 in 10% normal goat serum and PBS/0.1% Triton X-100. This was followed by 5X washes in PBS/0.3% Triton X-100 and subsequent mounting on slides for visualization.

Chapter 3: The apical membrane determinant Crumbs acts via the FERM-domain protein Expanded to control SWH-signaling in *Drosophila*

This chapter is adapted from the following published paper:

Robinson BS, Huang J, Hong Y, Moberg KH. *Crumbs Regulates Salvador/Warts/Hippo Signaling in Drosophila* via the FERM-Domain Protein Expanded. *Curr Biol.* 2010 Apr 13;20(7):582-90.

INTRODUCTION

Mutations in any of three *Drosophila melanogaster* genes required for the maintenance of apicobasal polarity - *Discs large (Dlg)*, *lethal giant larvae (lgl)*, and *scribble (scrib)* - result in disorganized overgrowth of epithelial tissues [116]. The discoveries that homologs of these genes are downregulated in cancer and targeted for inactivation by mammalian tumor viruses [127] have further advanced the hypothesis that defective epithelial polarization can drive ectopic cell proliferation and tissue overgrowth in metazoans. The mechanisms by which *Drosophila* Dlg, Lgl and Scrib restrict cell proliferation are not well understood, although it is assumed that they are an extension of their more primary roles in cell polarization.

The polarization of *Drosophila* epithelial cells is controlled by functional interactions between membrane-associated protein complexes [116]. In the embryonic ectoderm, the Dlg/Scrib complex localizes to the basolateral cell membrane and functionally antagonizes the apical Par6/Par3/aPKC (Par) complex. The Par complex recruits a second apically localized complex, composed of the Crumbs (Crb), Patj and Pals1/Stardust (Sdt) proteins, which represses activity of the Scrib complex. Mutations in *Dlg*, *lgl* or *scrib* lead to membrane 'apicalization' in which the Crb complex spreads ectopically into the basolateral membrane. Overexpression of Crb in discs leads to a similar spreading phenotype and produces overgrowth in a manner overtly similar to that seen in *Dlg*, *scrib*, or *lgl* mutants [31, 32]. Certain endocytic mutants that block Crb turnover also cause disc overgrowth [31, 118], although the role of Crb in this phenotype is not clear. Intriguingly, a *crb* transgene encoding the transmembrane region and the small 37 amino acid

intracellular tail is oncogenic when expressed in discs [31, 32], arguing that the Crb intracellular tail contains a growth regulatory domain. The Crb cytoplasmic tail has two recognized motifs, one that links to the spectrin and actin cytoskeleton and another that interacts with polarity regulatory factors such as Sdt, Patj, and Par6 [34]. The ability of Crb to drive tissue growth is thus either due to a previously described role for one of these motifs, or to a previously unrecognized growth regulatory domain embedded within the Crb cytoplasmic tail.

Here we show that the Crb cytoplasmic tail drives organ growth via the Salvador-Warts-Hippo (SWH) pathway, a conserved signaling network that restricts cell proliferation and promotes apoptosis by regulating the Yorkie (Yki) transcriptional co-factor [83]. The activities of the core SWH proteins are controlled by inputs from a variety of ‘non-core’ peripheral regulators that are required for growth inhibition by the SWH pathway, and in some cases render SWH responsive to different upstream inputs, including those from planar cell polarity pathways, morphogen gradients, and adhesion molecules [155]. We show that Crb restricts accumulation of Expanded [156], a FERM-domain protein that localizes to the apical-membrane and acts as a ‘peripheral’ regulator of the SWH pathway [157]. Moreover, this Ex-regulatory function maps to a small motif within the Crb cytoplasmic tail that coincides with juxtamembrane FERM-binding motif, which is distinct from the domain through which Crb binds polarity factors. These studies identify the Crb protein as a novel regulator of the SWH pathway via its effects on Ex, and suggest that discrete domains within Crb may allow it to simultaneously regulate apical polarity and tissue growth.

RESULTS

The intracellular domain of *crb* requires *yki* to drive tissue growth

Previous studies have shown that *engrailed-Gal4* (*en-Gal4*) driven expression of either a full-length *UAS-crb* transgene or one encoding only intact transmembrane and intracellular domains (*UAS-crbⁱ*) [32] produces wing overgrowth [31]. Because the *en>crb* genotype led to significant embryonic lethality (data not shown), the *en>crbⁱ* genotype was used to model the cell-autonomous effect of the Crb intracellular tail on wing development.

en>crbⁱ larval wing discs show posterior domain overgrowth and tissue disorganization (Figure 3.1D) [see also 31]. *en>crbⁱ* adult wings also show an enlarged posterior compartment and cuticular defects (Figure 3.1A). Quantification of posterior compartment size relative to the entire wing produces a value we termed the posterior compartment ratio (PCR) that is elevated in *en>crbⁱ* animals (Figure 3.1F). To understand the basis for this PCR phenotype, chromosomal deficiencies and selected alleles of pro-growth genes were screened for their ability to dominantly reduce *en>crbⁱ* wing phenotypes. Multiple alleles of pro-growth members of the SWH growth regulatory pathway, including the transcriptional co-factor *yorkie* (*yki*), the microRNA *bantam* (*ban*), and the transcription factor *scalloped* (*sd*), dominantly suppressed the *en>crbⁱ* PCR phenotype (Figure 3.1B,F). These alleles did not modify PCR of control wings, indicating their effects on *en>crbⁱ* wings do not reflect dosage-sensitive roles in wing growth (Figure 3.1F). Co-expression of the Sav protein, which antagonizes Yki [83], also suppressed growth

of larval and adult *en>crbi* wings (Figure 3.1C,E-F). Alleles of *Tor*, *rheb*, *rolled/ERK*, *stat92E*, and *Akt1* did not modify the *en>crbi* PCR phenotype (data not shown), indicating that *crbi*-driven growth is specifically sensitive to the dose of SWH pathway components.

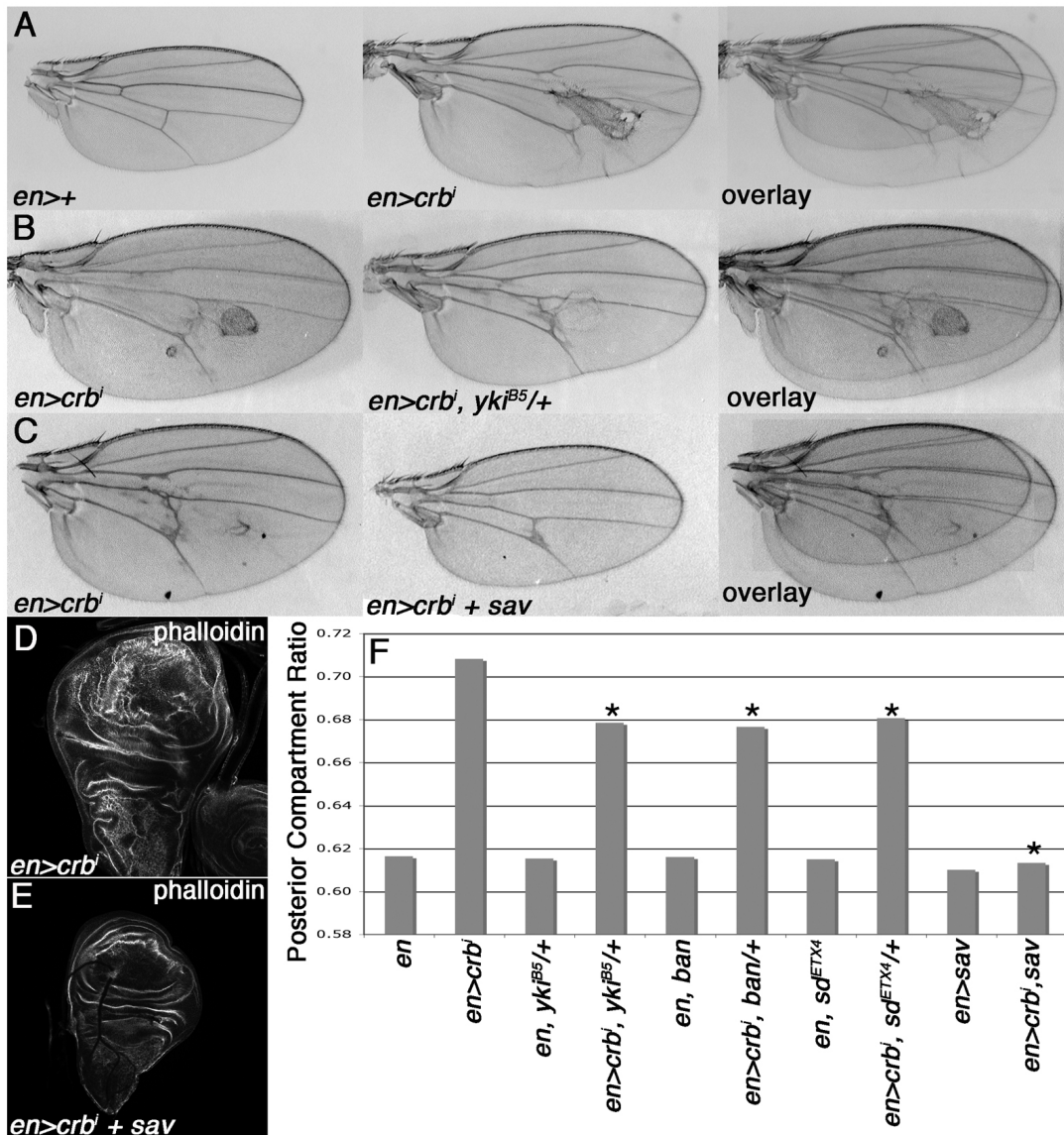


Figure 3.1. Overgrowth driven by the *crbⁱ* transgene is sensitive to the dose of SWH pathway genes. Images and overlays of (A) transgenic *en>crbⁱ* and control *en>+*, (B) *en>crbⁱ* and *en>crbⁱ,yki^{β5}/+*, (C) *en>crbⁱ* and *en>crbⁱ,sav* wings. (D-E) Phalloidin-FITC staining of *en>crbⁱ* and *en>crbⁱ,sav* larval wings. (F) PCR in the indicated genotypes (minimum 10 wings per genotype; * $p < 0.05$ compared to *en>crbⁱ* wings). PCR = Posterior Compartment Ratio.

***crbi* expression elevates Yki activity in developing epithelia**

Consistent with the pattern of genetic interactions between *crbi* and SWH alleles, the expression of multiple Yki targets [83] is elevated in *en>crbi* larval wing cells (Figure 3.2A-D). The *ex-lacZ* and *diap1-lacZ* enhancer traps, which respectively report Yki-dependent transcription of the *expanded (ex)* and *Drosophila Inhibitor of Apoptosis-1 (diap1)* genes, are elevated in the posterior domain of *en>crbi* wing discs (Figure 3.2A-A',C-C'). The *bantam-GFP* reporter, whose expression inversely correlates with activity of the Yki-target and pro-growth miRNA *bantam (ban)*, is also reduced in the posterior domain of *en>crbi* wing discs (Figure 3.2B-B'). Wg protein levels, which are normally repressed by the SWH pathway in the proximal wing hinge, are elevated in the corresponding area of *en>crbi* wing discs (Figure 3.2D). In parallel, the *en>crbi* genotype increased the amount of Yki that co-localizes with a DNA marker relative to the cortical pattern of Yki among cells in the anterior wing pouch (Figure 3.2F-F"). Finally, *crbi*-driven disc growth is also not associated with a dramatic shift in cell cycle phasing (Figure 3.2E) or cell size (data not shown), suggesting that *crbi* may promote balanced increases in the rates of cell growth and division as observed in core SWH mutants [83]. Thus the ability of multiple SWH pathway alleles to modify the *en>crbi* phenotype correlates with elevated Yki activity and with SWH-like phenotypes in *en>crbi* larval wing discs.

The Notch receptor interacts with the SWH pathway in certain tissues [147, 158, 159] and is regulated by *crb* in certain developmental contexts [141]. The effect of *Notch* heterozygosity on *en>crbi* PCR could not be reliably measured due to

significant wing-notching (data not shown). However expression of *crbi* had no significant effect on the Notch reporter *E(spl)mb-CD2* reporter [160] (Figure 3.3A-B) or expression of the Wg and Cut proteins at the dorsal/ventral margin of the wing (data not shown). Notch protein localization and levels in wing cells were also unaffected by expression of *crbi* (Figure 3.3C). Clonal loss of *crb* in the eye disc also did not affect *E(spl)mb-CD2* expression (Figure 3.3D). Thus, the *crbi*-induced changes in Yki activity do not coincide with detectable changes in Notch abundance, localization, or transcriptional induction of a Notch pathway reporter.

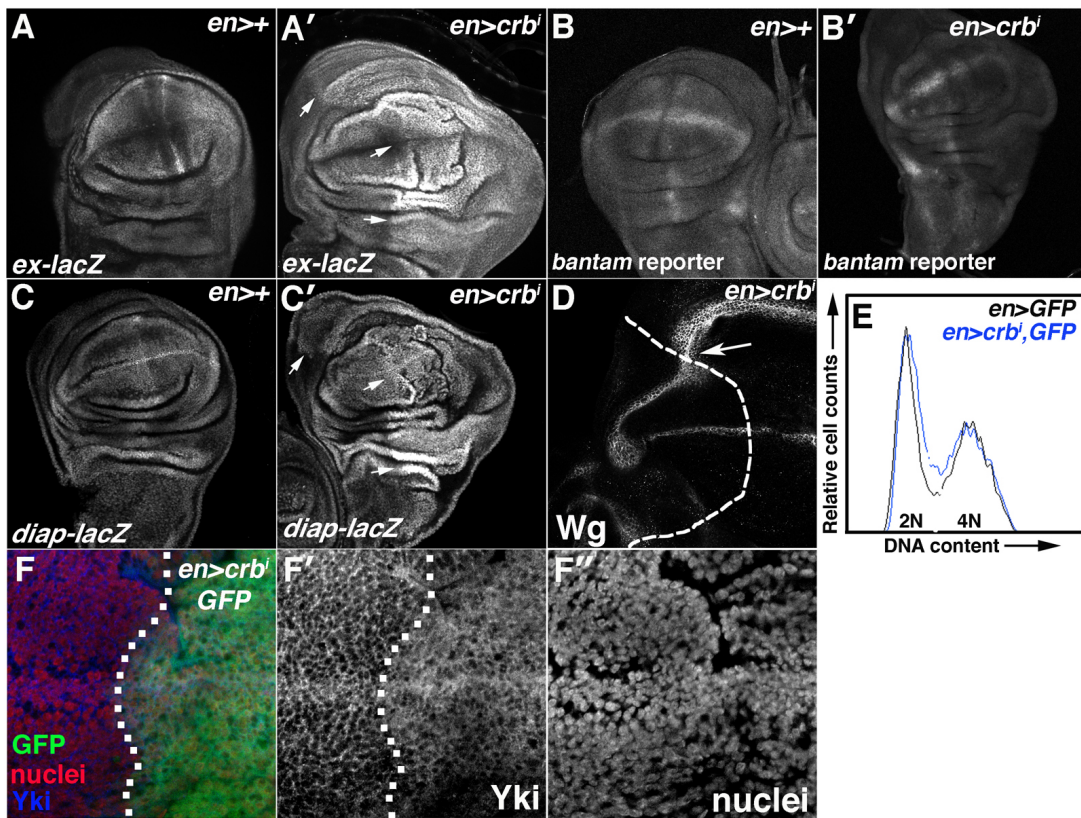


Figure 3.2. *crb¹* elevates Yki-activity. α - β -gal staining or GFP fluorescence in wing discs carrying (A) *ex-lacZ*, (B) *ban-GFP*, or (C) *diap1-lacZ* in the background of (A,B,C) *en>+* or (A',B',C') *en>crb¹*. Arrows in A' and C' highlight elevated *ex-lacZ* and *diap1-lacZ* expression. (D) a-*Wg* stain in *en>crb¹* wings discs (posterior = right of dashed line). (E) FACS-analysis of *en>GFP* (black) and transgenic *en>crb¹,GFP* (blue) wing discs. (F) Co-staining for Yki (blue) and HP1 (nuclei; red) in *en>crb¹,GFP* discs (posterior = right of dotted line).

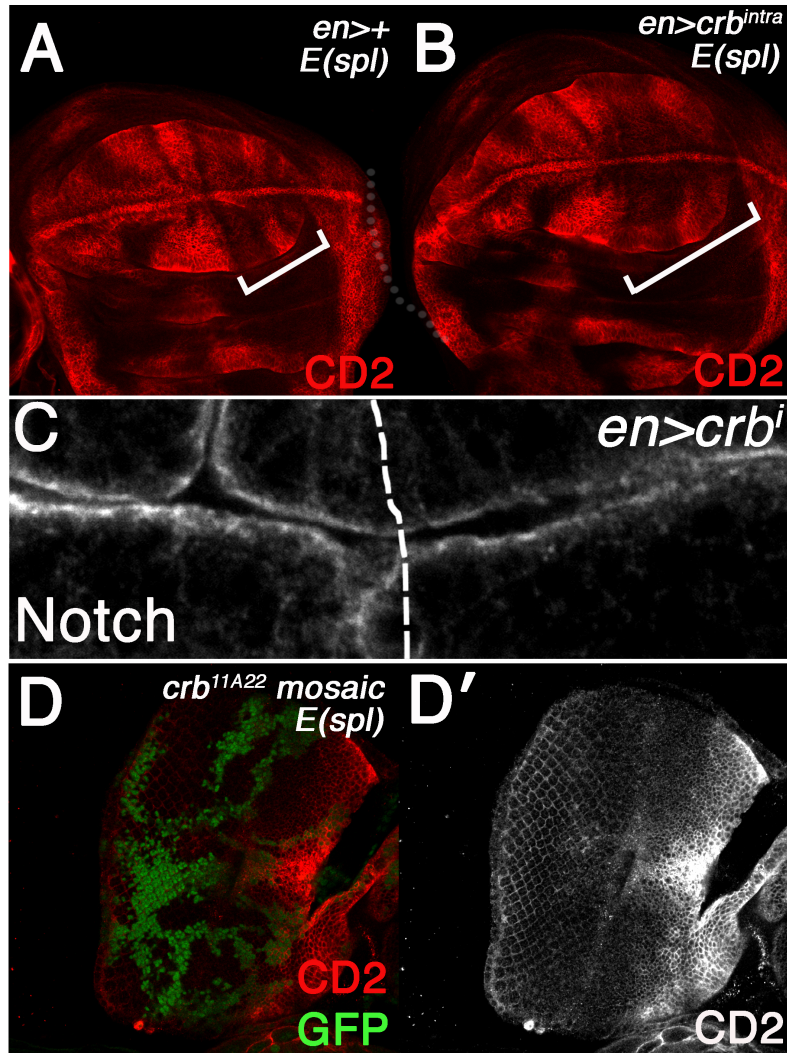


Figure 3.3. *crbi* does not effect Notch activity and localization. Activity of the Notch reporter *E(spl)m-b-CD2* in (A) *en>+* and (B) *en>crbi^{intra}* wings, and in (D) *crb^{11A22}* mosaic eye discs as assessed by a-CD2 staining (red). (C) Confocal images of and Notch in *en>crbiⁱ* larval wing discs. Posterior compartments are to the right of the dashed line.

***crbi* downregulates Ex protein levels in wing disc cells**

The localization of Crb to the apical membrane and apicolateral junctions of disc epithelial cells [33] suggests that expression of *crbi* might affect the activity of SWH proteins that also localize to these same domains. No significant alterations were noted in the levels and localization of either Fat or Merlin (Mer), two apically localized SWH regulators, in *en>crbi* wing discs (Figure 3.4A,B). Moreover, the Fat reporters *dachs-V5* (data not shown) and *four jointed-lacZ* [161] are unaltered in *en>crbi* wing discs (Figure 3.5A,B), and RNAi-knockdown of the palmitoyltransferase *approximated* (*app*), which is required for the overgrowth of *ft* mutant cells [162], did not suppress the *crbi*-driven enlarged wing phenotype (Figure 3.5C). Thus, *crbi* does not appear to control wing growth via a *ft*-dependent pathway. By contrast, the apical SWH regulator Ex is depleted from the apical membrane of *crbi*-expressing cells (Figure 3.6A-A’’). In parallel, expression of *en>crbi* leads to a drop in overall levels of Ex detected by immunoblot analysis (Figure 3.6D). The adherens junction (AJ) protein Armadillo was unaffected by *crbi* expression (Figure 3.7), indicating that the effect on Ex is not due to a general loss of AJ complexes in *en>crbi* cells.

As transcription of *ex-lacZ* is elevated in *en>crbi* discs, *crbi* thus appears to promote post-transcriptional down-regulation of Ex. A similar effect occurs in S2 cells expressing Ex from the constitutively expressed *pAct* plasmid [157]: Ex levels are reduced following induction of a *crb* transgene expression from the inducible *pMt* plasmid [163] (Figure 3.6E-F). Re-expression of Ex from a *UAS-ex* transgene is

also sufficient to revert the *en>crbⁱ* PCR phenotype (Figure 3.6B,C). In view of this link between Crb overexpression and Ex loss, it is notable that the array of phenotypes produced by *crbⁱ* overexpression are quite similar and those associated with the *ex* alleles in the intact organism (Figure 3.8), including large wings lacking posterior cross veins, small eyes with reduced numbers of ommatidia [156], a delay in morphogenetic furrow (MF) progression in the ventral portion of the eye disc and an ectopic MF produced dorsally [164], and an increase in the number of interommatidial cells in the pupal eye disc [157]. Thus, while it is likely that the intracellular tail of Crb has effects on additional cellular pathways, these phenotypic similarities indicate that a significant subset of the effects of Crbⁱ activity on developing tissues may be mediated via Ex.

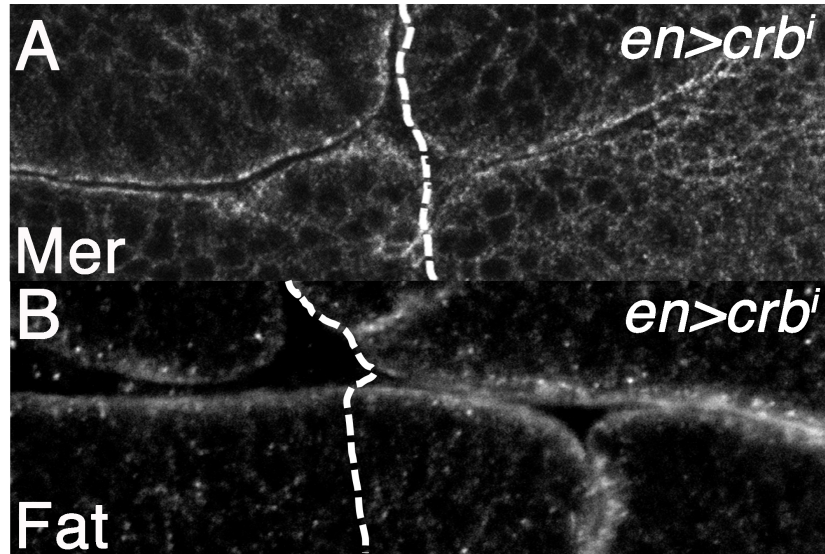


Figure 3.4. *crbi* does not effect the levels and localization of Mer and Fat. Confocal images of Mer (A) and Fat (B) in *en>crbi* larval wing discs. Posterior compartments are to the right of the dashed line.

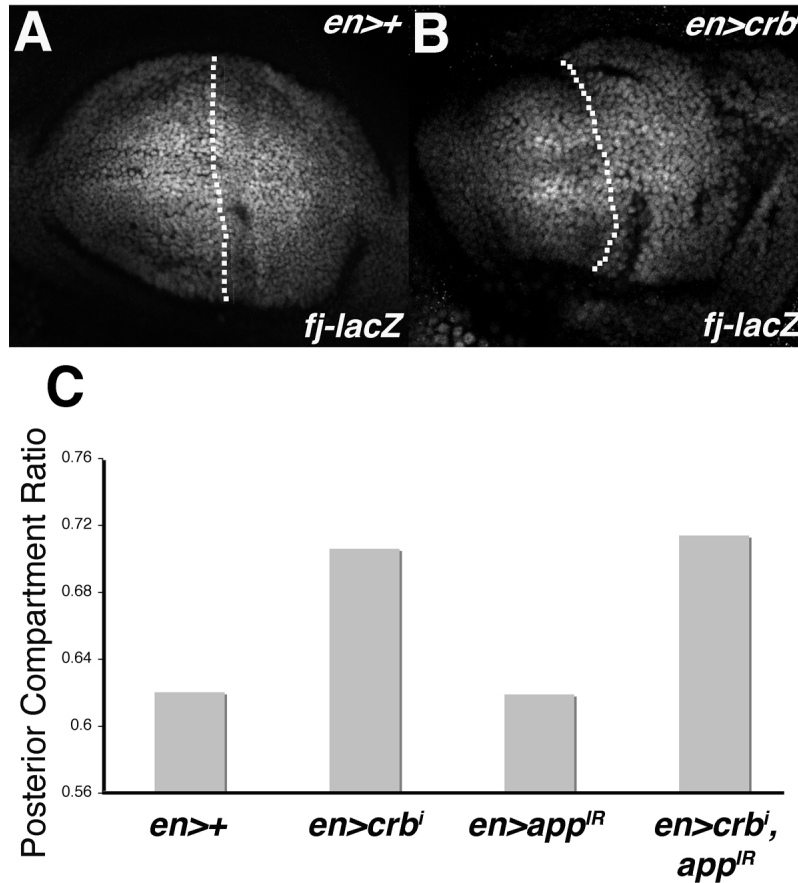


Figure 3.5. Excess Crb does not alter or require Fat pathway activity. Anti- β -gal staining to detect the Fat-pathway reporter *fj-lacZ* in (A) *en>+* and (B) *en>crbⁱ* wing discs. (C) Quantitative analysis of the posterior compartment ratio in indicated genotypes. A minimum of 10 wings was counted per genotype. No statistical difference was observed between *en>crbⁱ* and *en>crbⁱ,app^{IR}* posterior compartment ratios.

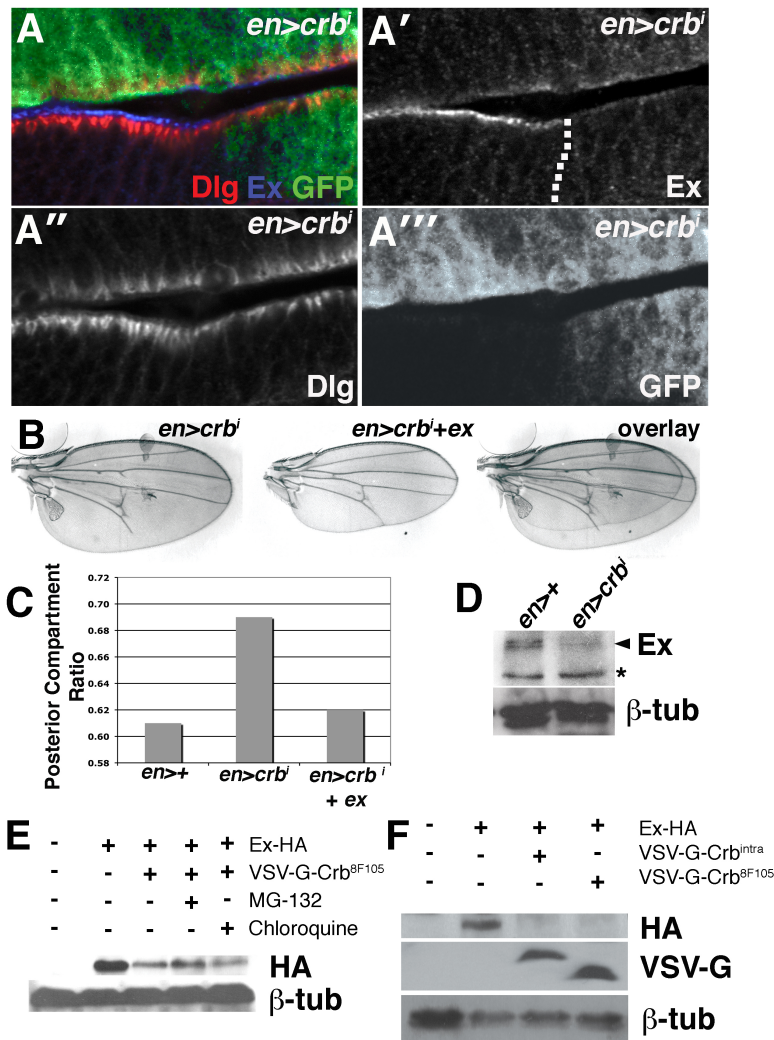


Figure 3.6. *crbⁱ* downregulates Ex levels. (A-A''') Lateral section of *en>crbⁱ,GFP* wing disc co-stained for Dlg (red) and Ex (blue). Dotted line denotes A:P boundary. (B) Images and overlays of *en>crbⁱ* and *en>crbⁱ,ex* wings. (C) PCR in the indicated genotypes. (D) Immunoblot of Ex in *en>+* and *en>crbⁱ* wing discs. Arrowhead denotes Ex based on comigration with overexpressed Ex (not shown) (* = non-specific band). Lower panel is a-b-tub loading control. (E) Immunoblot of HA-Ex in *Crb^{8F105}*-expressing cells treated with the MG132 (lane 4) or chloroquine (lane 5). (F) Corresponding a-HA, a-VSV-G, and a-b-tub immunoblots of S2 cells expressing

HA-Ex from the *pAct-HA-Ex* plasmid (lanes 2-4), and VSV-G-tagged forms of either *crbi* (lane 3) or *crb^{8F105}* (lane 4) from the *pMT* plasmid.

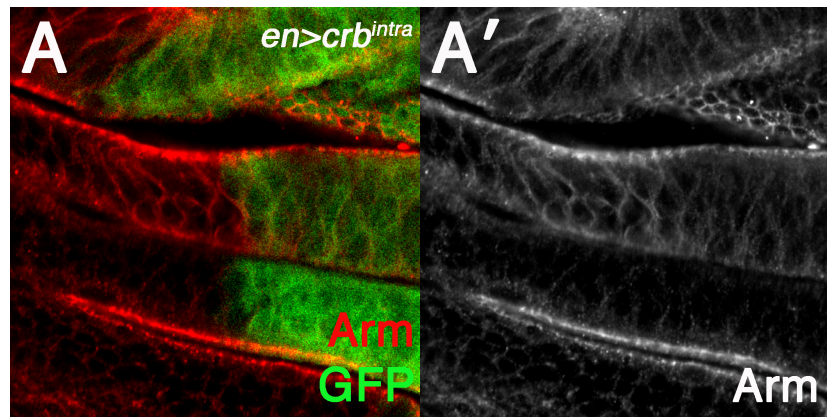


Figure 3.7. Arm protein is not altered in *en>crbⁱ* wing discs. Lateral confocal section of *en>crbⁱ;GFP* wing disc stained with anti-Arm to visualize AJs.

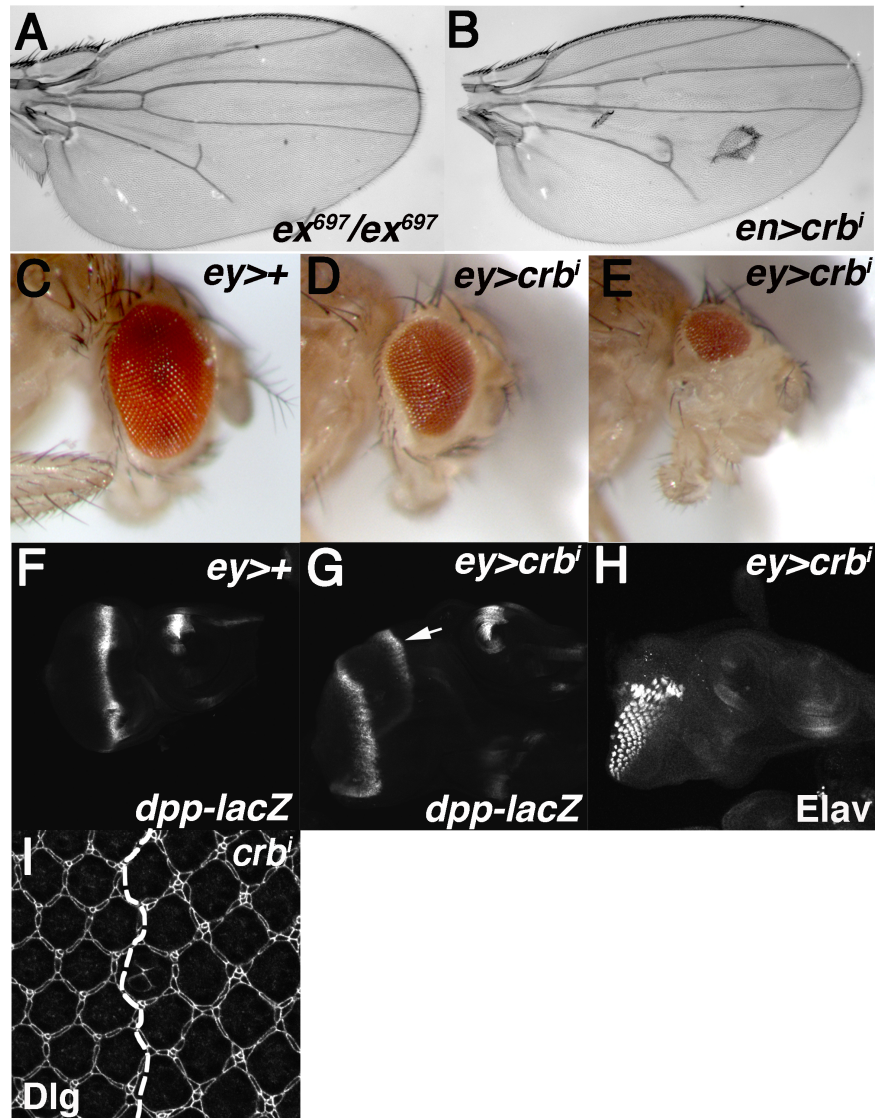


Figure 3.8. Expression of *crb1* phenocopies loss of *ex*. Representative images of adult wings of (A) *ex*⁶⁹⁷/*ex*⁶⁹⁷ and (B) transgenic *en>crb1* flies and adult eyes taken from control (C) *ey>+* and (D-E) *ey>crb1* flies. a-b-gal staining of (F) *ey>+* and (G) *ey>crb1* larval eye discs to visualize the MF marker *dpp-lacZ*. Arrow in G indicates ectopic furrow formation. (H) Expression for the neuronal marker Elav in *en>crb1* eye discs. (I) Confocal image of a-Dlg staining to mark apical cell profiles, in 48hr pupal discs. Image captures a boundary between normal cells and a MARCM-

generated *crbi*-expressing clone (right of dotted line). Note the excess interommatidial cells in the *crbi*-overexpressing clone as first reported by [165].

The Crb juxtamembrane domain regulates Ex

The 37 amino acid intracellular tail of Crb contains two functional motifs that are conserved across Crb proteins in multiple species: (i) the 15-amino acid juxtamembrane FERM-binding motif (JM), which mediates a direct interaction with the FERM-domain protein Yurt, and indirectly interacts with DMOesin (DMoe) and β_H -spectrin to link Crb to the underlying actin/spectrin cytoskeleton, and (ii) the C-terminal PDZ-binding motif (PBM), which is composed of the last 4 residues of the Crb tail (ERLI) and directs interactions with Sdt and Patj to form a polarity regulatory module commonly referred to as the Crb complex [34]. In order to better understand the mechanism whereby *crbⁱ* downregulates Ex and activates Yki, we used several previously utilized *crb* transgenes (Figure 3.9J) that inactivate either the JM domain or the PBM within the Crbⁱ protein [166] and assessed their ability to (i) increase wing size, (ii) activate Yki signaling, and (iii) eliminate apical Ex. Overexpression of a construct lacking the PBM, but maintaining the JM, increases PCR among adult wings to a similar degree as the intact *crbⁱ* transgene (Figure 3.9B,G). Expression of *crb-JM* also depletes apical Ex (Figure 3.9I) and increases Yki activity as detected by the *ex-lacZ* reporter, particularly in the pouch region of the wing disc (Figure 3.9B'). *crb-JM* thus phenocopies *crbⁱ* in its effects on Ex and on SWH pathway activity. By contrast, a construct containing the PBM and inactivating mutations within the JM (*crb-PBM*) does not increase PCR or significantly elevate *ex-lacZ* expression (Figure 3.9C-C',G), and has no effect on apical Ex (Figure 3.9H). Expression of *crb-PBM* did disrupt organization of the disc epithelium (Figure 3.10A-B) and wing morphology (Figure 3.9C-C') in a way not observed with *crb-JM*,

indicating that the failure of the *crb-PBM* transgene to affect Ex is not due to a general lack of biological activity. A construct lacking intact JM and PBM domains (*crb $\Delta\Delta$*) had no effect on wing size, structure or *ex-lacZ* (Figure 3.9D-D').

A similar link between the Crb JM domain and Ex was observed in S2 cells. Expression of either VSV-G-tagged Crbⁱ or VSV-G-tagged Crb^{8F105}, which contains a stop codon that prevents the translation of the last 23 amino acids (including the PBM) while preserving much of the JM [163], is sufficient to downregulate co-expressed Ex (Figure 3.6E-F). Treatment with the proteasome inhibitor MG132 was able to partially reverse this effect, whereas treatment with the lysosomal inhibitor chloroquine did not (Figure 3.6E). In parallel experiments in intact wing discs, *crbⁱ* is able to deplete levels of an Ex:GFP fusion protein [155] (Figure 3.11A). Genetic reduction of proteasome activity with a dominant-negative allele of the proteasomal subunit *Pros2 β* [167] also elevates levels of Ex:GFP levels in normal wing disc cells and partially restores Ex:GFP levels in discs that also express *crbⁱ* (Fig. 3.11A). Expression of *crbⁱ* did not stimulate endolysosomal routing of Ex:GFP as measured by the effect of treatment with the lysosomal inhibitor chloroquine on Ex:GFP localization (Figure 3.12). Thus, it appears that Ex protein levels are antagonized by the proteasome, and that blocking proteasome activity can retard the effect of Crbⁱ on Ex, although the rescue of *crbⁱ* PCR by *UAS-ex* (see Figure 3.6B) suggests that this mechanism cannot completely overcome the ability of overexpressed Ex to rescue PCR. Moreover, as in disc cells, the PBM domain is dispensable for the down-regulation of Ex in S2 cells, while constructs that retain the JM also retain the ability to regulate Ex.

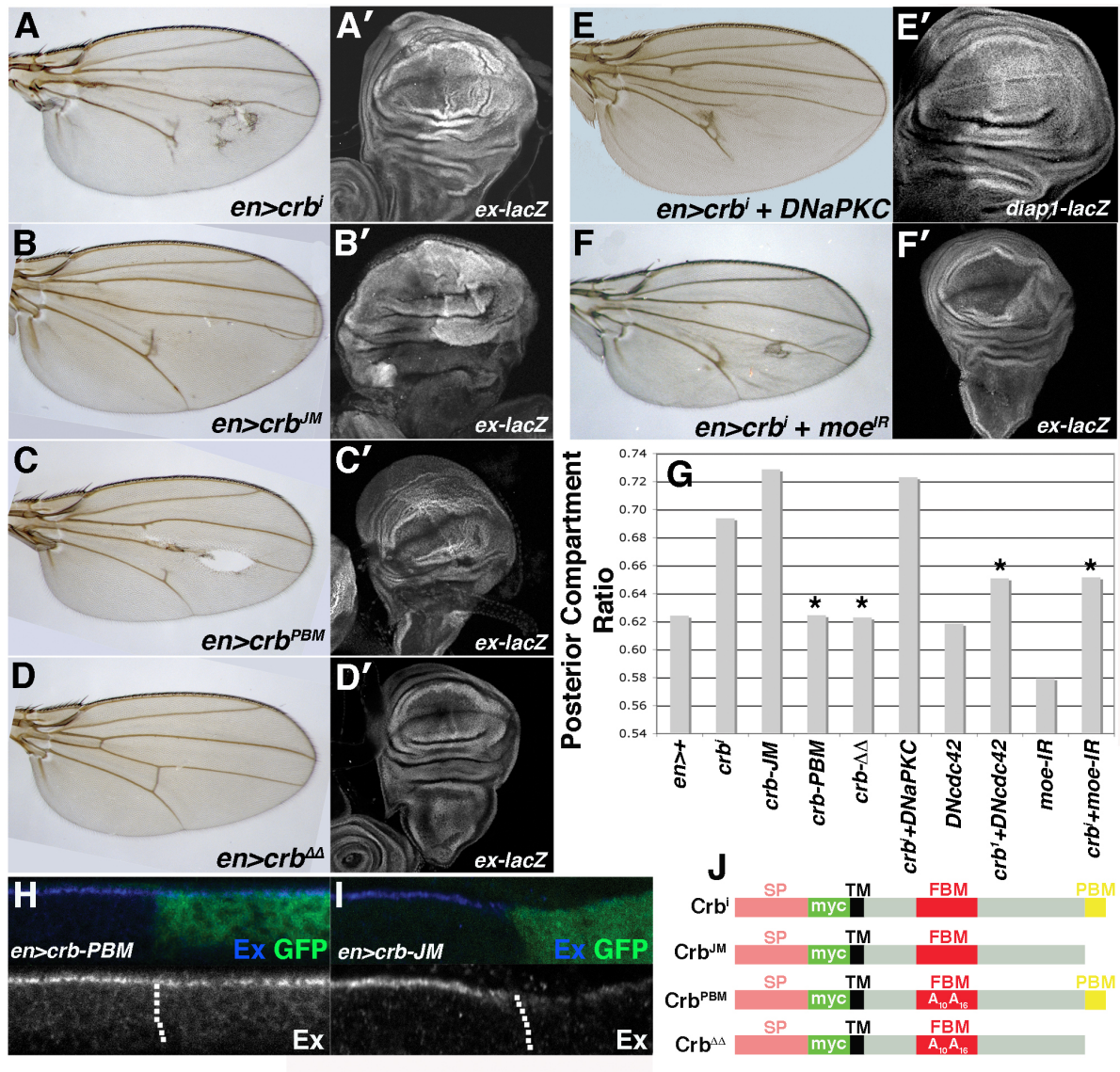


Figure 3.9. The Crb-JM controls Ex levels and Yki activity. Paired light microscopic (A-F) and confocal images of a-b-gal staining to detect activity of the *ex-lacZ* transgene (A'-D',F') or *diap1-lacZ* (E') in the indicated genotypes. (G) PCR values in the indicated genotypes. (* $p < 0.05$ compared to *en>crbⁱ*). a-Ex (blue) staining in (H) *en>crb-PBM,GFP* and (I) *en>crb-JM,GFP* wing discs. Dotted line marks the A:P boundary. (posterior = right). Cartoon of *crb* transgenes; signal peptide (SP), myc tag (Myc), transmembrane domain (TM), juxtamembrane FERM-binding motif

(JM), PDZ-binding motif (PBM), and amino acid substitutions are indicated [adapted from 168].

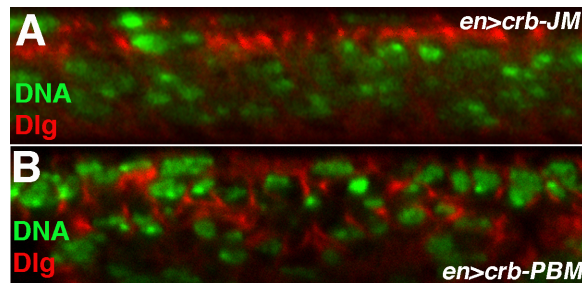


Figure 3.10. Tissue architecture of Crb-JM and Crb-PBM wings discs. Lateral image of nuclei (green) and Dlg (red) in posterior domain of (A) *en>crb-JM* and (B) *en>crb-PBM* wing discs. Apical is orientated up.

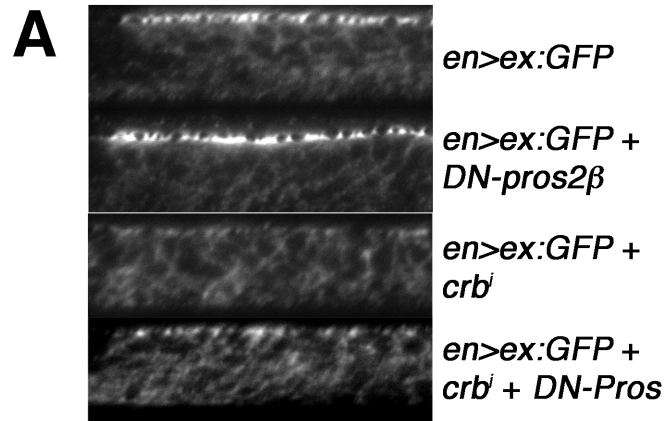


Figure 3.11. Crbⁱ-driven loss of Ex is sensitive to the activity of the proteasome.

Lateral images of Ex:GFP in the posterior region of the wing pouch in the indicated genotypes.

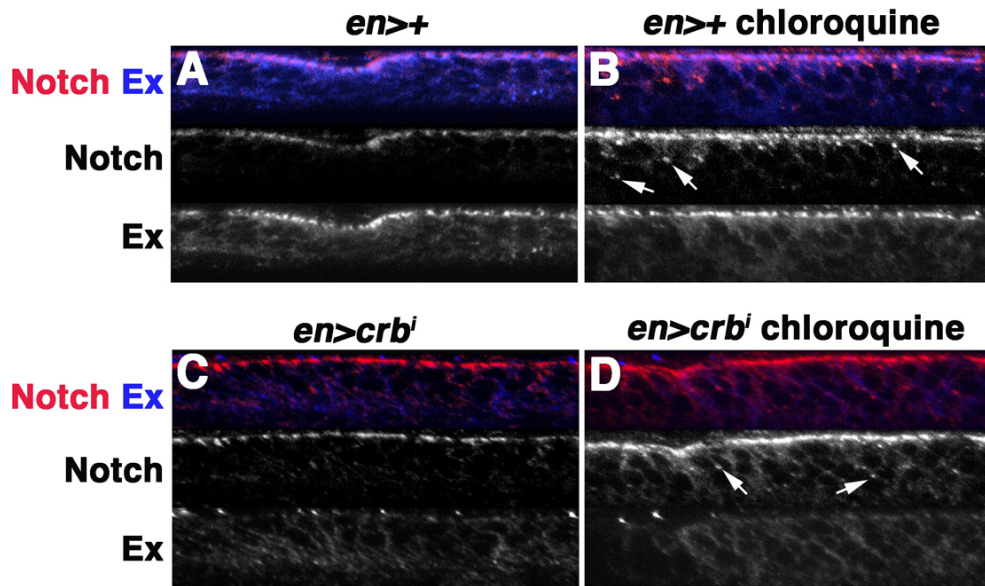


Figure 3.12. Loss of Ex following expression of Crbⁱ is not accompanied by routing of Ex:GFP into a chloroquine-sensitive lysosomal compartment. Lateral optical images of (A-B) *en>+* or (C-D) *en>crbⁱ* larval wing discs either (A,C) untreated or (B,D) treated with chloroquine and stained for Notch (red) or Ex (blue). Arrows in (B) and (D) denote intracellular Notch-positive puncta.

Effects of *crb* loss on Ex protein

The effect of *crbⁱ* on Ex suggests that under physiologic conditions *crb* might be required to restrict accumulation of Ex protein. Consistent with this, cells homozygous for the *crb^{11A22}* allele, which reduces endogenous Crb protein to background levels (Figure 3.13A-A'), show elevated Ex levels (Figure 3.13B-C) with no change in *ex-lacZ* expression (Figure 3.13D). A similar effect occurs in *crb^{11A22}* wing clones (Figure 3.13K). Levels and localization of the Dlg, Arm, and Mer protein are not affected by the *crb^{11A22}* allele (Figure 3.14), confirming that the effect of *crb* loss on Ex is fairly specific. Optical sections through the apical and basal planes of the eye disc indicate that while a portion of the excess Ex in *crb^{11A22}* localizes apically, a portion also drops more basally (Figure 3.13B',C'). Lateral sections through *crb^{11A22}* eye and wing clones confirm that Ex accumulates in a linear manner along what appears to be the basolateral membrane of cells (Figure 3.13I-I', J-J'). Since the excess Ex that accumulates in core SWH mutants remains at the apical domain [e.g. 157]), this Ex 'basal spreading' phenotype is not a secondary effect of elevating Ex levels in *crb* cells, but rather appears to reflect a role for *crb* in localizing Ex.

Site specific alleles support a role for the JM domain in the Ex-inhibitory role of *crb*: cells homozygous for the *crb^{8F105}* allele, which lacks the C-terminal PBM and the preceding 19 amino acids but maintains a largely intact JM [169], show a more mild effect on Ex levels than the *crb^{11A22}* allele (Figure 3.13F-F'). This weaker phenotype could be due to a role for the PBM region in regulating the Ex-regulatory

function of the JM, or to the loss of additional sequences between the JM and PBM that affect protein stability or function. The *crb^{8F105}* allele has been reported to reduce Crb levels and alter Crb protein distribution in embryonic epithelial cells [170] but no differences in Crb protein were detected in *crb^{8F105}* clones (Figure 3.13E-E'). To more finely map the sequences within Crb that are required to restrict Ex in vivo, a genomic *crb* allele carrying three missense mutations in the JM region (*crb^{Y10AP12AE16E}*) [5] was tested for its effect on Ex. While the *crb^{Y10AP12AE16E}* allele has no obvious effect on Crb levels or localization (Figure 3.13G-G'), it did elevate Ex levels in cells (Figure 3.13H-H'). Thus amino acids in the Crb JM are both necessary and sufficient to restrict Ex levels in vivo.

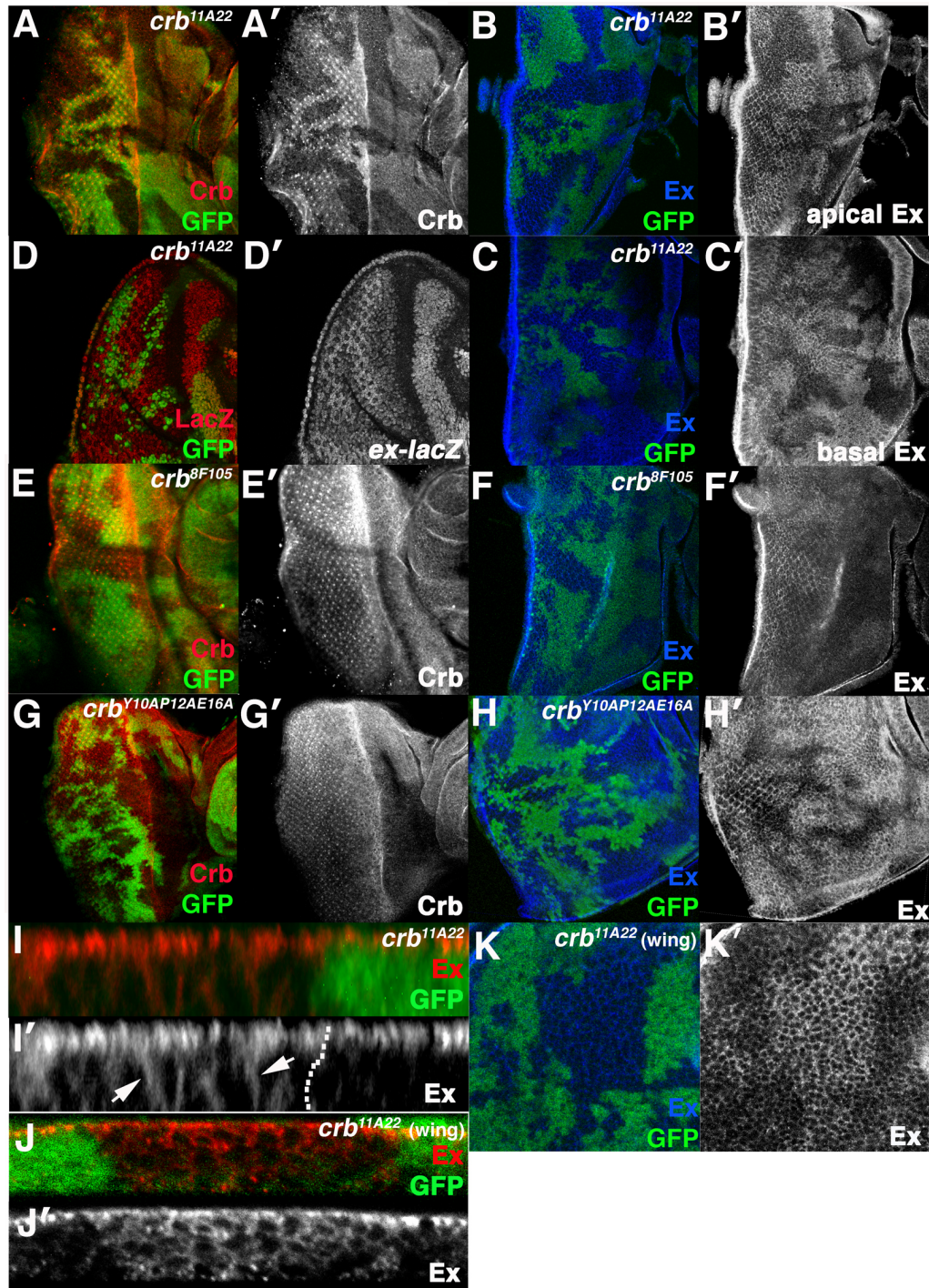


Figure 3.13. Effect of *crb* loss on Ex in disc cells. Confocal images of *crb*^{11A22} (A-D, I-K), *crb*^{8F105} (E-F), or *crb*^{Y10AP12AE16A} (G-H) clones in the eye (A-I) or wing (J-K) stained for Crb (A,E,G), Ex (B,C,F,H-K). (B) and (C) are apical and basal planes of the

same disc. Arrowheads in (I) denote excess Ex in *crb*^{11A22} cells that fails to localize apically. Disc in (I) is imaged through apical portion of epithelium; disc in (J) is imaged through entire epithelium. (D) α - β -gal staining to detect activity of the *ex-lacZ* transgene in *crb*^{11A22} eye clones.

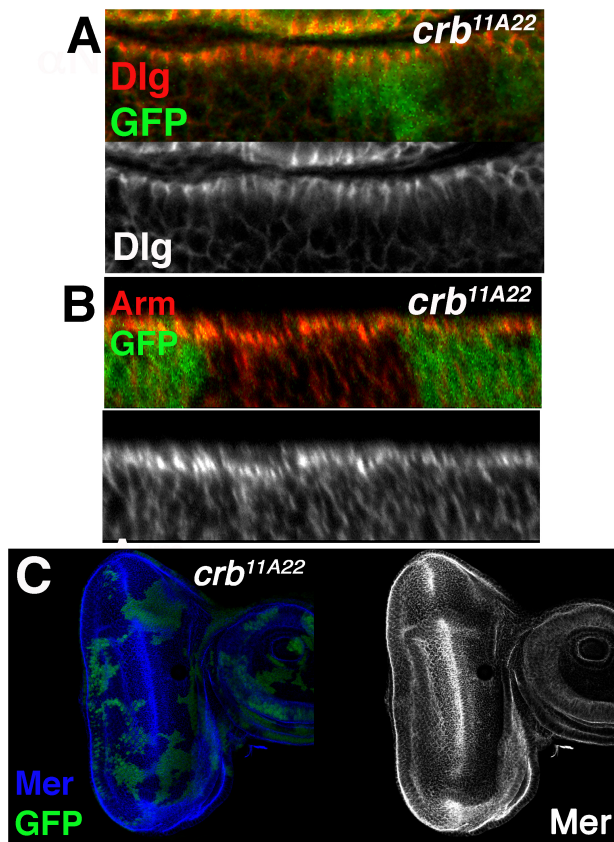


Figure 3.14. Dlg, Arm and Mer protein expression is unaffected in *crb^{11A22}* clones. Merged confocal sections of *crb^{11A22}* mosaic eye discs stained for (A) Dlg, (B) Arm, and (C) Mer. Mutant *crb^{11A22}* clones are marked by the absence of GFP (green).

Modification by Crb-interacting factors

The Crb JM interacts directly with the FERM-domain protein Yurt [171] and indirectly with the FERM-domain protein DMoe [163], both of which are structurally related to Ex. Although no evidence was found of a stable interaction between the Crb and Ex (see Discussion), genetic data suggest that the *DMoe* plays a role in the link between Crb and SWH activity. RNAi knockdown of *DMoe* [172] in *en>crbⁱ* discs suppressed both enlarged PCR (Figure 3.9F,G) and *ex-lacZ* expression (Figure 3.9F'), but did not rescue the drop in endogenous Ex induced by *crbⁱ* (Figure 3.15A) and had no independent effect on Ex:GFP (Figure 3.15B). Although this effect could be due to a non-specific effect of *DMoe* loss, the ability of *DMoe-IR* to uncouple Ex loss from Yki activation in *crbⁱ*-expressing cells argues that DMoe may play a more specific role downstream of Ex in a Crb/Ex pathway, or that DMoe acts in a parallel pathway that converges on Yki.

The Crb cytoplasmic tail is phosphorylated by the *Drosophila* atypical protein kinase C (*DaPKC*), a component of the Par complex that regulates polarity and endocytosis [25]. These modifications are thought to be involved in the ability of Crb to in turn participate in the establishment of epithelial polarity. As in these prior studies, a dominant-negative *DaPKC* transgene effectively suppressed the cuticular disorganization of *en>crbⁱ* wings (Figure 3.9E). However, it did not change *en>crbⁱ* PCR (Figure 3.9G), rescue the drop in Ex protein (Figure 3.9C-C''), or prevent induction of *diap1-lacZ* (Figure 3.9E'). By contrast, a transgene encoding a dominant-negative form of the GTPase Cdc42 (*dn-cdc42*) [173], whose effectors

include the Crb- and aPKC-interactor Par6, was an efficient suppressor of *en>crb* posterior compartment growth (Figure 3.9G). This variable effect could be due to differences in transgene strength or to functional differences between *aPKC* and *cdc42*, as observed in other studies [174]. Notably, the *dn-cdc42* allele is able to suppress the *crb-JM* PCR phenotype (Figure 3.15F), indicating either that Cdc42 can act on the Crb tail independent of the PBM, or that Cdc42 acts by a distinct pathway to control wing size.

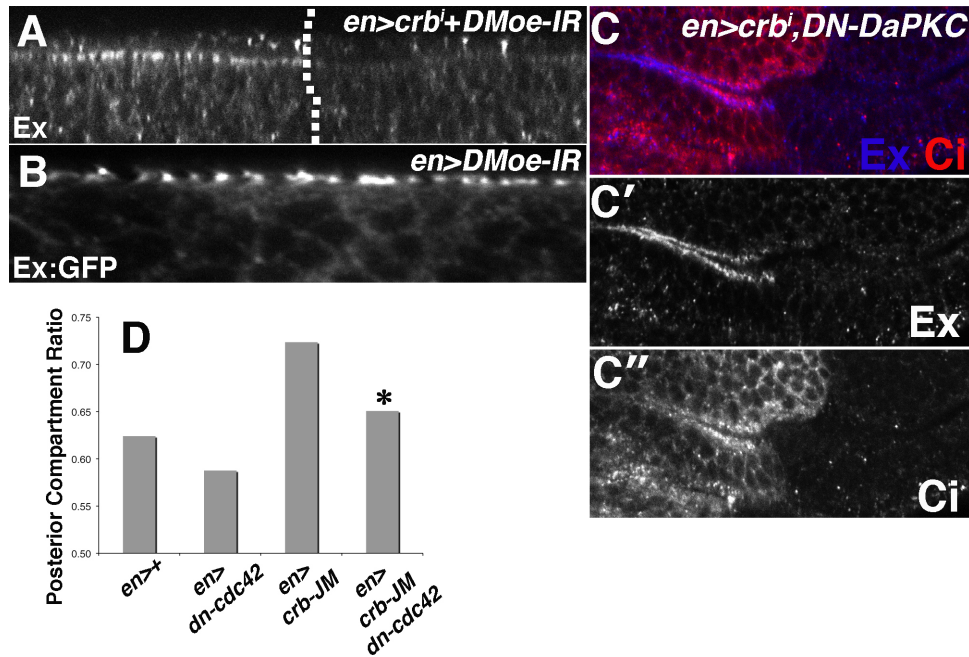


Figure 3.15. Functional interactions with putative Crb interactors. (A) Lateral image of endogenous Ex protein in an *en>crbⁱ+DMoe-IR* disc. Note absence of Ex in posterior to the right of the dotted line. (B) Ex:GFP fusion protein in posterior domain of an *en>DMoe-IR* disc. (C) Confocal image of an *en>crbⁱ,DN-DaPKC* larval wing disc stained for Ex (blue) and Ci (red) to mark the boundary between Ci-positive anterior cells and Ci-negative posterior cells that express the *crbⁱ* transgene. (D) Quantitative analysis of the PCR in indicated genotypes. A minimum of 10 wings was counted per genotype. Asterisk denotes a statistically significant interaction between *dn-cdc42* and *crb-JM* relative to controls as determined by two-way ANOVA analysis.

Effect of excess Ex in *crb* mutant cells

As transgenic overexpression of *ex* is growth-suppressive [155, 175], the excess Ex in *crb* mutant cells might be predicted to reduce Yki activity. However, RNAi knockdown of *crb* do not suppress organ overgrowth driven by a *UAS-yki:YFP* transgene [176] but rather enhanced them (Figure 3.16A-C). Expression of *diap-lacZ*, a sensitive readout of Yki activity [88], is also elevated in *crb^{11A22}* cells posterior to the MF (Figure 3.17A); DIAP1 protein shows a similar pattern in *crb^{11A22}* and *crb^{Y10AP12AE16A}* clones (Figure 3.17B-C). *crb^{11A22}* and *crb^{Y10AP12AE16A}* cells also display a clonal growth advantage in the eye relative to both control and *crb^{8F105}* chromosomes (Figure 3.16D-G). Thus, mutations in the JM are sufficient to deregulate DIAP1 levels and to confer a growth advantage in vivo. Moreover, the *crb^{11A22}* allele acts as a dominant enhancer of the increased wing-size phenotype associated with the *ex⁶⁹⁷* hypomorphic allele (Figure 3.17D-E), arguing that at a genetic level *crb* normally promotes *ex* activity, and that the effect of *crb* loss on Ex levels and localization may compromise signaling through the SWH pathway.

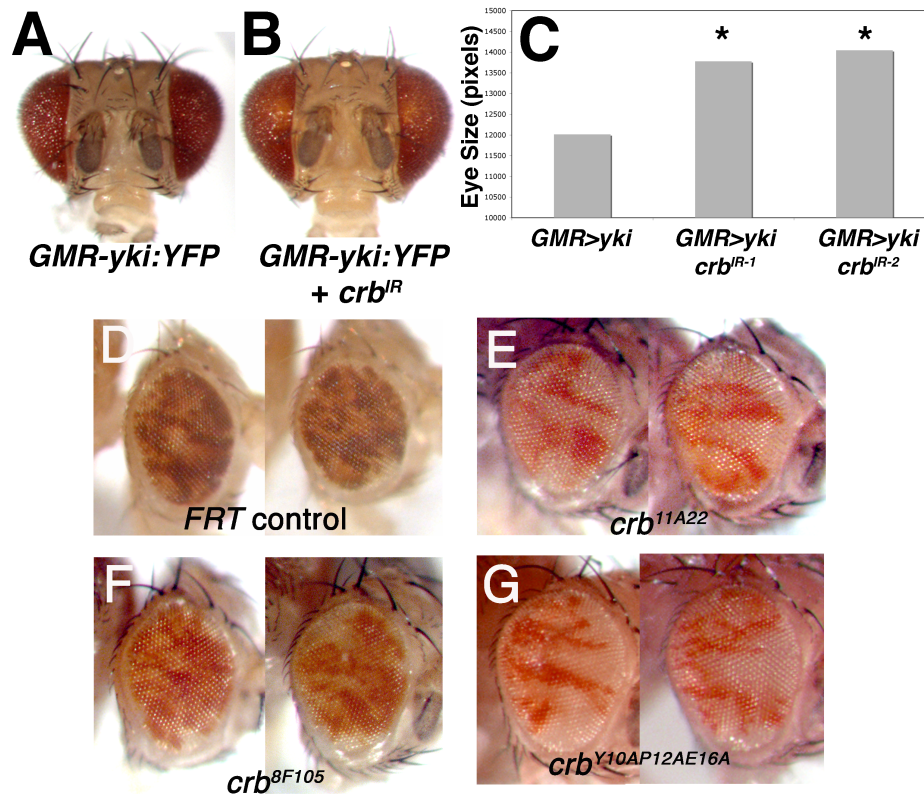


Figure 3.16. Growth phenotypes associated with loss of Crb. Representative images of (A) *GMR>yki:YFP* and (B) *GMR-yki:YFP,crb^{IR-2}* adult heads (images to scale), and (C) quantification of *en face* adult female eye size of *GMR>yki:YFP*, *GMR-yki:YFP,crb^{IR-1}*, and *GMR-yki:YFP,crb^{IR-2}* flies (minimum of 10 eyes was analyzed per genotype; Asterisk: $p < 0.05$ compared to *GMR>yki:YFP* eyes). Representative images of (D) *FRT82B*, (E) *FRT82B,crb^{11A22}*, (F) *FRT82B,crb^{8F105}*, and (G) *FRT82B,crb^{Y10AP12AE16A}* adult mosaic eyes. Mutant tissue is marked by the absence of pigment (red).

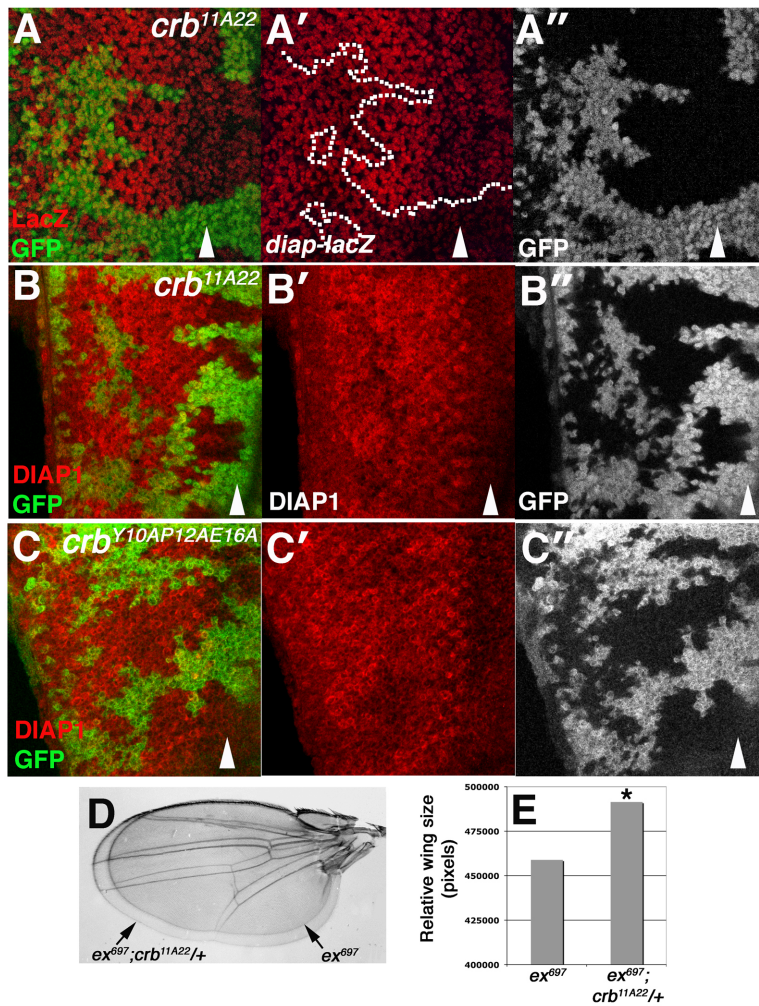


Figure 3.17. *crb* alleles interact with *ex* and elevate DIAP1 expression posterior to the furrow. Images of (A-B) *crb*^{11A22} or (C) *crb*^{Y10AP12AE16A} clones (lacking GFP) in larval eye discs stained with (A) α - β -Gal to detect *diap1-lacZ* (red) or (B-C) α -DIAP1 (red). Arrowheads denote position of the MF. (posterior = left). Dotted line in (A) highlights a *crb* clone that projects posterior to the MF and expresses elevated *diap1-lacZ*. (D) Optical overlay and (E) size adult wings of the indicated genotypes. (* $p < 1.5 \times 10^{-7}$ relative to *ex*⁶⁹⁷ wings).

DISCUSSION

Crb as dual regulator of polarity and growth

Crb nucleates apical membrane formation in the embryonic epidermis and other epithelial cell types in *Drosophila*. It exerts these effects primarily through two motifs in its intracellular tail: the C-terminal PBM and the juxtamembrane FERM-binding motif (JM). We find that Crb also acts as a peripheral regulator of the SWH pathway in larval discs via a previously unappreciated role for the JM domain in controlling levels of the Ex protein. Known peripheral regulators of the SWH pathway modulate signaling in response to upstream inputs including planar cell polarity pathways, morphogen gradients, and adhesion molecules [177]. Our data extend this theme by suggesting that Crb may serve as an interface between apicobasal polarity signals and the SWH pathway. Overexpression and loss of *crb* have opposing effects on Ex levels, and sequences in the Crb JM are both necessary and sufficient to control Ex *in vivo*. The ability of the Crb-JM to deplete Ex from cells suggests that mutations in endocytic genes that block Crb turnover and produce dramatic tissue disorganization and overgrowth (e.g. *avl* and *ept/tsg101*) [31, 118] may elicit their phenotypes in part via effects on Ex and SWH signaling. Indeed, *vps25* mutants have been shown to downregulate Ex levels [178]. A more complete analysis of the role of Crb and Ex in endocytic tumor mutants is required to understand this link more fully.

The link between *crb* loss and *diap1* expression is at present not clear. Since localization has been suggested to be an important determinant of Ex function

[155], our finding that a portion of the excess Ex found in *crb* cells is displaced basally suggests that the function of this fraction of Ex may be somehow altered or compromised. Prior work showing that loss of the tumor suppressor *ft* can also mislocalize Ex and compromise its function [14, 179, 180] provides precedent for this type of effect, but does not provide insight into what aspect of Ex function might be affected by *crb* loss. Moreover, since *ft* alleles elicit far stronger effects on Yki activity than do *crb* alleles, the consequences of Ex defects in each background would appear to be quite different. Future analysis of the effect of *crb* loss on the biochemical properties and subcellular localization of Ex may provide insight into this issue.

Ex stability appears to correlate inversely with expression of the Crb JM region, which is known to interact with FERM-domain proteins that are structurally similar to Ex. Attempts to detect a physical interaction between Ex and the Crb intracellular tail using multiple techniques have not been successful (BSR and KHM; unpub.). While this does not preclude a Crb:Ex complex, it does suggest that Crb controls Ex via unidentified intermediates. The modular structure of the Crb protein raises the possibility that factors that interact with the intracellular and extracellular portions of the intact protein may modulate the JM-dependent regulation of Ex. If so, then Crb-dependent changes in Ex levels might couple SWH activity to both changes in intracellular signals as cells begin to polarize their membranes, and to variations in extracellular adhesion during developmental tissue morphogenesis and wound repair. Given the ability of SWH pathway alleles to confer a proliferative advantage in cell competition scenarios [181], it may be that

crb that plays a more significant role as a SWH regulator in these types of regenerative and homeostatic growth regulatory programs. Major goals of future studies will therefore be to identify the precise mechanistic details of how Crb controls Ex, and how the intrinsic Ex-regulatory activity of the JM domain is linked to other functional domains of the Crb molecule.

The differential effect of the Crb-JM and Crb-PBM on growth and tissue architecture appears to conflict with a requirement for the JM in rescue of polarity defects in *crb* mutant embryos [166]. However, this is not without precedent [168] and may be explained by the well-documented differences between the roles of Crb in the embryonic epidermis and disc epithelium: loss of Crb disrupts the polarity of embryonic ectoderm and compromises tissue integrity [33], whereas loss of Crb in larval discs has minimal effect on the architecture, polarity, or organization of undifferentiated cells [122].

***crb* as a growth suppressor**

In addition to the circumstantial evidence of a growth advantage conferred by *crb* alleles, recent work has shown that reduced expression of the murine *crb3* gene, a homolog of *Drosophila crb*, can promote tumorigenicity of kidney epithelial cells and relieve contact inhibition [182]. A pro-proliferative effect of *crb* loss might seem at odds with recent work showing that loss of *crb* did not detectably alter overgrowth driven by *wts* inactivation [183, 184]. In these studies *crb* was analyzed as a downstream target of the SWH pathway; the data here show that it is also upstream of Ex. Loss of *wts* is thus predicted to be epistatic to the effects of *crb* loss on Ex. Rather, our data showing a upregulation of *diap1* expression in *crb* clones indicate

that *crb* alleles might enhance the effects of *wts* loss, although this would in all likelihood have little effect in the background of *wts* loss. Rather *crb* alleles may be more likely to synergize with mutations in other peripheral regulators of the SWH pathway such as *mer*, which functions redundantly to *ex* [157, 185].

Multiple polarity links to SWH activity

The link between Crb and Ex reinforces emerging links between polarity control and the SWH pathway. The polarity gene *Discs large (Dlg)* suppresses tumor growth of ovarian follicle cells via a pathway involving *warts* but independent of *ex*, *ft*, and *mer* [186]. The polarity factor Scribble can also interact with the Fat2 protein in the developing zebrafish kidney nephron [187]. In an accompanying study to the work presented here, Grzeschik et. al. have found that loss of *Drosophila lgl* can activate *diap1-lacZ*; significantly, this occurs without a loss of Ex protein. In view of the link uncovered here between *crb* and Ex levels in imaginal epithelial cells, it would thus seem that multiple mechanisms link polarity and the SWH pathway, and that multiple links can exist between apicobasal polarity factors and SWH activity even within a single cell type.

EXPERIMENTAL PROCEDURES

Genetics

Crosses performed at 25°C unless noted. Larval wing discs were harvested from animals kept at 20°C during embryogenesis. Animals were maintained at 20°C for adult wing analysis. Alleles used: *UAS-myc-crb^{intra}*; *UAS-Ex:GFP*; *UAS-sav*; *yki^{B5}*; *ban^{l(3)05967}*; *sd^{ETX4}*; *ex⁶⁹⁷*; *thj^{c58}*; *fj-lacZ*; *dpp-lacZ*; *ban-GFP*; *UAS-ex*; *FRT82B,crb^{11A22}*; *FRT82B,crb^{8F105}*; *crb^{Y10P12AE16A}*; *UAS-aPKC^{CAAX-DN}*; *UAS-cdc42^{N17.3}*; *UAS-moe^{IR-327-775}*; *UAS-yki-YFP*; *UAS-crb^{IR-1}* and *UAS-crb^{IR-2}* (VDRC #39178 and #39177); *lgl⁴*; *E-spl(m)β-CD2*; *UAS-app^{IR}*; *UAS-crb^{JM}* (also *UAS-Myc-Intra^{ERLI}*); *UAS-crb^{PBM}* (also *UAS-Myc-Intra^{Y10A/E16A}*); *UAS-crb^{aa}* (also *UAS-Myc-Intra^{Y10A/E16A/ERLI}*); *eyFLP;ubi-GFP,FRT80B*; *eyFLP;ubi-GFP,FRT82B*; *eyFLP;Act>CD2>Gal4;Rps17⁴,FRT80B*; *eyFLP;tub-Gal4;FRT80B,tub-Gal80*; *w;UAS-GFP,UAS-crbⁱ;FRT80B*.

Cell Culture & FACS

S2 cells were cultured under standard conditions. Constructs used: *pAc5.1-HA-Ex* (G. Halder), *pMT-VSV-G-crb-intra* and *pMT-VSV-G-crb-8F105* (A. Le Bivic). Transfected cells were analyzed 24-36 hours post-transfection (Cellfectin II, Invitrogen); where appropriate, CuSO₄ (0.5mM) was added for the final 12 hours. MG-132 (Sigma) was used at 50μM. Discs were treated with 100μM chloroquine (Sigma) as described previously [188]. Trypsin-dissociated discs were stained with 20 μM DRAQ-5 (Biostatus Limited), analyzed on a BD-LSR II cytometer via a 755 nM laser with a 780/60 nM BP collection filter, and analyzed on FlowJo (TreeStar).

Immunohistochemistry & Immunoblotting

Immunostaining, confocal microscopy, and immunoblotting performed as described previously [189]. Antibodies: mouse α - β -gal 1:1000 (Promega); mouse α -Wg 1:800 (DSHB); rabbit α -yki 1:1000 (K. Irvine); mouse α -HP1 1:20 (DSHB); 1:500 rat α -Crb (H. Bellen); mouse α -Dlg 1:20 (DSHB); rabbit α -GFP (Molecular Probes); guinea pig α -Ex 1:5000 (R. Fehon); rabbit α -Ex 1:200 (K. Irvine); goat α - β -tub 1:10000 (Santa Cruz); mouse α -HA 1:1000 (Sigma); goat α -VSV-G 1:1000 (Bethyl Labs); mouse α -Arm 1:20 (DSHB); mouse α -DIAP1 1:50 (B. Hay); mouse α -rat CD2 1:100 (Research Diagnostics, Inc.); mouse- α -Notch 1:10 (DSHB, clone 9C6); guinea pig α -Mer 1:7500 (R. Fehon), rabbit α -Fat 1:200; rat α -Elav 1:200 (DHSB); Alexa-488 phalloidin, 1:100, and YOYO-1, 1:20,000 (Molecular Probes).

Wing/Eye Measurements

Eyes/wings were imaged on a Leica DFC500 CCD camera and quantified with Adobe Photoshop. Posterior compartment ratio (PCR) = posterior compartment size/total wing size.

Chapter 4: Blockade of the Endolysosomal Pathway Affects SWH-signaling Via the c-Jun N-Terminal MAP Kinase Pathway in *Drosophila*¹

¹ A portion of this chapter is adapted from:
Robinson BS and Moberg KH. *Blockade of the Endolysosomal Pathway Affects Hippo/Mst-2 Signaling Via the c-Jun N-Terminal MAP Kinase Pathway in Drosophila*. (Submitted).

INTRODUCTION

Genetic studies performed in *Drosophila* have identified an assortment of genes required to restrict growth in *Drosophila* epithelia. Of these, there exists a relatively small subset of genes, termed neoplastic tumor suppressor genes (nTSG), whose inactivation results in the transformation of an epithelium into one that is highly proliferative, highly invasive, lacks a capacity to differentiate, and displays profound defects in apical-basal polarity and tissue architecture (reviewed in [43]). Many studies have linked *Drosophila* nTSGs to tumor formation in vertebrates [130, 190]; thus, understanding the molecular basis of how loss of these genes elicits their effects will inform our understanding of neoplastic transformation in humans. Moreover, as deregulation of proliferation, differentiation, polarity control, and adhesion are central features of *Drosophila* nTSGs, examination of *Drosophila* nTSGs will allow for a greater understanding of the framework under which these processes are regulated in cells.

In a genetic screen performed to identify genes that restrict growth in the *Drosophila* eye, we identified *erupted* (*ept*) as a gene that elicits a neoplastic phenotype when eliminated from *Drosophila* epithelia [118]. Studies have demonstrated that *ept* functions as a member of the endolysosomal pathway, a pathway that targets transmembrane and membrane-associated proteins for degradation of in the lysosome (reviewed in [191]). *ept* is a member of the endosomal-sorting complex required for transport-I (ESCRT-I) complex which functions to promote multivesicular body (MVB) biogenesis of late endosomes, a step required for complete exposure of target proteins to the proteolytic

environment of the lysosome [192, 193]. Interestingly, studies have shown that mutations in genes at multiple steps of the endolysosomal pathway result in neoplasia, though how these defects mediate these growth effects remains poorly understood (reviewed in [117]). Genetic and molecular studies of *ept*-mutant cells show central roles of the Notch and JAK-STAT signaling pathways in *ept* phenotypes [118, 194, 195]. However, because the phenotypes of these animals cannot be fully rescued by reducing Notch and JAK/STAT-signaling, and because neoplasia ensues in other endocytic mutants which lack activation of these pathways (e.g., *syx7/avl*;^[31]), it is likely that other signaling pathways are altered in these backgrounds ([194, 195]).

One pathway linked to growth control is the Salvador-Warts-Hippo (SWH) pathway, an emerging tumor suppressor network that was discovered in flies and is functions across metazoans to control organ size (reviewed in [82]). SWH-signaling functions through a core kinase cassette composed of two kinases (e.g., Hippo and Warts) and their scaffolding proteins, Salvador (Sav) and Mob-as-tumor-suppressor (Mats). Activation of Hippo (Hpo) by 'upstream signals' promotes its association with Sav, allowing for the phosphorylation of Warts (Wts) by Hpo-Sav. Wts, which is bound with Mats in the cytosol, acts on the pro-growth transcription factor Yorkie (Yki), rendering Yki inactive via 14-3-3-dependent cytosolic sequestration. To date, many proteins have been linked to alteration of SWH-activity in cells, yet precise mechanisms detailing how they exert these effects is lacking [90]. Thus, uncovering the network of regulatory inputs in the SWH-signaling will allow for a more

comprehensive view of its regulation and modality in cells, and potentially describe its role in diseases like cancer.

In order to better understand how mutations in *ept* promote neoplastic transformation in *Drosophila*, we explored the activity of the Salvador-Warts-Hippo (SWH)-pathway in the background of *ept*-deficient cells. We find that SWH-activity is altered in *ept* mutant cells, and that this alteration is enhanced when *ept* is combined with a block in cell death. Unlike Notch and JAK-STAT signaling, we find that altered SWH-activity is found at each step in the endolysosomal pathway. Analysis of endocytic-mutants shows that the expression of the apical pathway member Expanded (Ex) is altered in late endocytic mutants, but not in early mutants. However, in all mutants we find deregulation of JNK-signaling is altered in each step, a MAP kinase pathway that has been linked to *Drosophila* neoplasia and control of SWH-outputs in neoplastic cells [79, 80, 149, 150, 152, 196]. These studies highlight a novel role of endocytosis in regulating SWH-outputs, and place *Drosophila* endocytic nTSGs into an established tumor suppressor network that involves two major signaling pathways implicated in oncogenesis.

RESULTS:

***ept* mutant cells display altered *yki*-activity**

Loss of the endocytic gene *erupted* (*ept*), which functions as a member of the ESCRT-I complex to promote multi-vesicular body (MVB) biogenesis [192, 193], results in neoplastic transformation of imaginal disc epithelia in *Drosophila* [118]. Because deficient SWH-signaling is linked with altered contact inhibition and excessive proliferation [197], two key features of neoplasia in *Drosophila*, we examined whether SWH-signaling was modified in an *ept*-deficient background. To test this model, we generated *ept* clones in the *Drosophila* larval eye disc, and analyzed the expression of a well-characterized SWH-reporter, *expanded-lacZ* (*ex-lacZ*), in this background [156].

In *ept* clones generated in the eye the expression of the *ex-lacZ* reporter varies widely and displays no consistent pattern of activity with respect to the morphogenetic furrow, nor the dorsal-ventral and anterior-posterior axis. Some *ept* clones display an autonomous activation of *ex-lacZ* that coincides with non-cell autonomous activation in adjacent cells (Figure 4.1A, [151]), while others do not. Such phenotypes have been observed in the contexts of tissue regenerative and cell competition, where surrounding cells upregulate JNK and SWH signaling to outcompete and eliminate their genetically or biochemically defective neighbors [80, 151]. Moreover, it has been well documented that clones of *ept*-deficient cells display a cell-autonomous apoptotic phenotype [118]. Because of the concern that these apoptotic processes may obscure an otherwise cell-autonomous effect on

SWH signaling in *ept*-deficient cells, we combined an *ept* null allele with a small deletion (*Df(3L)H99* or *H99*) that removes three genes, *reaper*, *grim*, and *hid* that are required for apoptosis in *Drosophila* [198]. This produces clones of cells that are *ept,H99* double mutant and cannot die.

Animals mosaic for *ept,H99* produce large neoplastic eye discs, in contrast to *ept* mosaic animals alone, suggesting that *ept*-dependent signaling may be distinct in the background of blocked cell death [194]. Consistent with this idea, we observe that *ept,H99* clones in the eye display a strong cell-autonomous activation of the *ex-lacZ* reporter that is not accompanied with non-cell autonomous activation (Figure 4.11B). Thus, loss of *ept* can lead to a strong cell-autonomous inactivation of SWH-signaling when combined with a blocked in cell death.

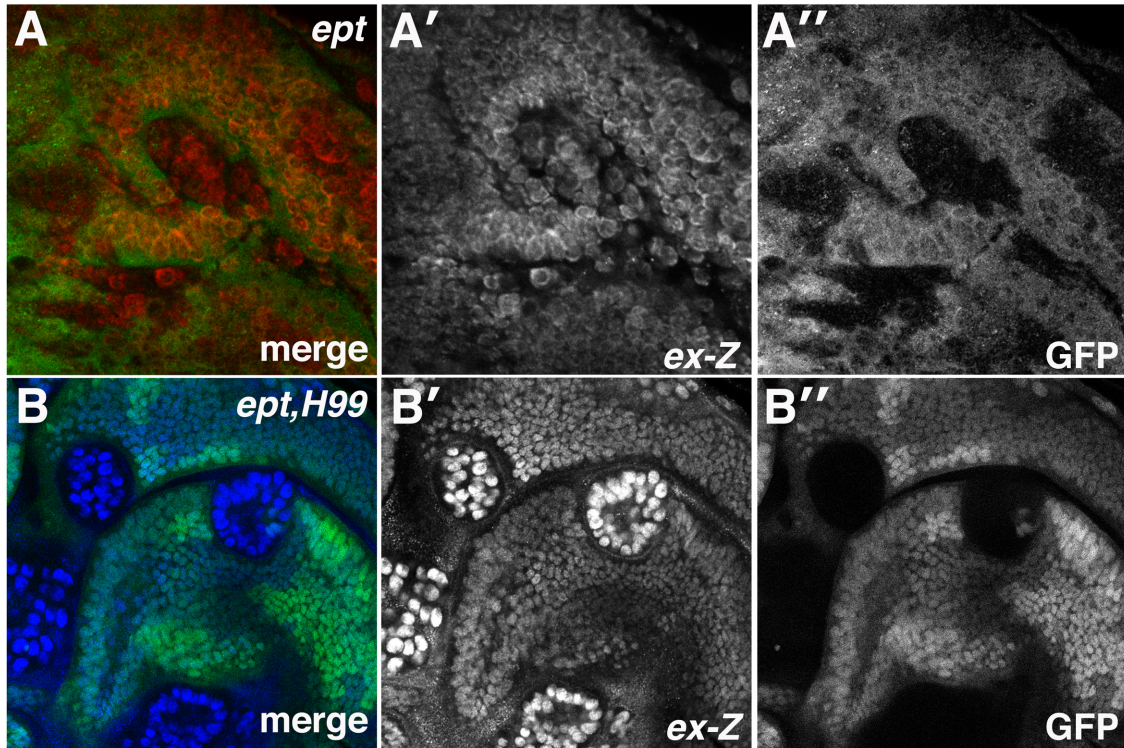


Figure 4.1. *ept* elevates Yki-activity. α - β -gal staining or GFP fluorescence of larval imaginal eye discs in which (A,B) the *ex-lacZ* reporter has been placed into the background of (A) *ept* or (B) *ept,H99* flies.

Loss of both early and late endocytic nTSG elevates yki-activity *in vivo*

As a member of the ESCRT-I complex, *ept* acts in the later stages of the endolysosomal pathway that targets transmembrane and membrane-associated proteins for ultimate degradation in the lysosome [192, 193]. To test whether the SWH-inactivation observed with loss of *ept* is unique to *ept*, or can be tracked to certain members or distinct stages within the endolysosomal pathway, we reduced the activity of specific endolysosomal pathway members and assessed the expression of the SWH-reporter *ex-lacZ*. For this analysis, we manipulated the gene expression of endolysosomal pathway members by using the posterior wing driver *engrailed-GAL4 (en)* and transgenic animals in which UAS elements had been placed in tandem to inverted-repeats (IR) directed at certain members of the endolysosomal pathway. Because antibodies do not exist for each of the target proteins, we were unable to confirm the efficiency of knockdown for each transgene by immunofluorescence. However, we did observe that for each of the IRs being used, expression resulted in neoplastic transformation of the epithelium and altered localization of the transmembrane protein Crumbs, consistent with functional reduction of the endolysosomal pathway (BSR personal communication; [195]).

Reduction of the adaptor protein AP-2 σ , which is required for protein internalization [199], produces a clear activation of *ex-lacZ* in the posterior compartment of the *Drosophila* wing discs (Figure 4.2B). Similarly, reduction of *syntaxin-7 (syx7 or avl)* and *rab-5* activity, two proteins previously characterized for their requirement in early endosome formation in *Drosophila* [31], results in strong activation of the *ex-lacZ* SWH-reporter (Figure 4.2C,D). As with our clonal

phenotype observed in the eye, we also find that reduction of a protein that acts in the later stages of this process, the ESCRT-II complex member *vps25*, results in activation of *ex-lacZ* (Figure 4.2E). In parallel, we also analyzed a separate SWH reporter, *thread-lacZ* (*th-lacZ*), and found that it is elevated in AP2 σ -deficient cells, albeit to a lesser degree than as *ex-lacZ*. These data suggest that different sensitivities may exist for SWH-reporters activated by altered endocytosis (Figure 4.3), as has been noted in other studies [200]. In summary, reduction of several members of the endolysosomal pathway can elevate *yki*-activity. Moreover, this link between SWH-signaling and endocytic genes appears to map to multiple steps along the pathway including cell-surface internalization, early endosome formation, and MVB biogenesis.

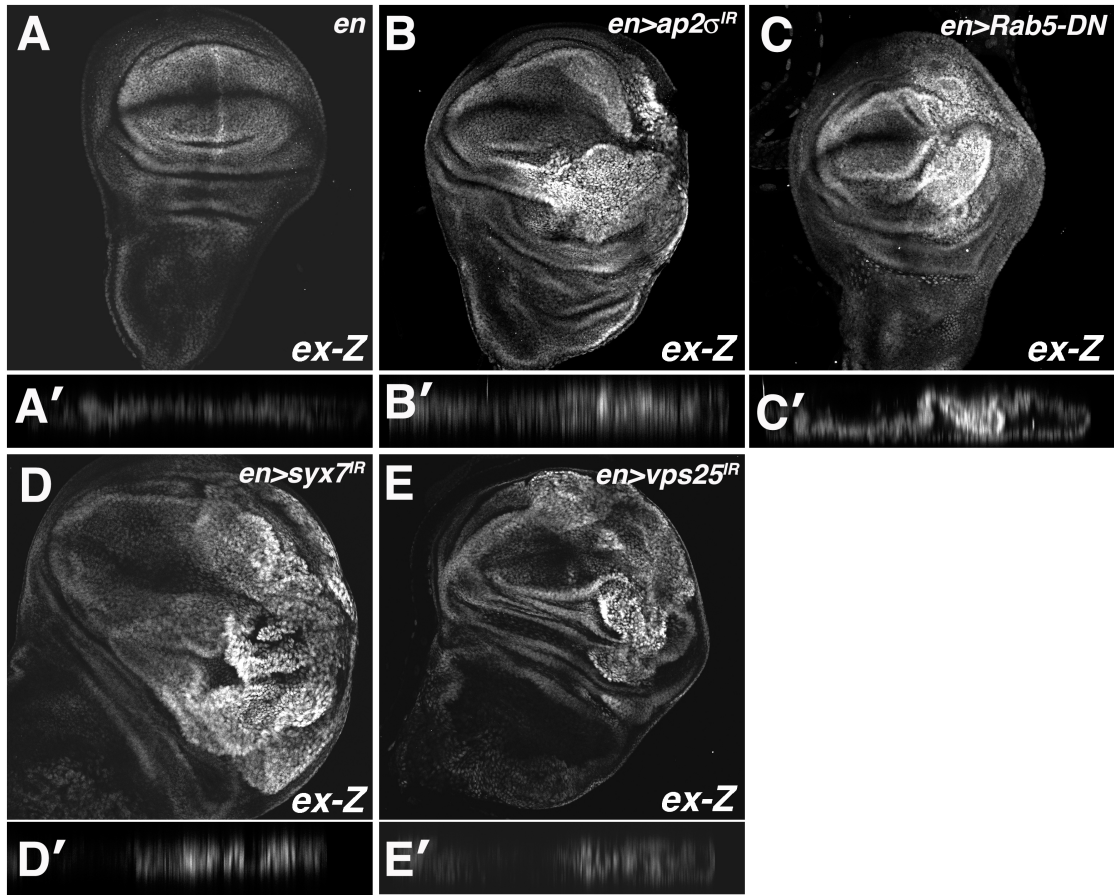


Figure 4.2. Multiple blocks in the endolysosomal pathway elevate Yki-activity. α - β -gal staining of larval imaginal wing discs in which the *ex-lacZ* SWH-reporter has been placed in the background of (A) *en*, (B) *en>AP2 σ^{IR}* (C) *en>Rab5^{DN}* (D) *en>syx7^{IR}* and (E) *en>vps25^{IR}* animals.

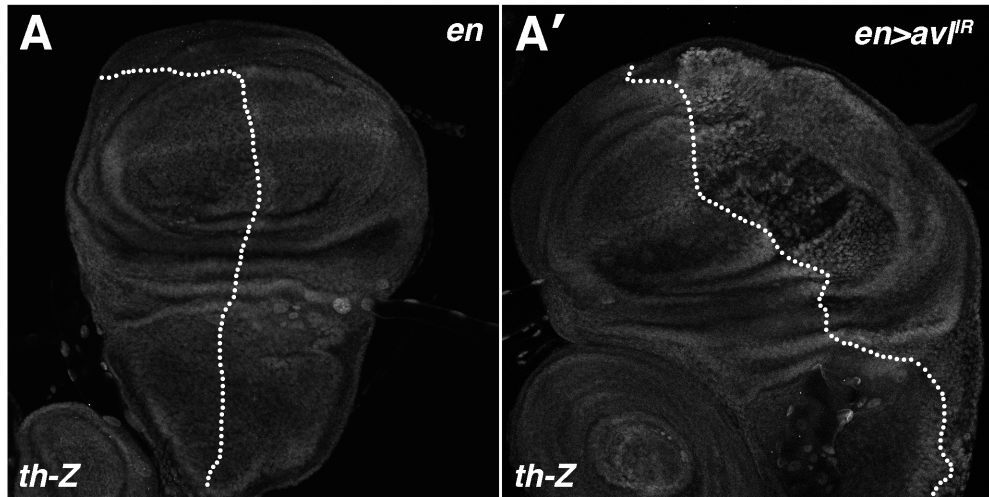


Figure 4.3. *avI^R* elevates the *th-lacZ* Yki-reporter. (A) α - β -gal staining of larval imaginal wing discs in which the *th-lacZ* reporter has been placed into the background of *en>avI^R* flies.

Endocytic neoplastic tumor suppressor genes require *yki* to overgrow

Given the effect of altered endocytosis on *ex-lacZ*, we next tested whether *yki*, the pro-growth effector of the SWH-pathway, was required for any of the phenotypes observed in endolysosomal mutants. One hallmark of *Drosophila* neoplasia is a strong reduction and/or absence in pupariation (reviewed in [43]). We utilized the *eyeless-FLP* system to generate eye-antennal discs that are entirely-mutant for *syx7/avl*, and analyzed whether overexpression of Salvador (Sav), a scaffolding protein that suppresses *yki*-activity, could affect *avl*-driven phenotypes [17, 48]. Interestingly, while *avl*-mutant animals normally die during an extended larval stage and rarely form pupae [31], *avl*-mutant animals in which Sav was overexpressed not only pupariate more frequently (Figure 4.4B) but sometimes eclose as adult animals with overgrown eyes (Figure 4.4A). Importantly, Sav overexpression itself has only a mild effect on overall eye growth, suggesting that *avl*-deficient cells are especially sensitive to the dosage of Sav (Figure 4.4A).

Next, we asked whether *yki* itself was required for the transcriptional effect on *ex-lacZ* in endocytic mutants. To test this, we co-depleted AP2 σ and Yki from cells by *en-GAL4* driven expression of *UAS-AP2 σ^R* and *UAS-yki^{IR}* (*yki^{IR}*) transgenes. As with the *avl*-deficient animals noted above, we noted a significant reduction in pupariation delay when *yki*-activity is reduced in this background (Figure 4.4C). Moreover, in the background of *yki^{IR}*, *AP2 σ^R* is no longer able to elevate *ex-lacZ* activity, arguing that *yki* is required for the effect of an endolysosomal block on SWH-signaling (Figure 4.4D).

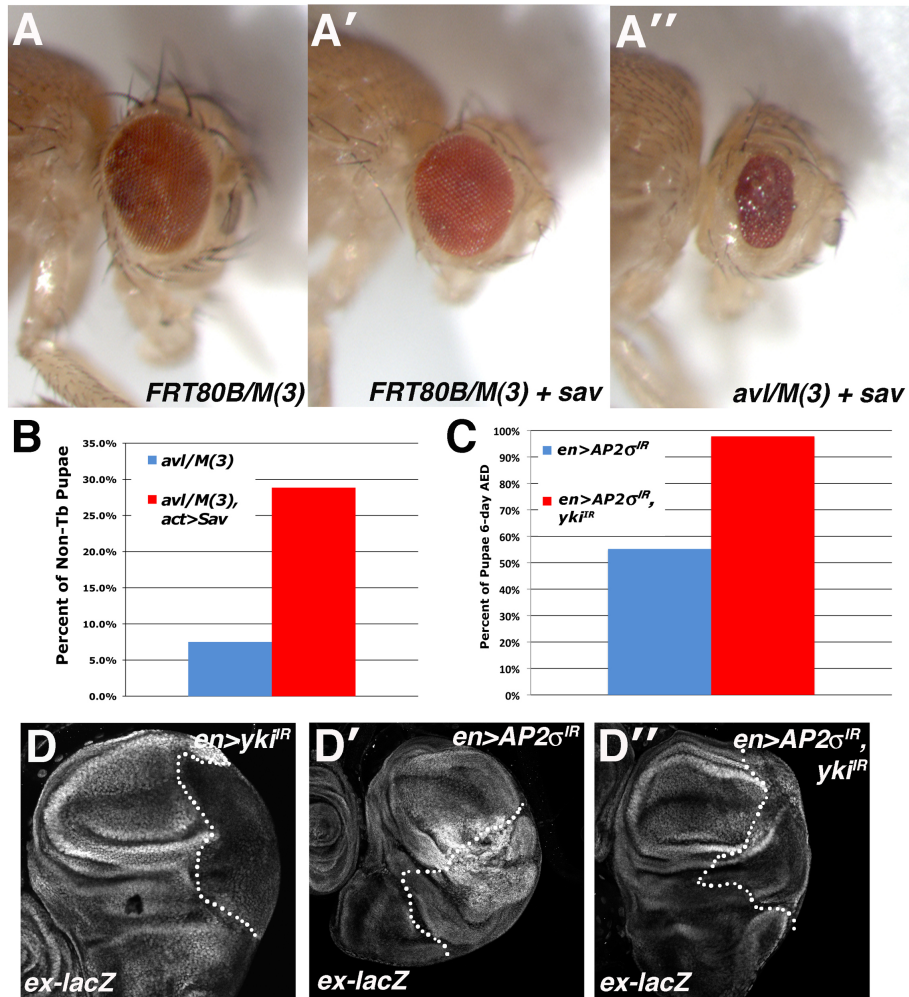


Figure 4.4. endolysosomal growth phenotypes are sensitive to the dose of Yki. Light microscopic images of (A) *eyFLP;FRT80B/M(3)*, (A') *eyFLP;Act>CD2>Gal4,UAS-sav;FRT80B/M(3)* and (A'') *eyFLP,Act>CD2>Gal4,UAS-sav;avl¹/M(3)* adult eyes, in which *sav* is overexpressed using the *Act>CD2>Gal4* 'Flp-out technique'. (B,C) Quantitative analysis of the percent of pupae at 6 days AEL in the indicated genotypes. A minimum of 50 animals were counted per genotype. (D) α - β -gal staining of larval imaginal wing discs in which the *ex-lacZ* reporter has been placed into the background of (D) *en>yki^{IR}* (D') *en>AP2 σ^{IR}* and (D'') *en>AP2 σ^{IR} ,yki^{IR}* flies.

Endocytic neoplastic tumor suppressor genes elevate JNK activity *in vivo*

Next, we sought to determine the mechanism whereby a block in endocytosis activates Yki-signaling in cells. One recently identified SWH-pathway component is the transmembrane polarity factor Crb [33], which acts to restrict the levels and localization apical SWH-pathway component Expanded [143-145, 201]. As with previous studies looking at the late-endocytic gene *vps25* [178], we found reduced levels of *expanded* in *ept*-deficient cells (Figure 4.5A-B). However, analysis of *AP2 σ* cells did not yield similar results (Figure 4.5C), arguing that loss of *ex* may not be the primary driver of widespread *yki*-activation we observe with a block in endocytosis. Thus, we investigated other mechanisms.

Among the first genes identified to restrict neoplasia in *Drosophila* were the apical-basal polarity factors *lethal (2) giant larvae (lgl)* and *discs-large (dlg)* [125, 126]. Recent studies show that loss of *dlg* and *lgl* polarity elevates *yki*-signaling via an effect mediated by the pro-apoptotic c-Jun N-terminal Kinase (JNK) signaling pathway [80], a pathway that also promotes Yki-activation in *Drosophila* intestinal stem cells [149, 150, 196]. To see whether a similar mechanism operate in endocytic nTSGs, we analyzed the activity of JNK-signaling in the background of blocked endocytosis. JNK-pathway signaling begins with upstream activation of MAPKKK, which leads to the eventual phosphorylation and activation of Basket (Bsk), the terminal JNK kinase in *Drosophila* (reviewed in [77]). Phosphorylation of *bsk* promotes its activity in cells, leading to the phosphorylation of the transcription factor Jun, which then heterodimerizes with the transcription factor Fos to form an active transcriptional complex (e.g., AP-1) in the nucleus. Several transcriptional

targets of the active AP-1 complex have been identified in *Drosophila*, including *matrix-metalloprotease-1 (mmp1)* and *puckered (puc)* [202, 203].

First, we analyzed the expression of the JNK-pathway target MMP-1 in *ept* clones. As predicted by a model whereby a block in endocytosis activates JNK-signaling, MMP-1 protein levels are elevated in *ept* and *ept,H99* clones mutant clones compared to surrounding wild-type tissue (Figure 4.6A,C). Next, in order to see whether activation of JNK-signaling occurs in endolysosomal mutants other than *ept*, we analyzed MMP-1 expression in *en>ap2 σ^{DR}* , *en>syx7 IR* , and *en>vps25 IR* animals. As with the SWH-reporter *ex-lacZ*, MMP-1 expression is elevated in the posterior compartment of each of these genotypes (Figure 4.7A-C). Similar results were observed with the JNK-reporter *puc-lacZ*, which was elevated in *en>ap2 σ^{DR}* and *en>syx7 IR* animals (Figure 4.7D-F). Finally, we analyzed phosphorylation of JNK itself, which also serves as a marker JNK-pathway activation, in various endocytic mutants. As with MMP-1 expression, we observed increased p-JNK staining in *ept* clones, *ept,H99* clones (Fig 4.6B,D), and in the posterior compartment of *en>ap2 σ^{DR}* , *en>syx7 IR* , and *en>vps25 IR* animals (Fig 4.7G-I). In summary, these data suggest that altered endocytosis is accompanied by elevated JNK-signaling, consistent with a model whereby neoplasia induces activation of Yki by elevating JNK-signaling in cells.

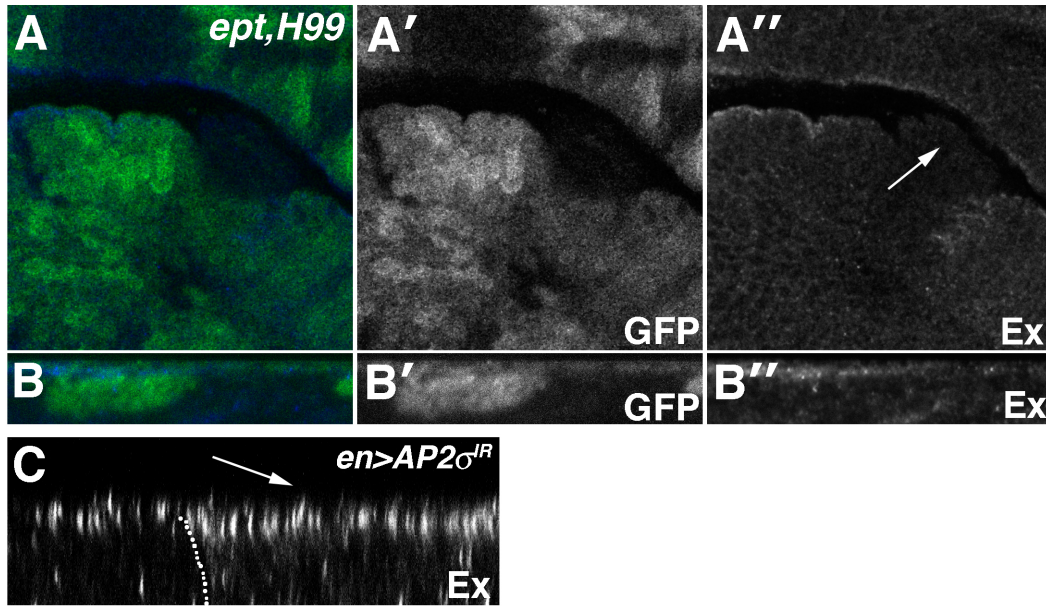


Figure 4.5. Ex Expression is altered in endolysosomal mutants. Confocal images of (A-B) *ept^{x1}, H99* clones in the eye and (C) *en>AP2 σ^R* wings discs stained for Ex protein. *ept^{x1}, H99* clones marked by the absence of GFP. Arrow in A indicates loss of Ex from a GFP-negative *ept^{x1}, H99* clone. Arrow in C indicates the presence of Ex in the posterior compartment of *en>AP2 σ^R* animals in which AP2 has been reduced.

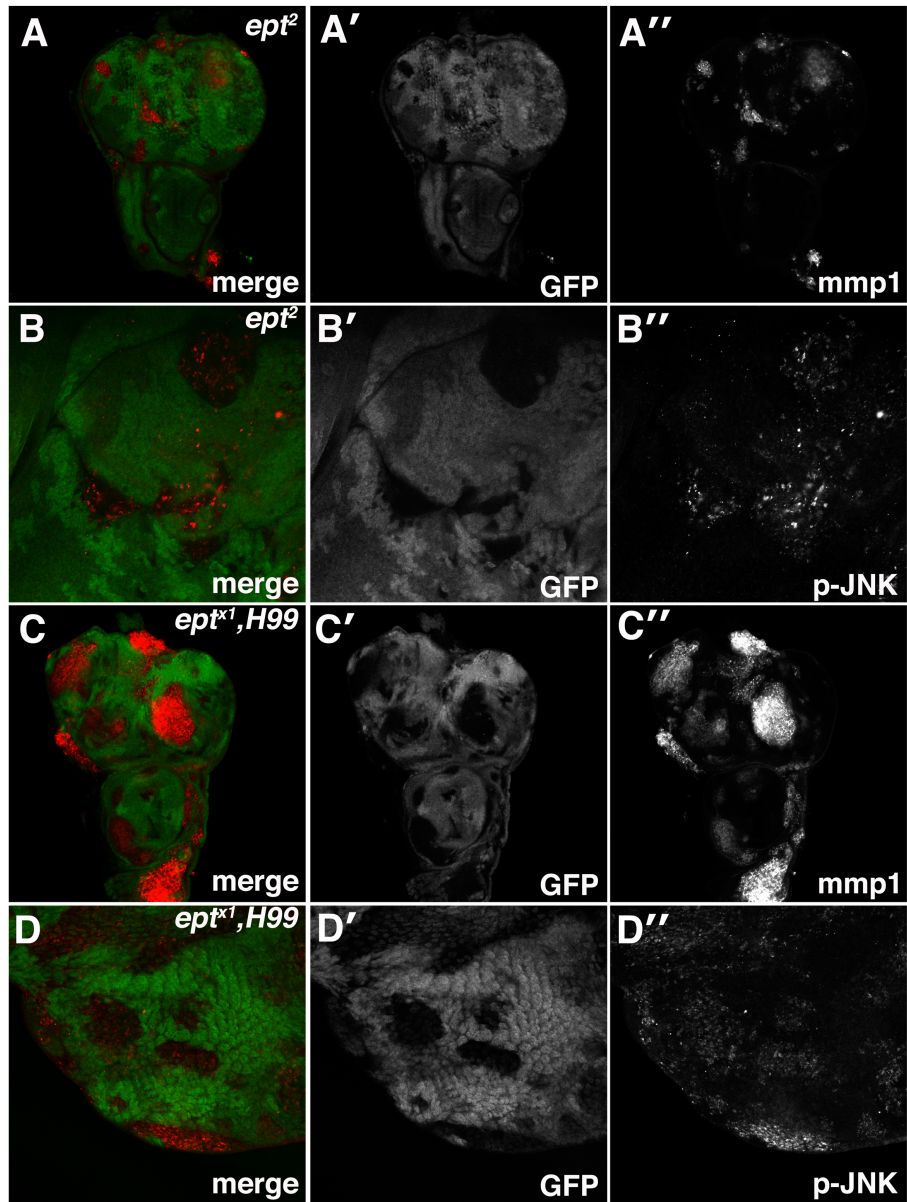


Figure 4.6. Loss of *ept* elevates JNK-activity. Confocal images of (A-B) *ept*² and (C-D) *ept*^{x1,H99} marked by the absence of GFP stained for (A,C) MMP1 and (B,D) phosphorylated-JNK.

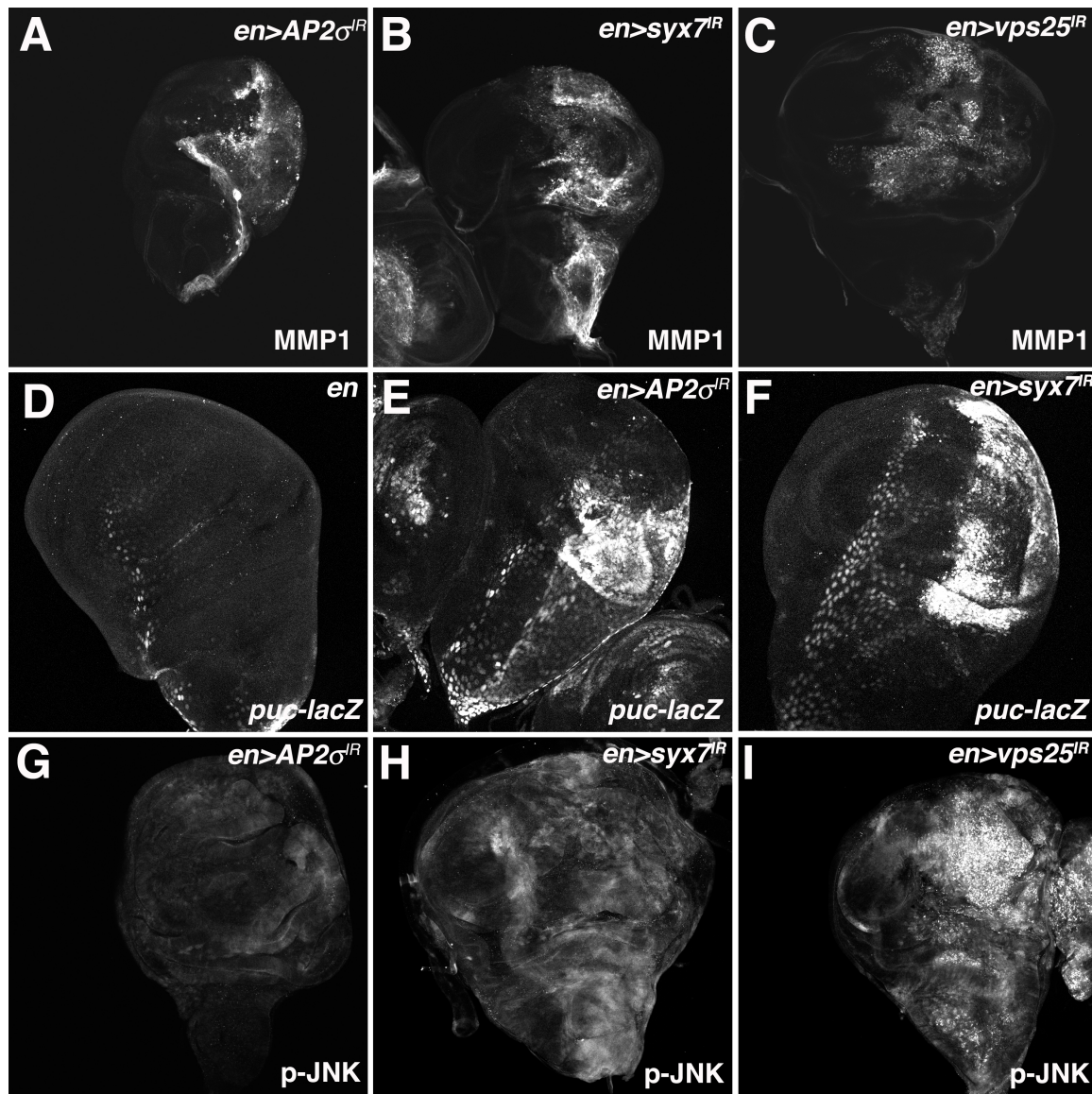


Figure 4.7. Loss AP2 σ , Syx7, and Vps25 elevate JNK-activity. Confocal images of larval imaginal wing discs from (A,G) *en>AP2 σ^{IR}* , (B,H) *en>syx7 IR* , and (I) *en>vps25 IR* flies stained for (A-C) MMP1 and (G-I) phosphorylated-JNK. (D-F) α - β -gal staining of larval imaginal wing discs in which the *puc-lacZ* reporter has been placed into the background of (D) *en*, (E) *en>AP2 σ^{IR}* , and (F) *en>syx7 IR* flies.

DISCUSSION

The link between neoplastic transformation and mutations in any number of the genes required for endocytic trafficking to the lysosome in *Drosophila* is well established. Here, we detail this link further by highlighting a connection between endocytic neoplastic tumor suppressor genes (nTSG) and two major growth regulatory pathways, the JNK pathway and the SWH pathway. We find that loss of endocytic nTSG is associated with altered activity of the SWH-pathway. Moreover, we show that endocytic nTSGs display unique sensitivity to the dosage of SWH-pathway components. Finally, we find in addition to altered SWH-pathways activity, loss of endocytic nTSGs is accompanied with significant upregulation of JNK-pathway activity, a pathway linked to neoplasia and SWH-regulation in flies [79, 80, 149, 150, 152, 196].

The data presented here reinforce an emerging role for JNK-signaling in driving the proliferative phenotypes in neoplastic tissue. This is a bit surprising, given the well-established role of JNK-signaling in driving apoptosis [70, 71]. However, studies examining *lgl* and *Scrib*-driven neoplasia show a requirement for JNK-signaling in driving the growth of these tumors [79, 204]. Moreover, recent studies examining the proliferation *lgl* and *dlg*-deficient cells show a primary role for JNK-signaling in driving the proliferation of cells through activating Yki [80], a potent effector of the SWH-pathway in *Drosophila*. Mechanistic insight into how JNK-signaling activates Yki is lacking, and likely to be topic of extensive investigation given that JNK-activation is continuing to be connected to Yki-signaling in a variety of developmental contexts [149, 150, 196]. Moreover, our

observation that endocytic nTSG activate JNK-signaling in a manner similar to polarity nTSGs raises other important questions as well, including mechanistic insight into how neoplasia promotes JNK-activity in cells. Recent studies demonstrating a linear pathway involving the polarity factor *cdc42*, *rho1* and JNK hint that JNK-activation likely occurs via altered cell polarity [152]. However, as studies have shown a role for polarity proteins in modulating endocytic programs (reviewed in [205]) and the JNK-pathway receptor Wengen is trafficked in cells [206], it is indeed plausible that altered endocytosis may be more primary in driving neoplastic activation of JNK-signaling.

These data also lend insights into *ept*-driven phenotypes in cells. Proliferation of *ept*-deficient cells has been linked to JAK-STAT and Notch signaling [118, 194, 195], however, our findings suggest that when cell death is blocked altered SWH-signaling may contribute as well. This is significant given the well-established role of the SWH-pathway in controlling cell proliferation and tumorigenesis [83]. These data may seem to contradict previous findings investigating the late endocytic gene *vps25* [178], which demonstrated SWH-activation as a primary driver of apoptosis in endocytic nTSG cells. However, these studies used Ex as a readout of SWH-activity. Given the recent findings that Ex can be downregulated by excess levels of the transmembrane factor Crb [145, 201], which accumulates in late endocytic mutants [118], the ability to interpret Ex protein levels as a readout of SWH-activity may be diminished. In fact, the data presented here point towards elevated JNK-signaling as the causative factors in the cell-autonomous apoptotic phenotype observed *ept*-deficient cells, mirroring similar

studies looking at the ESCRT-III component *vps4* [207]. This JNK-dependent apoptosis is significant, for it may explain the controversy concerning the vertebrate ortholog of *ept* Tumor Susceptibility Gene-101 (TSG101) in tumorigenesis, where some studies show TSG101 as a tumor suppressor while others do not [208-212]. Perhaps it is possible that only in the context of a block in cell death that TSG101-nulls cells can fully express their oncogenic properties.

Experimental Procedures

Genetics

Crosses were performed at 25°C unless otherwise noted. For analysis of larval wing discs, crosses were maintained at 28°C to enhance GAL4 activity. For analysis of adult wings, crosses were maintained at 20°C. Alleles used: *ept²*; *ept^{x1}*, *Df(3L)H99* (gift of M. Gilbert); UAS-*sav* (G. Halder); *ex⁶⁹⁷* [156]; *thi^{c58}* (B. Hay); UAS-AP2 σ ^{IR} (Bloomington Stock Center, stock 27322); UAS-*syx7*^{IR} (Bloomington Stock Center, stock 29546); UAS-*rab7*^{IR} (Bloomington Stock Center, stock 27501); UAS-*vps25*^{IR} (Bloomington Stock Center, stock 26286); *av1¹* (D. Bilder); UAS-Rab5-DN (M. Scott); UAS-Yorkie-IR-KK (Vienna Drosophila RNAi Center). Clonal analysis was performed using: *eyFLP;ubi-GFP,FRT80B*. ‘Flp-out’ analysis was performed using: *eyFLP;Act>CD2>Gal4;Rps17⁴,FRT80B*.

Immunohistochemistry & Immunoblotting

Immunostaining and confocal microscopy were performed as described previously [189]. Antibodies used: mouse α - β -gal 1/1000 (Promega); mouse α -MMP-1, 1/100 of 1:1:1 aliquot of clones 5H7B11, 3B8D12, 3A6B4 (Developmental Studies Hybridoma Bank); guinea pig α -Ex 1/5000 (R. Fehon); rabbit α -phospho-JNK 1/1000 (Promega); rat α -Crb-Extra 1/500 (U. Tepass and E Knust).

Pupariation Analysis

Briefly, adults were allowed to deposit embryos for a span of 24-hours, after which their progeny was tracked and the number of pupae and larvae were compared at 144-hours AED. A minimum of 50 flies was analyzed per genotype.

Chapter 5: The Nuclear Receptor Co-Activator Taiman promotes a Yorkie-dependent growth program in *Drosophila*.

INTRODUCTION

Developmental control of cellular proliferation and apoptosis occurs via an array of signaling pathways that are tightly regulated in order to ensure the proper formation of organ size. Genetic screens performed in *Drosophila* have identified numerous factors required for this process, including genes that function in known growth-regulatory and apoptotic pathways as well as multiple genes that define entirely new growth-regulatory networks [116]. This latter case is perhaps best exemplified by the Salvador-Warts-Hippo (SWH) pathway, a tumor suppressor network that was first elaborated through EMS-based screens looking for mutants that confer a clonal growth advantage in the *Drosophila* eye, which was subsequently found to operate universally across metazoans in regulating organ size [85].

The SWH pathway operates primarily through two cytoplasmic kinases, Hippo and Warts, which phosphorylate pro-growth transcriptional co-activator Yorkie (Yki) and promote its retention in the cytoplasm (reviewed in [82]). Several proteins have been shown to aid in this process including the adaptor proteins, Salvador (Sav) and Mob as Tumor Suppressor (Mats), which function to physically link Hippo and Warts together producing a functional kinase cassette. Additionally, several 'upstream-regulators' have been identified, including the apically localized transmembrane proteins Fat (Ft) and Crumbs (Crb), the cytosolic FERM-domain containing proteins Expanded (Ex) and Merlin (Mer), and the WW-domain containing linker protein Kibra (Kib). Precisely how these proteins function together and/or independently to restrict SWH-pathway activity is still unclear and

the topic of considerable research (reviewed in [90]). Additionally, how Yki functions in the nucleus to drive concomitant proliferation and cell survival programs remains unclear, although studies have demonstrated that Yki can associate with multiple DNA-binding factors, including Scalloped (*sd*), Teashirt (*tsh*), and Homothorax (*hth*) as well as cooperate with several other growth-regulatory programs to augment organ size in vivo [86-89, 134, 213].

Here we identify alleles of *tai*, the *Drosophila* ortholog of human SRC-3/AIB1, as a modifier of a growth phenotype driven by altered activity SWH-activity in *Drosophila* [113]. We find that ectopic expression of *tai* elevates several SWH-pathway outputs, while reciprocally, loss of *tai* reduces basal SWH-reporter activity. Tai activity appears to converge on *yki*, a nuclear transcriptional co-activator that drives the expression of several pro-growth and anti-apoptotic genes to produce hyperplasia noted in mutant animals [214]. These studies highlight a novel role for *tai* in regulating SWH signaling in *Drosophila*, and potentially place *tai* as a regulator of an emerging tumor suppressor network in metazoans.

RESULTS

***taiman* regulates imaginal disc growth**

The overexpression of the intracellular tail of the apical polarity factor Crumbs (Crb) can drive excessive proliferation and overgrowth in *Drosophila* imaginal disc epithelia [31, 201]. In a screen designed to identify loci that could alter growth within this background, we found a genomic deficiency, *Df(2L)N22-14*, that dominantly suppressed the ability of *crb^{intra}* (*crbⁱ*) to drive overgrowth in the wing (Figure 5.1). Subsequent mapping utilizing smaller overlapping deficiencies that lie within *Df(2L)N22-14*, reveal a smaller deficiency, *Df(2L)ED680*, that is sufficient to recapitulate the original genetic suppression associated with *Df(2L)N22-14* (Figure 5.1). We obtained all available alleles of genes within this region, and found that several alleles of a gene called *taiman* (*tai*), which is known for its role in transcriptional co-activation and border cell migration [113, 215], are able to dominantly suppress *crbⁱ*-dependent overgrowth, including *tai^{61G1}*, *tai^{k01351}*, and *tai^{k15101}* (Figure 5.1).

The ability of *tai* alleles to suppress *crbⁱ*-dependent overgrowth suggested that *tai* may be able to regulate tissue growth in *Drosophila*. Since, to date, no studies have been performed analyzing a role of *tai* in this process, we used the Gal4-UAS system to see whether ectopic expression or reduction of *tai* could alter growth in developing *Drosophila* epithelia. *engrailed-Gal4* (*en-GAL4*) driven expression of a *UAS-tai* transgene led to expansion of the posterior domain of larval wing discs, particularly in the wing pouch (Figure 5.2A'). Furthermore, phalloidin staining of *en>tai* imaginal discs reveals extensive tissue folding and outpouching of

wing pouch cells (Fig 5.3), and a BrdU-incorporation assay show increased uptake in the posterior compartment indicative of elevated proliferation response in this area (Fig 5.2D). Reciprocally, *en-GAL4* expression of an inverted-repeat directed at *tai* (*UAS-tai^{IR}*), which binds to the *tai* 3'-UTR and reduces protein expression (Figure 5.4), distinctly shrinks the posterior compartment of wing discs (Fig 1A''). As a control, we stained discs in each of these background with an antibody directed towards Cubitus Interruptus (Ci), which marks the anterior domain of discs cells, and observed no general change in anterior compartment size, indicating that the alteration in posterior compartment size is likely not due to an alteration in developmental staging but rather to an autonomous effect of *tai* on tissue growth. To test the consistency of these effects by the *UAS-tai* and *UAS-tai^{IR}* transgenes, we dissected wing discs from ≥ 10 animals and quantified the posterior and anterior compartment size and found that while the anterior compartment remained unchanged, there was a statistically significant alteration in posterior compartment size with both ectopic expression and reduction of *tai* in these domains (Figure 5.2B, $p = 3.8E-02$ and $4.4E-06$ respectively, when compared to control wing discs).

Lastly, we sought to determine how representative the growth phenotypes we observed with *en-Gal4* driven overexpression were to *tai*-driven overgrowth. First, we observed similar overgrowth phenotypes in the eye-antennal disc when *tai* was overexpressed (Figure 5.3), indicating that this pro-growth effect of *tai* growth is not restricted to the wing epithelia. Moreover, using the 'flp-out' technique to analyze the effect of elevated *tai* in clonal fashion [216], we observed that *tai* clones were on average 34% larger ($n = 79$ for control and 112 for *UAS-tai*; $p = .025$) than

those from control animals (expressing only GFP), consistent with a pro-growth role for *tai* in *Drosophila* imaginal discs (Figure 5.2C).

A

Deficiency	Posterior Compartment Ratio	Associated p-value	Cytologic Deletion
Df(2L)N22-14	0.67	2.93E-07	29C1-30C9
Df(2L)ED680	0.67	2.70E-08	30A4-30B12
Df(2L)ED611	0.70	-	29B4-29C3
Df(2L)ED623	0.69	-	29C1-29E4
Df(2L)ED647	0.69	-	29E1-29F5
Df(2L)Exel7042	0.69	-	30B10-30C1
Df(2L)Exel7040	0.69	-	29F1-29F6
Df(2L)Exel7039	0.68	-	29D5-29F1
Df(2L)Exel7038	0.69	-	29C4-29D5
Df(2L)Exel6022	0.70	-	30B5-30B11
Df(2L)Exel6021	0.68	4.60E-02	29F7-30A2
Df(2L)BSC17	0.70	-	30C3-30F1

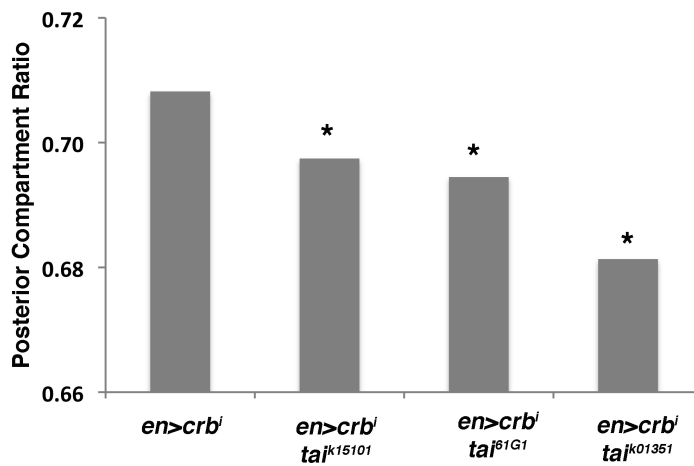
B

Figure 5.1. Mapping of the *crbⁱ* modifier Df(2L)N22-14. (A) Table showing the effect of the *en>crbⁱ* suppressor Df(2L)N22-14 and several smaller overlapping genomic deficiencies within this loci to map the region responsible. (B) Subsequent analysis show that three alleles of a gene called *taiman* (*tai*), which was uncovered by both Df(2L)Exel680 and Df(2L)Exel6021, reproducibly suppress *crbⁱ*-driven overgrowth.

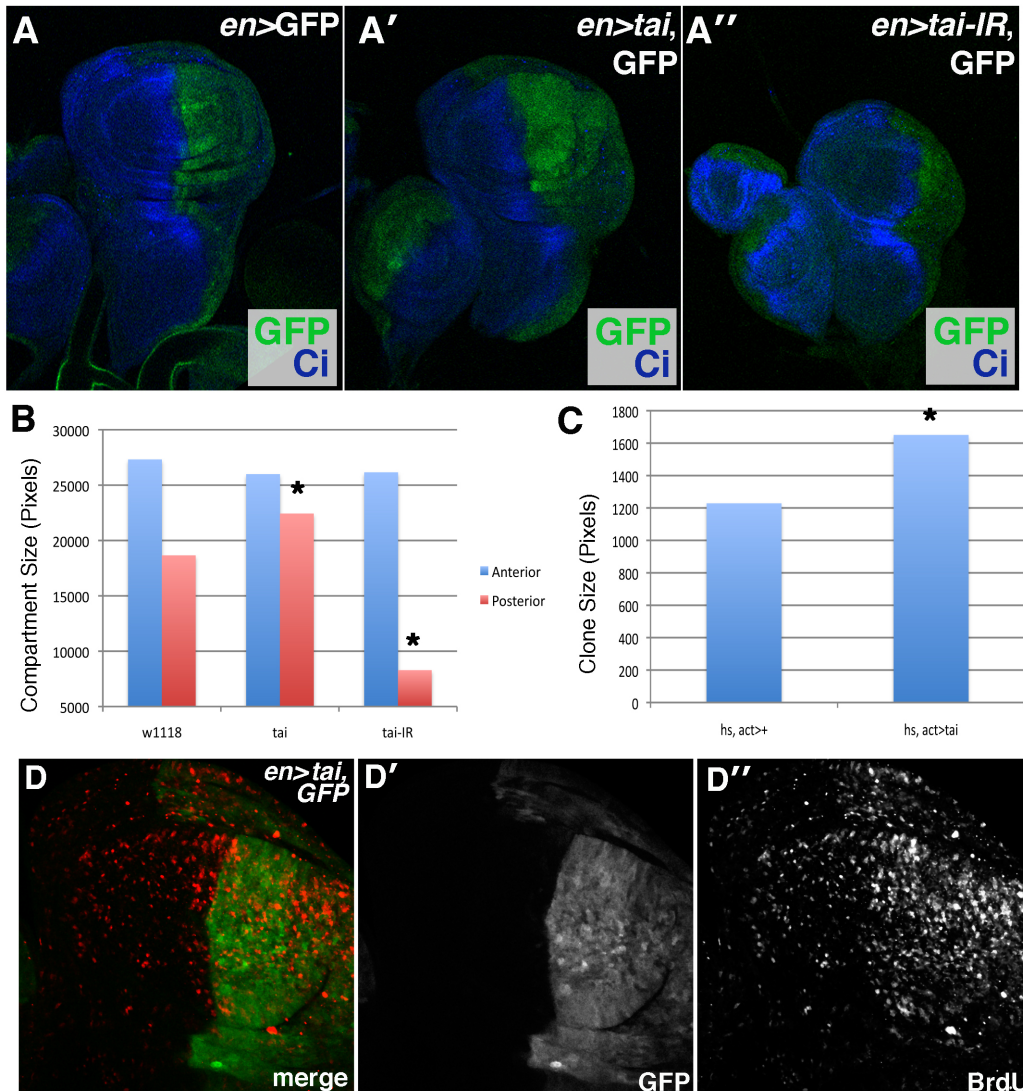


Figure 5.2. *tai* controls larval imaginal wing disc growth. (A) Ci staining and GFP fluorescence in (A) *en>GFP*, (A') *en>GFP,tai*, and (A'') *en>GFP,tai^{IR}* flies. Ci marks the anterior compartment. (B) Anterior and posterior compartment size of larval wing discs from flies of the indicated genotypes. (C) Average size of 'flp-out' clones 48-hours after induction in the indicated genotypes. (D) BrdU-incorporation assay of larval wing discs from *en>GFP,tai* animals. * denoted p-value of <.05 when compared by students t-test to control animals.

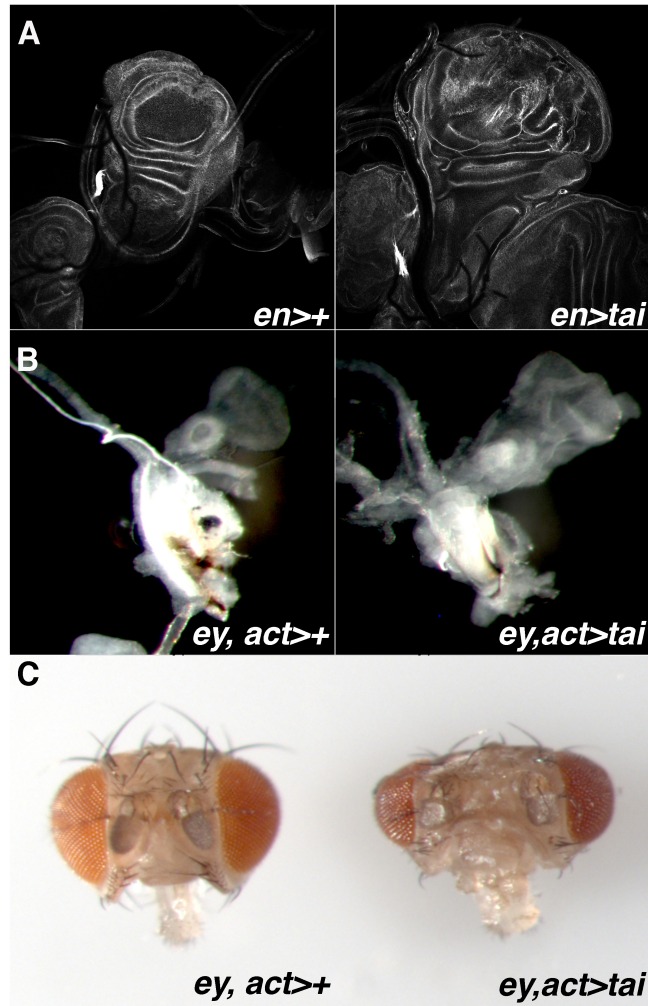


Figure 5.3. *tai* controls the growth of multiple *Drosophila* epithelia. (A) Phalloidin staining of larval imaginal wing discs from *en* and *en>tai* flies. Note the extensive folding in the wing pouch of *en>tai* discs. (B) Larval imaginal eye discs and (C) adult heads from indicated genotypes. Note extensive tissue folding in the eye discs and the enlarged head width in background of *ey, act>tai*.

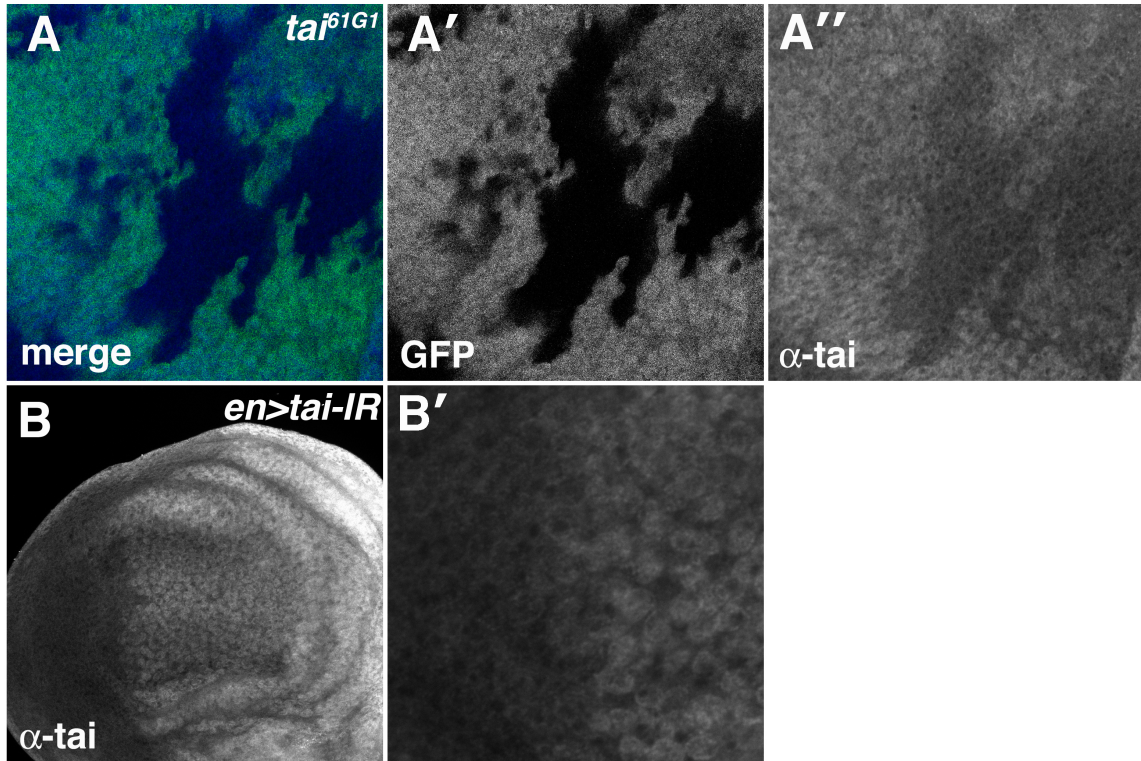


Figure 5.4. *tai*^{IR} and *tai*^{61G1} clones have reduced levels of *tai*. Images of (A) *tai*^{61G1} clones (lacking GFP) in larval eye disc and (B) *en>tai*^{IR} larval wing discs stained with α-*tai*. Posterior is to the left.

Excess *tai* elevates *yki*-activity

The ability of *tai* to suppress *crbi*-dependent overgrowth suggests that *tai* may function downstream of Crb to regulate a common growth-regulatory pathway. Crb was recently identified as an upstream regulator of the Salvador-Warts-Hippo (SWH) pathway that regulates the localization and levels of the apically located FERM-domain containing protein Expanded [143-145, 201]. Therefore, we sought to address whether the growth phenotypes produced by excess *tai* could be attributed via an as-of-yet unrecognized role of *tai* in regulating SWH-signaling, and analyzed several well-characterized reporters of SWH-activity in the background of excess *tai*.

In *Drosophila*, SWH-signaling converges on a transcriptional co-activator, Yorkie (Yki), which is known to drive the expression of several genes, including the apoptotic regulator *Drosophila Inhibitor of Apoptosis-1* (*DIAP1*) or *thread* (*th*), the apical FERM-domain containing protein Ex, the microRNA *bantam*, and several others pro-growth effectors [83]. We analyzed the activity of two β -galactosidase enhancer traps for *ex* and *DIAP1/th* respectively, and found a striking elevation in reporter activity in the posterior compartment of *en>tai* animals that was not observed in control animals (Figure 5.5A,B,E,F). We further investigated the effect of *tai* on the *DIAP1*-promoter by examining the activity of the *DIAP4.3-GFP* reporter, which is a fusion of the 4.3 kb *yki*-responsive element found within the *DIAP1* promoter to GFP. As with the *th-lacZ* enhancer trap, the *DIAP4.3-GFP* reporter was elevated in the posterior compartment of *en>tai* animals (Figure 5.5C-D). Finally, we analyzed the expression of the *yki*-target miRNA *ban* using the *ban*-GFP reporter,

which reports *ban* levels indirectly through the expression of a GFP-construct that contains a *ban* binding site in its 3-UTR [217]. As with the other reporters investigated, *ban* activity is markedly elevated in *en>tai* expressing cells (Figure 5.5G-H).

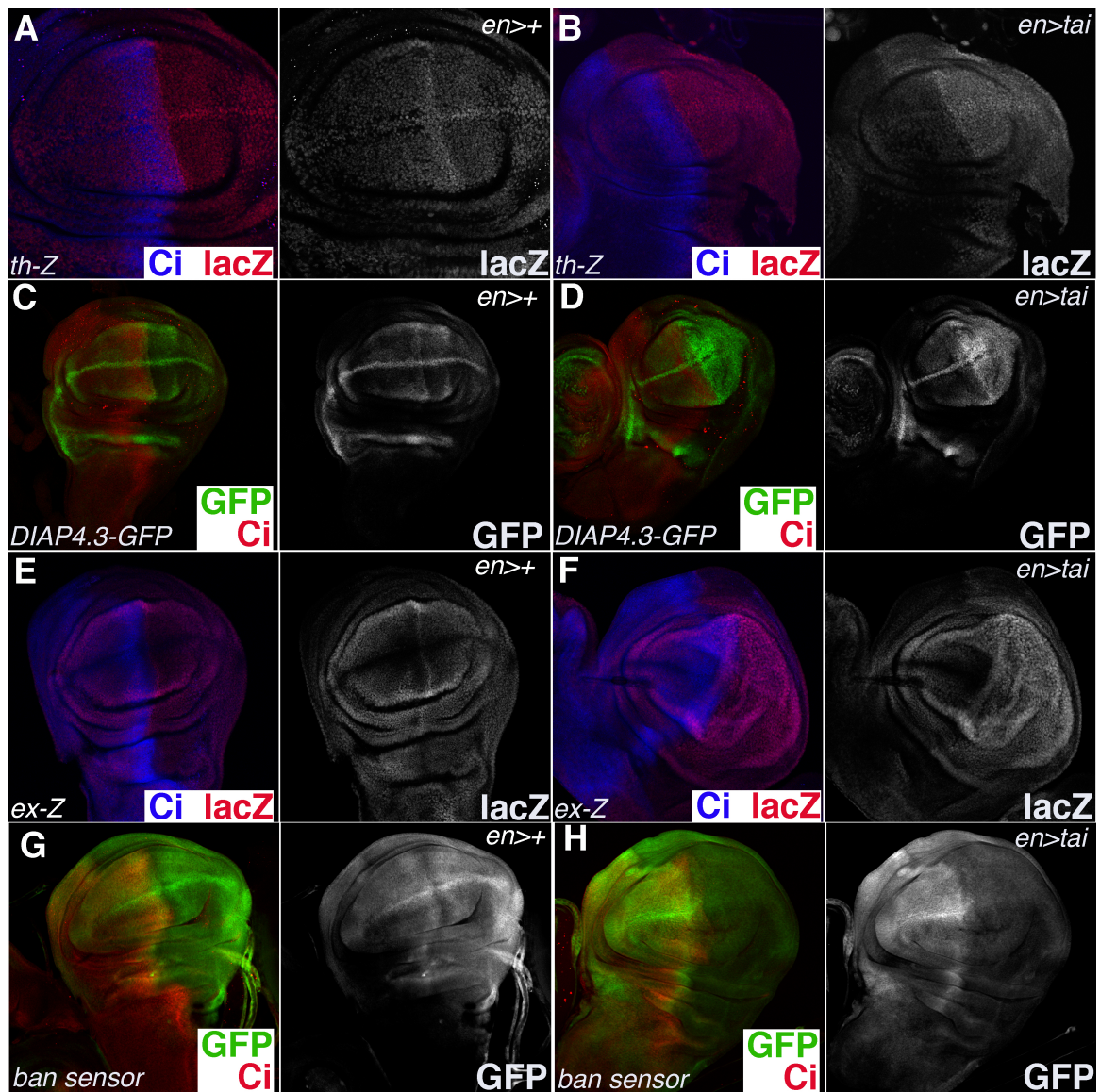


Figure 5.5. *tai* elevates Yki-activity. α - β -gal and Ci staining or GFP fluorescence in wing discs carrying (A-B) *th-lacZ*, (C-D) *DIAP4.3-GFP*, (E-F) *ex-lacZ*, or (G-H) *ban-GFP* in the background of (A,C,E,G) *en>+* or (B,D,F,H) *en>tai*. Ci staining marks anterior wing compartments.

Loss of *tai* reduces *yki*-activity

Given the ability of exogenous *tai* to elevate *yki*-signaling, we next explored the role of endogenous *tai* in regulating SWH-signaling in developing imaginal discs. In contrast to *en>tai* animals, *en>tai^{IR}* animals demonstrate a marked reduction in the activity of the *ex-lacZ*, *th-lacZ*, and *DIAP4.3-GFP* reporters in the posterior wing disc compartment (Fig 5.6A-C). Next, we utilized the FLP-FRT system to generate mitotic clones of the strong loss of function allele of *tai^{61G1}* in the eye. These *tai^{61G1}* clones are marked by the absence of GFP and show a pronounced decrease in *tai* steady-state levels (Figure 5.4A). As with the *en>tai^{IR}* animals in the wing, *tai^{61G1}* cells in the eye display a marked reduction of *th-lacZ* activity, especially behind the morphogenetic furrow (Figure 5.6). Thus ectopic *tai* can elevate *yki*-signaling, and reduction of *tai* can dampen *yki*-activity, suggesting a role for *tai* in regulating SWH-pathway activity.

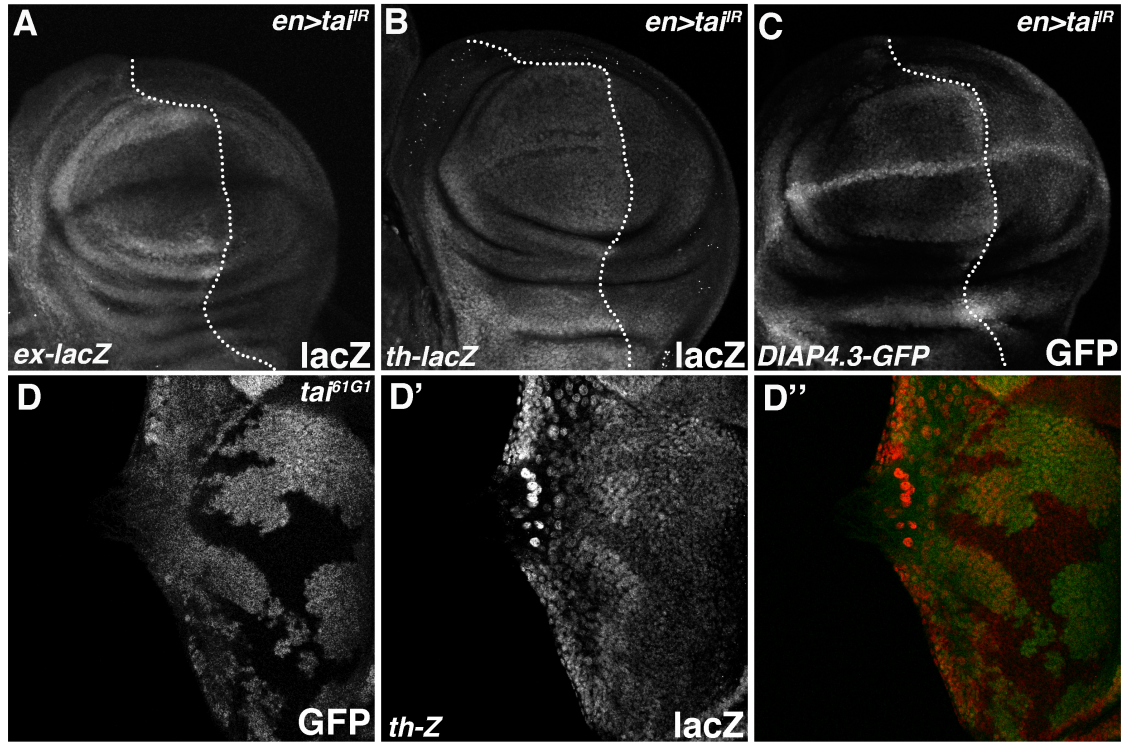


Figure 5.6. *tai* is required for basal Yki-target gene expression. α - β -gal staining or GFP fluorescence in (A-C) *en>tai^{IR}* wing discs and (D) *tai^{61G1}* eye clones carrying (A) *ex-lacZ*, (B,D) *th-lacZ*, or (C) *DIAP4.3-GFP*. *tai^{61G1}* clones are marked by the absence of GFP.

***yki* is required for *tai* to elevate *ex-lacZ* and drive imaginal discs growth**

Given the well-documented role of *tai* and its mammalian ortholog NCOA-3 (Nuclear receptor co-activator 3) in transcriptional co-activation [218], it is plausible that *tai* may operate in a pathway independent of *yki* to elevate SWH-reporter activity. Thus, we utilized an inverted-repeat directed at *yki* to reduce *yki*-levels in the background of excess *tai*, and analyzed the activity of *ex-lacZ* to determine whether *yki* was required for *tai* to elevate *ex-lacZ* in the wing. As noted above, ectopic expression of *tai* elevates *ex-lacZ* in the posterior compartment of *en>tai* animals (Figure 5.7A-B). However, when *yki^{IR}* is introduced into the background of *en>tai* animals, there is a marked reduction in *ex-lacZ* activity compared to *en>tai* animals alone (Figure 5.7B,D), indicating that *tai* requires *yki* to elevate *ex-lacZ* activity. Intriguingly, not all areas of *en>tai* discs are suppressed by *yki^{IR}*; in fact, we noted a consistent elevation in a portion of wing hinge in the posterior compartment of *en>tai^{IR},yki^{IR}* wing discs, indicating that cells in this portion of the wing hinge may be able to bypass the requirement of *yki* to elevate *ex-lacZ*. We also quantified the growth of the posterior compartments in these backgrounds and found, that as with the ability to activate *ex-lacZ*, *tai* requires *yki* to drive growth in the wing imaginal discs (Figure 5.7E).

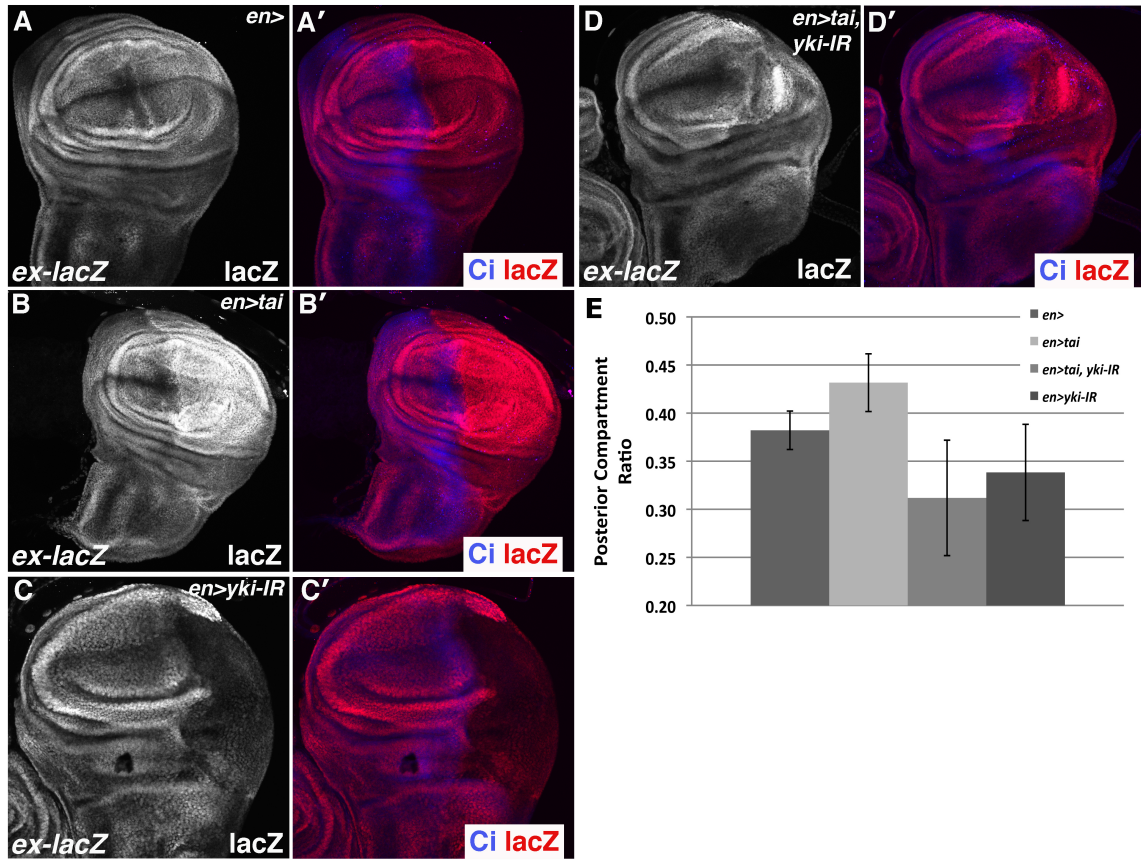


Figure 5.7. *yki* is required for *tai*-driven overgrowth. α - β -gal and Ci staining in (A) *en*, (B) *en>tai*, (C) *en>yki^{IR}*, or (D) *en>tai,yki^{IR}* wing discs carrying *ex-lacZ*. Ci marks the anterior domain where no transgene is being expressed. (E) Posterior compartment analysis of larval wing discs in the indicated genotypes. GFP was co-expressed to mark posterior domains. Ci-staining was used to mark anterior domains.

***tai* growth phenotypes occur independently of the bHLH and *ecdysone* signaling**

We next focused on determining the role of known regulators of *tai* in modulating *tai*-dependent growth phenotypes. The Tai polypeptide contains two N-terminal protein-protein interaction domains, including a β -Helix-loop-helix (β -HLH) and PAS (Per-Arnst-Sim) domain, a central LXXLP motif critical for physical interactions with steroid receptors, and a C-terminal 'activation-domain' that contains several poly-glutamine tracks that are critical for transcriptional co-activation [113]. Studies have demonstrated that JAK-Stat signaling can restrict Tai via the BTB protein Abrupt that physically interacts with the Tai β -HLH and promotes Tai turnover [215]. We utilized a transgenic construct of *tai* that lacks the β -HLH domain [215], *tai^{iB}*, and assessed its ability to drive overgrowth and *yki* activation *in vivo*. As with the wild-type transgene, ectopic expression of *tai^{iB}* drives significant overgrowth of the eye and activates the *ex-lacZ* SWH-reporter in the wing, both clonal fashion and when expressed with *en-GAL4* (Figure 5.8). Furthermore, *tai^{iB}*-driven overgrowth appears to be stronger than the wild-type *tai* transgene, as the tissue in these animals appears more disorganized (BSR unpublished data). Moreover, expression of MMP-1, a marker of neoplasia [22], is higher in *tai^{iB}* cells and there is a pronounced defect in pupariation when overexpressed in the eye (Figure 5.9; BSR unpublished data). These data argue that the β -HLH is not required for *tai*-dependent growth phenotypes and, in fact, may function to suppress them.

Next we examined the role of *ecdysone* signaling in regulating SWH-activity, given the well-documented connection between *tai* and *ecdysone*, and studies highlighting role of *ecdysone* in regulating autonomous imaginal disc growth in *Drosophila* [112, 219]. First, we tested whether a construct containing only the *tai^{LXXLP}* motif could phenocopy *tai*-driven growth phenotypes; it could not (Figure 5.10A). Next, we expressed a previously utilized inverted-repeat directed at all the *ecdysone*-receptor isoforms [219] and found that it was unable to reduce *ex-lacZ* activity (Figure 5.10B). Finally, we transgenically overexpressed *EcR* isoforms to see if they could recapitulate the phenotypes observed by transgenic overexpression of *tai* and found that unlike *tai*, *EcR* isoforms are unable to elevate *ex-lacZ* expression in wing disc epithelia (Figure 5.10C-F). These data suggest that *ecdysone* signaling does not appear to regulate Yki-activity in *Drosophila*, and thus *tai* does not likely operate through this pathway to ectopically activate *yki*-activity *in vivo*.

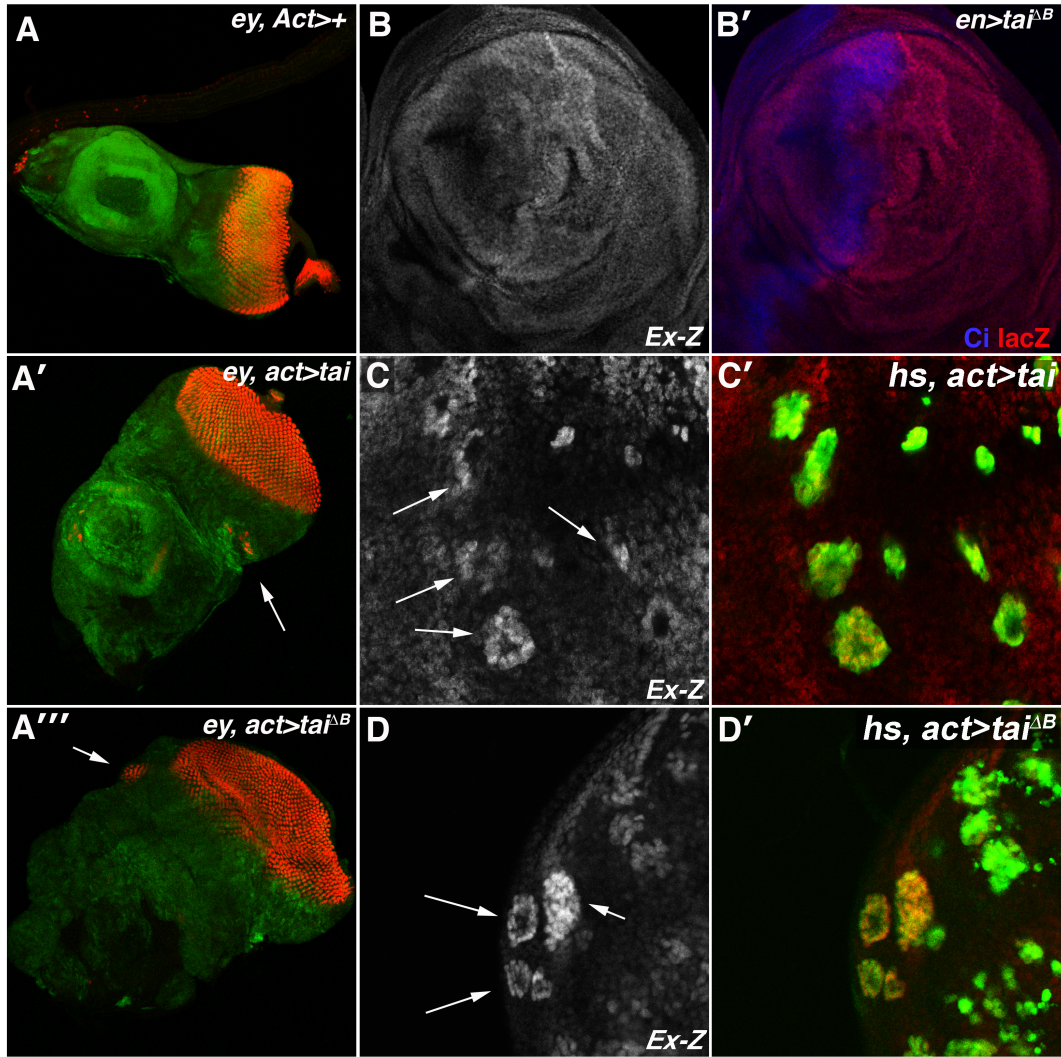


Figure 5.8. The *tai* β -HLH domain is not required for *tai*-driven overgrowth.

(A). α -elav staining and GFP fluorescence in (A) *ey, act>+*, (A') *ey, act>tai*, and (A'') *ey, act>tai^{ΔB}* flies carrying UAS-GFP. Arrows denote ectopic furrows in *ey, act>tai* and *ey, act>tai^{ΔB}* animals. (B). α - β -gal and Ci staining in (B) *en* and (B') *en>tai^{ΔB}* flies carrying *ex-lacZ*. Ci marks the anterior domain where no transgene is being expressed. (C-D). 'flp-out' clones expressing (C) *tai* and (D) *tai^{ΔB}* transgenes in flies carrying *ex-lacZ*. Arrows denoted elevated *ex-lacZ* in clones.

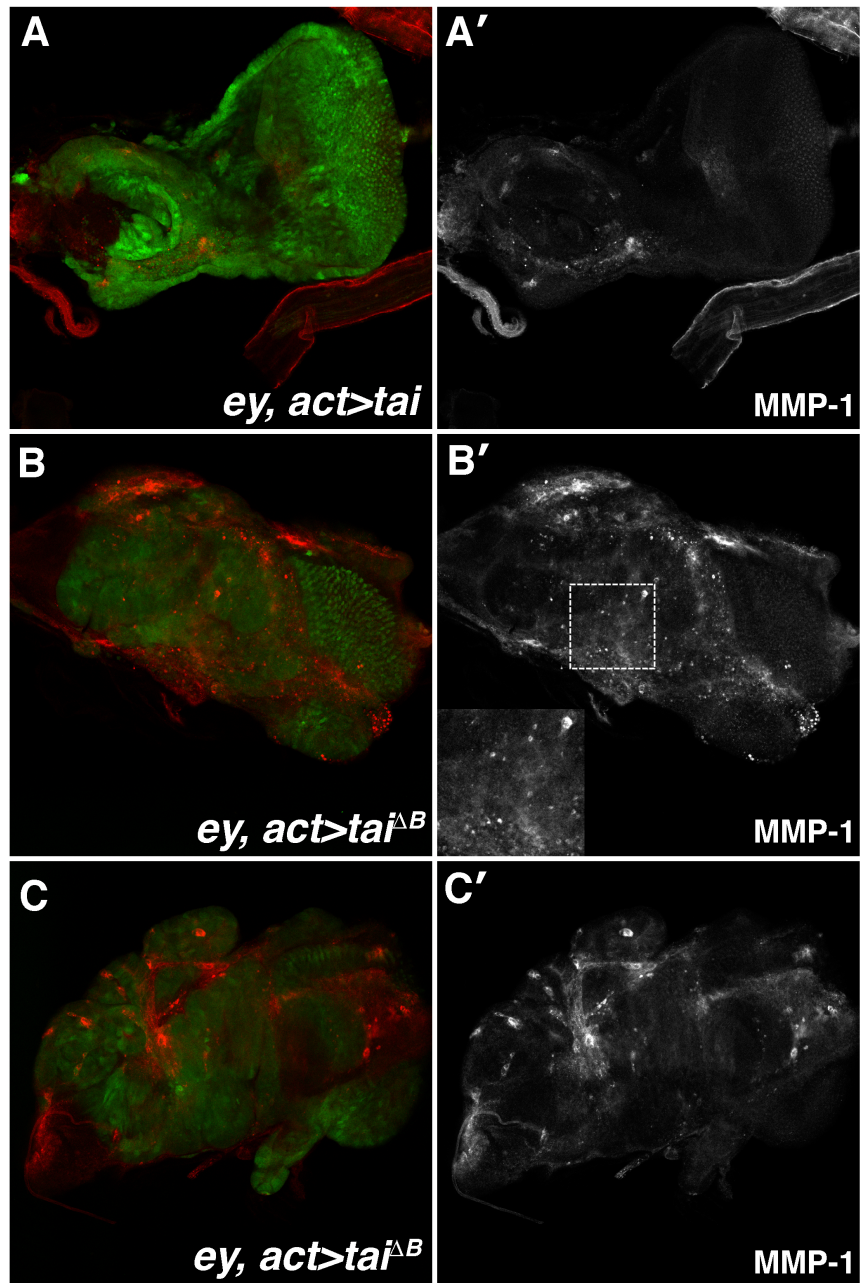


Figure 5.9. Tai elevates MMP-1 expression. α -MMP1 staining and GFP fluorescence in (A) *ey, act>tai*, and (B-C) *ey, act>tai^{ΔB}* flies carrying UAS-GFP.

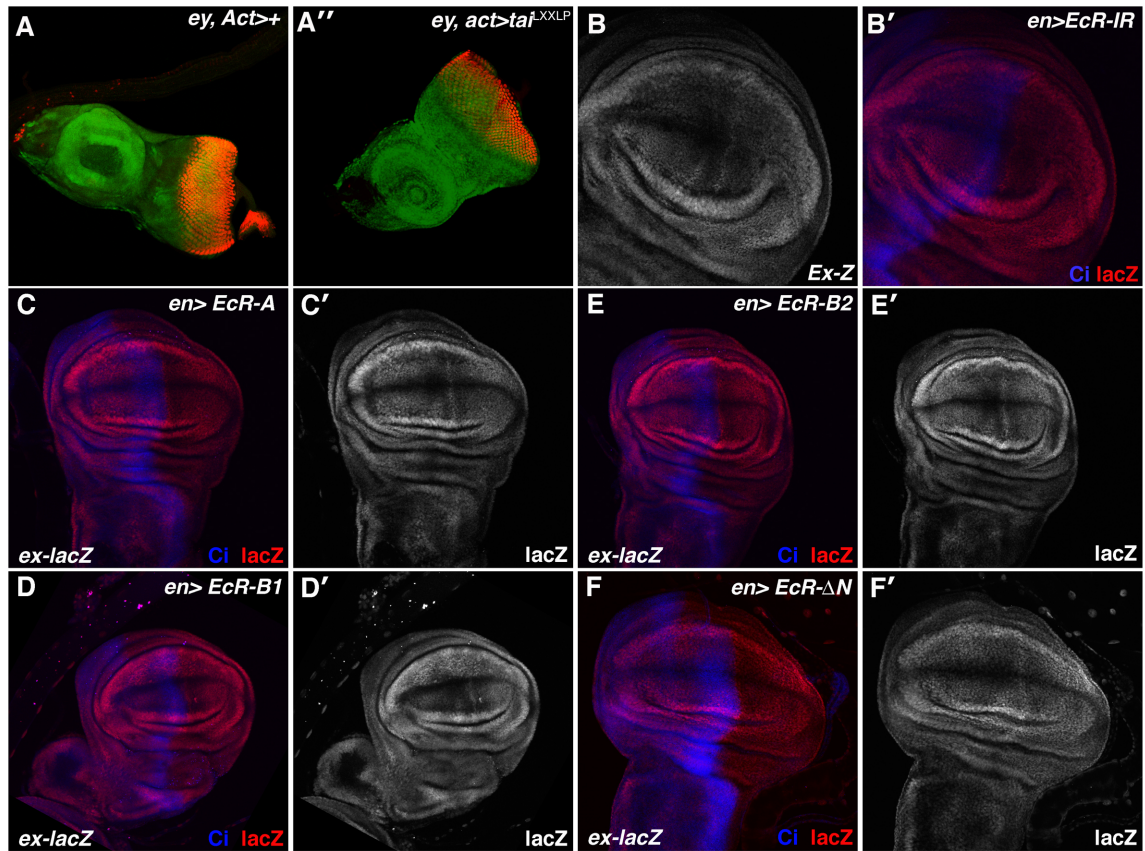


Figure 5.10. The *tai* β -HLH domain is not required for *tai*-driven overgrowth.

(A). α -elav staining and GFP fluorescence in (A) *ey, act>+* and (A') *ey, act>tai^{LXXLP}* flies carrying UAS-GFP. (B-F). α - β -gal and Ci staining in (B) *en>EcR^{IR}*, (C) *en>EcR^A*, (D) *en>EcR^{B1}*, (E) *en>EcR^{B2}*, or (F) *en>EcR^{ΔN}* flies carrying *ex-lacZ*. Ci marks the anterior domain where no transgene is being expressed.

***tai* functions genetically downstream of core pathway components to control organ size**

To clarify how *tai* functions to regulate *yki* reporters in cells we examined epistatic relationships between *tai* and known SWH components. The Wts kinase phosphorylates Yki on many sites, including S168, and this prevents Yki nuclear co-activation of pro-growth programs via 14-3-3 protein binding and cytosolic sequestration [85]. A serine-to-alanine mutant of Yki at S168 (Yki^{S168A}) uncouples Yki from this Wts-mediated inhibition and hyperactivates Yki-signaling in cells. *GMR-GAL4* (Glass Multimer Reporter) driven transgenic expression of *UAS-Yki^{S168A}* results in animals that eclose with a hyperplastic eyes [176]. We reasoned that if *tai* acts upstream of *wts* activity to regulate Yki reporters, *tai^{IR}* would *not* be unable to suppress the enlarged eye size of *GMR>yki^{S168A}* animals. Reciprocally, we reasoned that if *tai* acts downstream of the core cassette to activate Yki reporters, *tai^{IR}* might suppress the *GMR>yki^{S168A}* growth phenotype. Consistent with this latter model, we observed that *GMR>yki^{S168A}, tai^{IR}* animals eclose with substantially less growth phenotypes than *GMR>yki^{S168A}* animals (Figure 5.11). Conversely, we also observe that transgenic overexpression of Tai (*UAS-tai*) in the *GMR>yki^{S168A}* background enhances eye overgrowth (Figure 5.11). Together, these data suggest that *tai* acts downstream of the core kinase cassette (i.e., *hpo* and *wts*) to enhance Yki nuclear outputs.

Our analysis of the *ex-lacZ* reporter suggested, in part, that Tai expression could rescue reduced *yki*-activity in cells. In order to better understand how *tai* may with Yki in the nucleus to control Yki-outputs, we next assessed the ability of Tai to

activate a 32-bp β -galactosidase reporter derived from the *thread* promoter (e.g., the hippo response element or HRE-lacZ) that is activated by loss of *wts* [88]. We reasoned that if Tai acted to control Yki overgrowth through direct interactions of Yki-Sd, it would activate this reporter when overexpressed. However, if Tai mediated its effects through cooperative interactions with Yki-Sd on the *thread* promoter, it would not. As with this latter model, we did not observe activation of the 32-bp HRE with Tai overexpression (Figure 5.12)

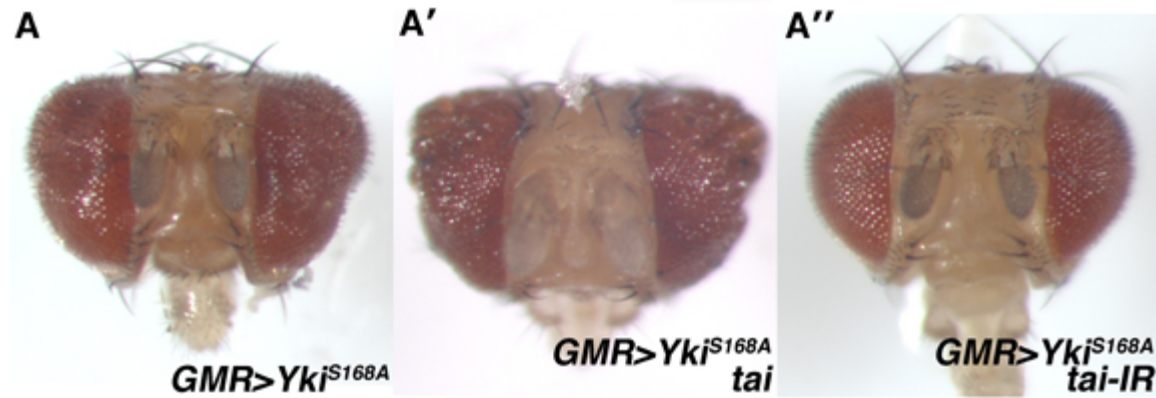


Figure 5.11. *tai* modifies Yki^{S168A} -driven overgrowth. Light microscopic images of (A) $GMR>yki^{S168A}$, (A') $GMR>yki^{S168A},tai$ and (A'') $GMR>yki^{S168A},tai^{IR}$ eyes and heads. Images were taken using identical microscope setting.

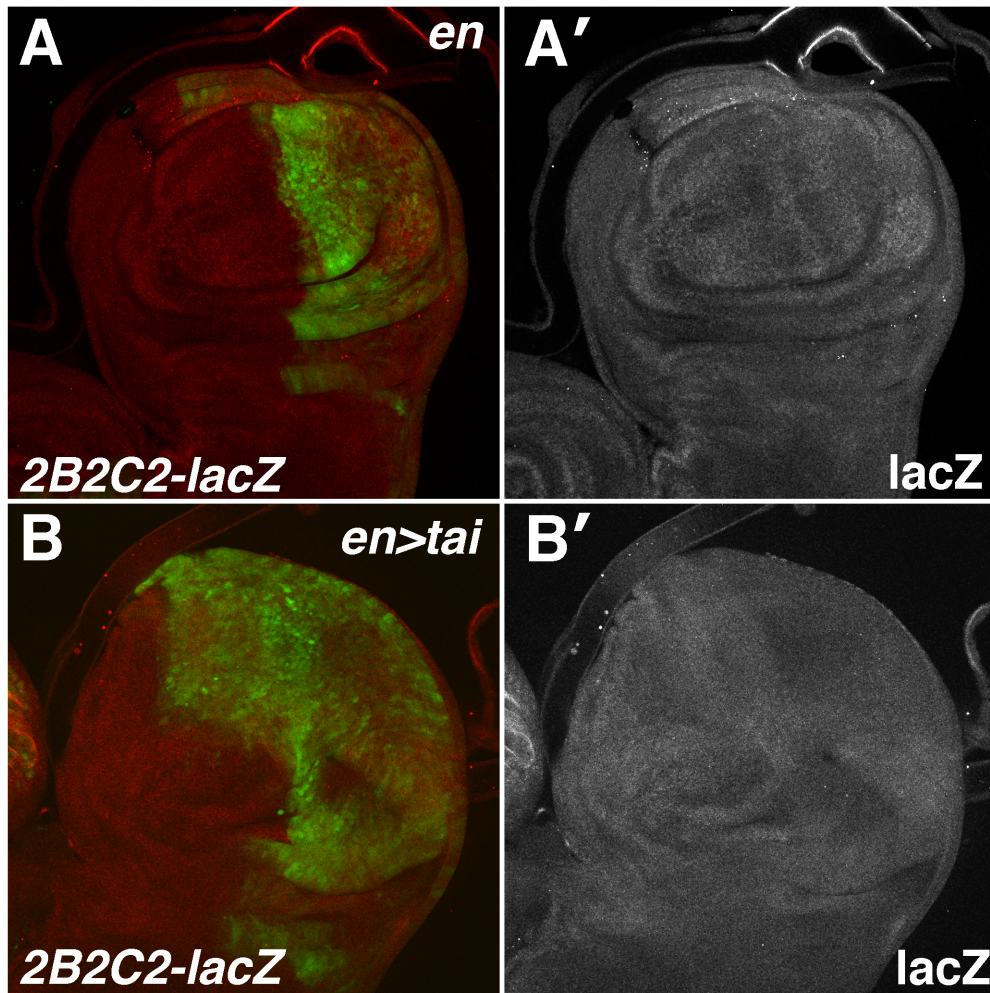


Figure 5.12. *tai* does not activate the 32bp-HRE. α - β -gal staining and GFP fluorescence in (A) *en* and (B) *en>tai* flies carrying the *yki*-responsive 32-bp HRE (2B2C2-lacZ) and UAS-GFP. HRE = Hippo response element

DISCUSSION

The control of organ size operates through the coordination of cell size, division, and death programs. Here we show a novel role for the transcriptional co-activator *taiman* in regulating the outputs of the Salvador-Warts-Hippo (SWH) pathway, a signaling module that coordinates cell growth, division, and death programs in cells to control organ size in metazoans [220]. We find that ectopic expression of *tai* elevates SWH-pathways outputs, while reduction of *tai* reduces them. Moreover, we show that *tai* and Yki cooperate together to elicit these effects: Tai cannot fully activate SWH-signaling without *yki*, while reciprocally, Yki cannot drive overgrowth in the absence of *tai*.

While we are learning more everyday about upstream inputs into SWH-signaling, less is known about how Yki functions within the nucleus to drive proliferative programs. Several studies have uncovered Yki-binding partners required for Yki localization to target promoters [86-89]. Moreover, emerging data suggests that Yki can cooperate with other transcriptional programs to elicit proliferative responses in cells [134, 213]. The data presented here appear to place Tai in this latter scenario, in light of our observations that (1) ectopic expression of *tai* can rescue *ex-lacZ* expression in *yki*-deficient cells and (2) *tai*-overexpression is unable to activate the 32-bp *wts*-responsive-response-element on the *th* promoter (BSR personal communication). It will be interesting to understand how *tai* mediates these effects, whether through co-activating similar promoters at distinct sites or through directly binding to Yki or known Yki-binding partners and modulating their activity in cells (see model, Figure 5.12). Indeed precedence exists

for both these scenarios in vertebrate systems, as studies have highlighted a role for SRC-3 binding to and potentiating the YAP-binding partner TEAD-1 (e.g., *sd*) and E2F1 [221, 222], a collaborator of Yki/Sd target promoters in *Drosophila*.

Detailing the signals that promote *tai* co-activation of SWH-promoters in cells will be important as well. Our data suggest that *tai* co-activation occurs in the absence of Ecdysone and JAK-STAT signaling, two inputs previously linked to *tai*-activity in *Drosophila* [113, 215]. Moreover, we find that *tai*-dependent regulation of SWH-outputs appears to be context specific; *tai* loss reduces *th-lacZ* expression in both the wing and the eye, but in the eye this effect is limited cells behind the morphogenetic furrow. Also, we observed that while Tai overexpression can elevate the Yki-target *ban*, reduction of Tai does not have reciprocal effects (BSR personal communication). Understanding these contexts, as well as in what other systems Tai and Yki cooperate together, like the follicular epithelium where *tai* has been studied more exhaustively, will be revealing too as studies in these epithelia have already providing insight in SRC-3's tumor-promoting properties in vertebrates [223]. Lastly, determining which of the post-translational modifications that impinges on SRC-3 in vertebrate systems—including sumoylation, phosphorylation, and acetylation—also impinge on Tai will also be helpful into understanding *tai*-dependent regulation of organ size control [224].

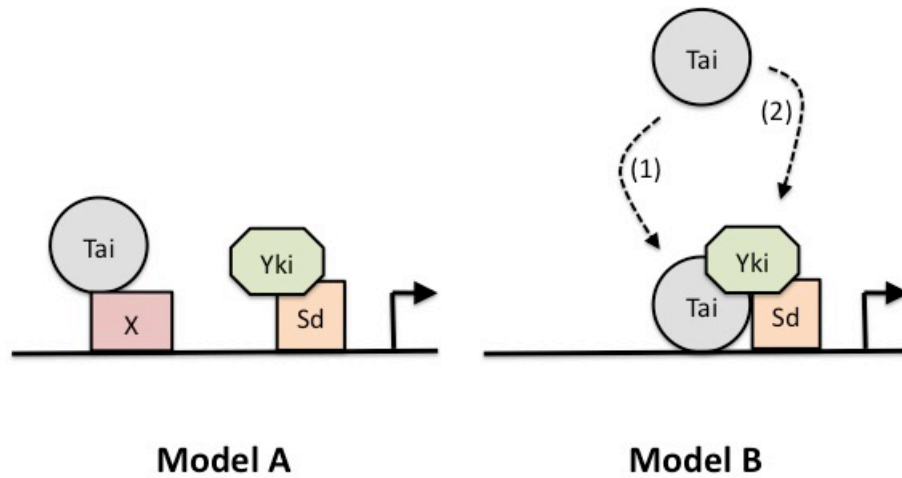


Figure 5.13. Models of *tai*-dependent regulation of SWH-signaling. In Model A (left), *Tai* influences *Yki*-*Sd* target gene expression by binding to distinct promoter elements and cooperating with *Yki*-*Sd* gene activation. In Model B, *Tai* directly influences *Yki* and/or *Sd* through either (1) complexing with it on promoters or (2) regulating *Yki* and *Sd* levels and/or activity in cells.

EXPERIMENTAL PROCEDURES

Genetics

Crosses performed at 25°C unless noted. Alleles used: *UAS-tai*; *UAS-tai^B*; *UAS-tai-IR* (Bloomington stock center, #28971); *UAS-tai^{LXXLP}*; *tai^{61G1}*; *ex⁶⁹⁷*; *thi^{c58}*; *DIAP4.3-GFP*; *ban-GFP*; *UAS-yki-IR* (VDRC, KK line); *2B2C2-lacZ*; *UAS-ECR-IR* (BSC, #9327); *UAS-ECR-A*; *UAS-ECR-B1*; *UAS-EcR-B2*; *UAS-EcR-ΔN*; *UAS-yki^{S168A}-YFP* (K. Harvey). ‘Flp-out’ analysis used: *eyFLP;Act>CD2>Gal4;Rps17⁴,FRT80B*; *hsFLP*; *Act>CD2>Gal4*. Clonal analysis used: *eyFLP;ubi-GFP,FRT40A*.

Immunohistochemistry & Immunoblotting

Immunostaining and confocal microscopy were performed as described previously [189]. Antibodies used: mouse α - β -gal 1/1000 (Promega); mouse α -MMP-1, 1/100 of 1:1:1 aliquot of clones 5H7B11, 3B8D12, 3A6B4 (Developmental Studies Hybridoma Bank); rabbit α -Tai 1/1000 (D. Montell); rat α -elav 1/1000 (DSHB); mouse α -Ci 1/50 (DSHB).

Wing Measurements

Larval imaginal wing discs were imaged using confocal microscopy and quantified with Adobe Photoshop. Adult wings were imaged on a Leica DFC500 CCD camera and quantified with Adobe Photoshop. Posterior compartment ratio (PCR) = posterior compartment size/total wing size.

BrdU incorporation Assay

Briefly, wing discs were dissected in Schneiders media and transferred into 500 μ l

of Schneider's containing 10mM BrdU for 30' incubation. Discs were then washed 2X in PBS, pH 7.4 and fixed overnight at 4° in 1.5% formaldehyde/0.01% Tween-20 in PBS. Following overnight incubation, discs were then washed 5X with PBS and treated with DNase for 45' at 37°C (RQ1 DNAase Promega). Discs were then washed 3X with PBS/0.3% Triton X-100 and incubated with anti-BrdU (1:100) in 10% normal goat serum and PBS/0.1% Triton X-100. Following at least a 2-hour incubation in primary antibody, discs were then washed and incubated with goat-anti-mouse-cy3 in 10% normal goat serum and PBS/0.1% Triton X-100. This was followed by 5X washes in PBS/0.3% Triton X-100 and subsequent mounting on slides for visualization.

Chapter 6: Future Directions

FUTURE DIRECTIONS

The work presented here defines previously unrecognized links between polarity, endocytic, and nuclear receptor programs with an emerging tumor suppressor network, the SWH-pathway (Figure 6.1). In the section that follows, I will briefly summarize where I feel each of the studies performed herein fit within our greater understanding of growth control, followed by a brief discussion of the questions I believe should be addressed in the immediate future. I will then conclude with a brief discussion of the larger context of the SWH-pathway in the field of growth biology and speculate on its future in the coming years.

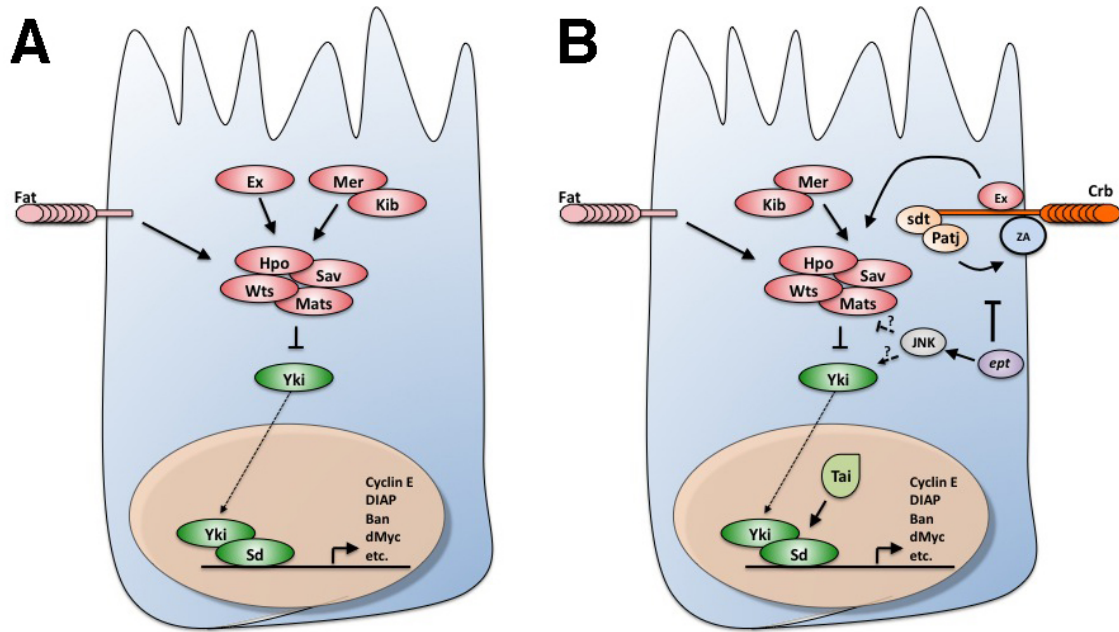


Figure 6.1. Elaboration of the SWH-signaling network. Schematic representations of our understanding of SWH-signaling both (A) before and (B) after studies performed in this dissertation.

The Crbⁱ Dominant-Modifier Screen

The most significant finding from the Crbⁱ Dominant-modifier screen is the genetic interaction observed between Crbⁱ and the SWH-pathway. These observations led to the identification of a clear molecular link between Crb and the SWH-component Expanded, which has since been confirmed by several other labs [143-145]. In view of this link, it now appears that the Crbⁱ dominant-modifier screen may potentially represent a screen against excess SWH-activity in cells. This is significant, given our relative lack of knowledge of how SWH-activity is controlled in cells, and the well-characterized role of SWH-signaling in diseases like cancer (reviewed in [82]). Thus, determining the gene or genes responsible for the modification of Crbⁱ we observed in the deficiency dominant modifier screen is imperative.

This will not be an easy task, given the initial 'hit-list' contains over 20 deficiencies that reproducibly modify Crbⁱ-driven overgrowth. Moreover, as each of these loci remove anywhere from 100-1000 genes, loci identification by simply crossing an allele of every gene in the uncovered region may prove laborious. I found this to be true, even when I narrowed down the modifying region using smaller overlapping deficiencies (as was the case for the identification of *taiman* as a Crbⁱ-modifier). If the hope is to find genes that function act to control SHW-activity in cells, my approach would be to take the original ~20 deficiencies and test their ability to modify other SWH-phenotypes. This should generate a smaller list of modifiers that more likely represents SWH-pathway components, making deficiency-modifier mapping both more manageable and productive. For instance, one may predict that any Crbⁱ-modifier that acts downstream of Crbⁱ to control Yki

activity may also modify an *en>ex-IR* or *en>crb-JM* growth phenotype, since the overgrowth attributed to both these phenotypes is increased Yki-activity in cells. To extend this analysis, you could perform epistatic analysis as well; screening against *wts-IR* or *yki-S168A* phenotypes will allow for the identification of loci that act downstream of the core kinase cassette (e.g., Wts) to promote SWH-dependent proliferation. Finally, given that Crb is connected other functions in cells (i.e., polarity formation) this approach need not be limited to SWH-pathway analysis solely. For instance, testing Crbⁱ-modifiers against *dlg-IR*, *lgl-IR*, or *crb-PBM* phenotypes may delineate additional regulators of apicobasal polarity formation in cells.

In addition to isolating the unidentified gene or genes responsible for dominant modification of *en>crbⁱ* animals, future studies should also focus on determining the molecular basis for the genetic interactions we observed between Crbⁱ and those genes we have mapped to a specific locus. These genes include *taiman (tai)*, *rho1*, *CTP:phosphocholine cytidyltransferase 1 (cct1)*, *rpt1*, *TNF-receptor associated factor-4 (traf4)*, *ventral veins lacking (vvl)*, and *target of wingless (tow)*. Considerable work in this thesis has been performed to understand the molecular basis of *tai* (see Chapter 5, or discussion later in this chapter). In my opinion the other candidates are equally as attractive, despite having a less apparent connection to tumor formation in vertebrates. Cct1 is an enzyme required for the rate-limiting step in phosphatylcholine production at the plasma membrane, and mutants show defects in efficient endocytosis in cells (though not in endolysosomal transit) [225, 226]. Mutants in CCT1 show defects in Notch and

EGFR signaling [226]. It will be interesting to determine whether mutants also display defects in SWH-signaling, given the recent data showing reliance of SWH-signaling on phospholipid composition at the plasma membrane [227]. RhoA is a well-characterized small GTPase, whose connection to apicobasal polarity proteins is well documented [228]. Given the emerging data connecting of RhoA to JNK [152, 229], and JNK to SWH [80, 149-151, 196], it will be intriguing to see whether a linear pathway exists in the background of excess Crb. Moreover, given the recent data showing that Ex becomes hyperphosphorylated when localized to membranes [143], and our data showing that RhoA is among the strongest suppressors of Crb-driven overgrowth, it will be interesting to determine whether RhoA activates a kinase (i.e., ROCK) that phosphorylates Ex and promotes its degradation in cells (see later discussion in this chapter). Vvl and Tow are two proteins thought to operate in the nucleus [230, 231]; it will be interesting whether their regulation impinges on nuclear inputs of SWH-signaling like Tai. Finally, Traf4 was identified in a yeast-two-hybrid as a protein that binds to and activates the ste-20 kinase Mishappen, the upstream MAP kinase kinase kinase kinase of JNK [154]. We observed that co-expression of Traf4 significantly suppressed Crbⁱ-driven overgrowth; perhaps this suppression, as with RhoA, is either an indication of a reliance on JNK-signaling for Crbⁱ-driven overgrowth or via an ability of Traf4 to suppress other ste-20-like kinases such as Hippo in cells.

The Crb-Ex Regulatory Network

Our identification of Crb as an upstream regulator of the SWH-pathway is significant for a number of reasons. First, it comes at a time when few upstream inputs into the core kinase cassette (i.e., Hippo and Warts) of SWH-signaling are known. Second, it reiterates an emerging concept that adhesive proteins emanating from the cell periphery can suppress cell proliferation through a singular signaling network [232]. Third, and perhaps most significant, it provides insight into how polarity factors can influence the proliferation of cells.

Shortly after publishing our findings that Crb regulates the levels and localization of the apical SWH-component Ex [201], several other studies showed similar results [143-145]. These studies both confirmed our findings, and added new insights as well. Crb is clearly required for the proper localization of Ex to the membrane, as multiple studies demonstrate that *crb* clones show an absence of Ex from the sub-apical membrane of cells [143, 144, 201]. Moreover, Ling et al. demonstrate that Crb can bind to Ex in cultured cells and recruit it to membrane fractions [143]. Chen et al. found that Ex is lost from the membrane of wild-type cells that are surrounded by cells lacking Crb, indicating that trans acting homophilic interactions of Crb are required for these effects [144]. Thus these studies, as with ours, show that Crb clearly can act as a tumor suppressor by recruiting Ex to the sub-apical region and promoting its activity in cells (see Figure 6.2).

Our findings indicate that Crb can also exert inhibitory actions on Ex as well, though how it exerts these effects is less clear. We observe that overexpression of

Crbⁱ results in depletion of Ex from cells, that is dependent on the activity of the proteasome. Intriguingly, Ling et al. found that myristoylation of Ex can promote its phosphorylation and turnover in cultured cells. Thus, perhaps Crbⁱ recruits Ex to the subapical region in cells, where Ex is then phosphorylated and subsequently degraded in cells. Consistent with this model, studies in mouse fibroblasts show that the activity and localization of proteins structurally similar to Ex, the ERM proteins, can be regulated by Rho-kinase [233, 234].

Future studies should clarify several unanswered questions remaining from these studies. Is Ex phosphorylated *in vivo*? If so, what is the kinase responsible? aPKC may be an ideal kinase, given its apical-lateral localization in cells. However, in light of the suppression of Crbⁱ-driven overgrowth we observed with alleles of RhoA, perhaps a kinase downstream of RhoA is more primary. Determining how Ex is degraded in the background of excess Crbⁱ will also be important. Is it via proteosomal degradation, as our data suggest? Studies examining (1) Ex ubiquitination in cells and (2) whether any E3-ligases effect Ex levels may prove insightful. Finally, understanding the contexts with which this system operates is critical. In what tissues does Crb act to restrict SWH-activity? Is this system involved in epithelial-to-mesenchymal transitions, where adhesive contacts act to restrict cellular proliferation? What is the role of the large extracellular domain of Crb in regulating SWH-activity? To what degree is the Crb-Ex pathway conserved across metazoans?

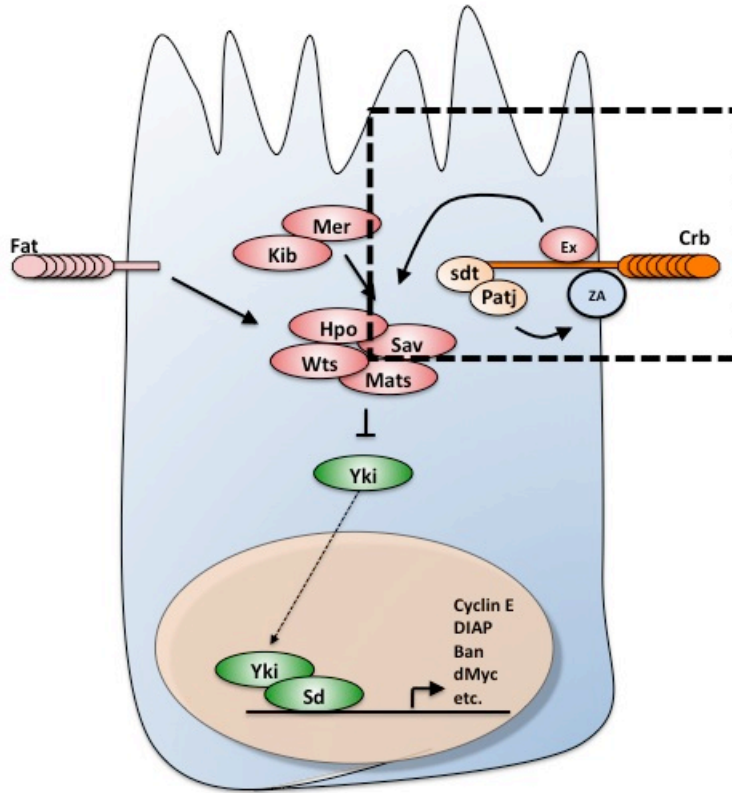


Figure 6.2. Model of the Crb-Ex regulatory network. Crb functions as a dual regulator of polarity and growth by recruiting factors Sdt and Patj to the apical-lateral domain via interactions with its C-terminus, and the SWH-regulator Ex via interactions with its juxtamembrane domain. Not represented is the inhibitory role of Crb on Ex expression, where Crb promotes Ex turnover in cells. See text for detailed explanation.

Endocytic Regulation of SWH-signaling

The observation that *Crbⁱ* overexpression can elevate SWH-outputs led us to ask whether similar phenotypes exist in mutants that contain excess amounts of *Crb* *in vivo*. To date, endocytic neoplastic tumor suppressor genes (nTSGs) are the only class of genes with such a phenotype. Thus, the observation that (1) all endocytic nTSGs contain elevated *yki*-activity and (2) late endocytic nTSGs display reduced Ex levels is significant for it provides *in vivo* confirmation of our transgenic *en>crbⁱ* system (see Figure 6.3).

However, the conclusions from these results should be tempered, as we also observed an elevation in JNK-signaling in the background of reduced endocytosis, which has been linked to Yki-signaling in several contexts [80, 149-151, 196]. Thus, determining the relative contribution of each of these systems to the elevated Yki-signaling observed in endocytic nTSGs will be important in interpreting these results we obtained. Does reduction of JNK-signaling with a dominant-negative JNK transgene completely rescue the altered SWH-signaling observed in *erupted* mutant cells? Or does some altered SWH-signaling persist? Conversely, is JNK-signaling altered in the background of excess *Crbⁱ*? If so, what if any does this contribute to the effect on Yki-signaling?

The observation that endocytic nTSGs alter SWH-signaling while concomitantly deregulating JNK-signaling, and that this deregulation occurs at each step of the endolysosomal pathway raises several additional questions. First, does the elevated Yki-signaling observed in endolysosomal mutants require JNK-activation? If so, how is JNK mediating this effect? Is it via transcriptional elements

(i.e., Jun/Fos) or through altered phosphorylation of SWH-components by Jnk? Second, how is JNK-signaling activated in the background of altered endocytosis? Many studies suggest that 'altered polarity' can contribute [79, 80, 204, 206], but even these studies lack mechanistic insight into how altered polarity promotes JNK-signaling. Is altered trafficking of the JNK-pathway receptor Wengen critical to the phenotype? Is RhoA aberrantly activated? Finally, it is clear that late-endocytic mutants display more severe activation of JNK-signaling and Yki-signaling than early-endocytic or internalization mutants: what is the molecular basis of this phenotype?

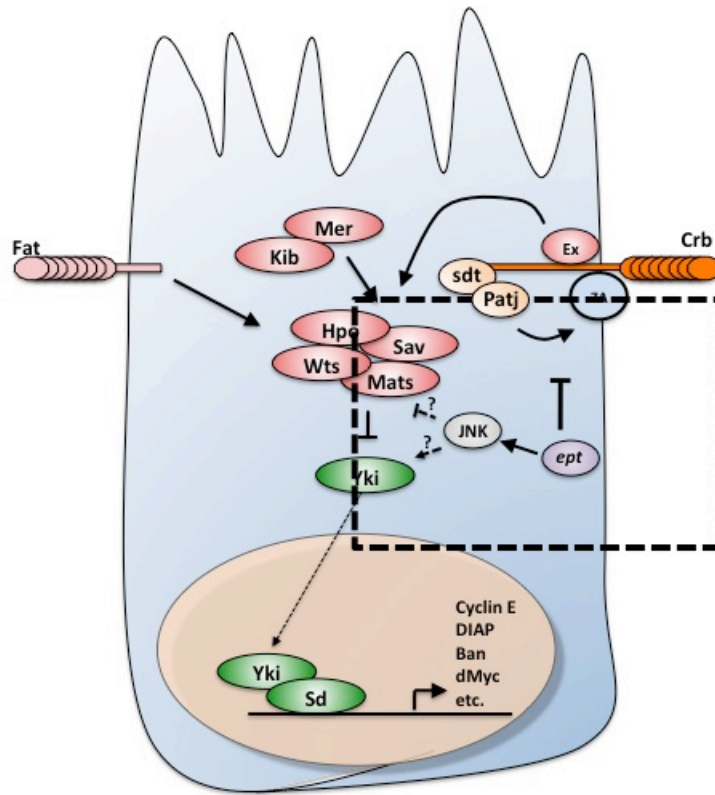


Figure 6.3. Model of SWH-control by endocytic regulators. Endocytic proteins like *ept* control the turnover of Crb leading to its buildup in cells, and activation of SWH-signaling. These proteins also deregulate JNK-signaling, leading the SWH-activation through unknown mechanisms. See text for detailed explanation.

Taiman

From both a developmental and disease perspective, the elucidation of *tai* as a potential regulator of SWH-signaling is significant (Figure 6.4). Relatively little is known regarding regulatory influences of Yki/YAP in the nucleus (reviewed in [82]). The observation that *tai* controls SWH-signaling within the nucleus lends insight into nuclear factors required efficient expression of SWH-outputs. Moreover, as *tai* is orthologous to human SRC-3/AIB1, a well-established oncogene linked to tumor formation in several organs (reviewed in [115]), the observation that *tai* regulates the basal expression and can ectopically elevate SWH-outputs delineates potential oncogenic mechanisms SRC-3 in humans.

Several unanswered questions remain from our examination of *tai*. Foremost among them is clarification of how *tai* mediates its effects on SWH-outputs. Does Tai physically associate with the promoter of known SWH-targets? If so, does Tai associated with known Yki-binding sites or with distinct regions (See Figure 5.13)? Moreover, determining the influence of *tai* on the levels and localization of any known nuclear SWH components (e.g., Yki, Sd, E2F1, etc) may prove useful. Perhaps the effects of *tai* on Yki-activity is mediated through control of E2F1, a known SWH-collaborator that has been shown to bind to SRC-3 in vertebrates [134, 221]? This hypothesis seems less likely given the dramatic difference observed between Tai and E2F1 overexpression phenotypes however should be explored. Additionally, it will be important to determine the context with which this system operates. How does the absence of the ecdysone nuclear receptor influence the ability of *tai* to activate Yki-signaling in cells? Are any of the other 17 nuclear receptors in

Drosophila required for these effects [235]? Does this system operate in vertebrates cells? This latter work may prove more tedious, as there are three SRC proteins in vertebrates, which behave redundantly in some contexts (reviewed in [218]). Similarly, vertebrates contain two orthologs of Yki, YAP and Taz, which exert different effects depending on the context with which they are activated. Given the well-characterized role of Taz in epithelial-to-mesenchymal transitions [236], and similar functions attributed to *tai* in the follicular epithelium [113], perhaps an interaction between SRC-3 and Taz should be explored first.

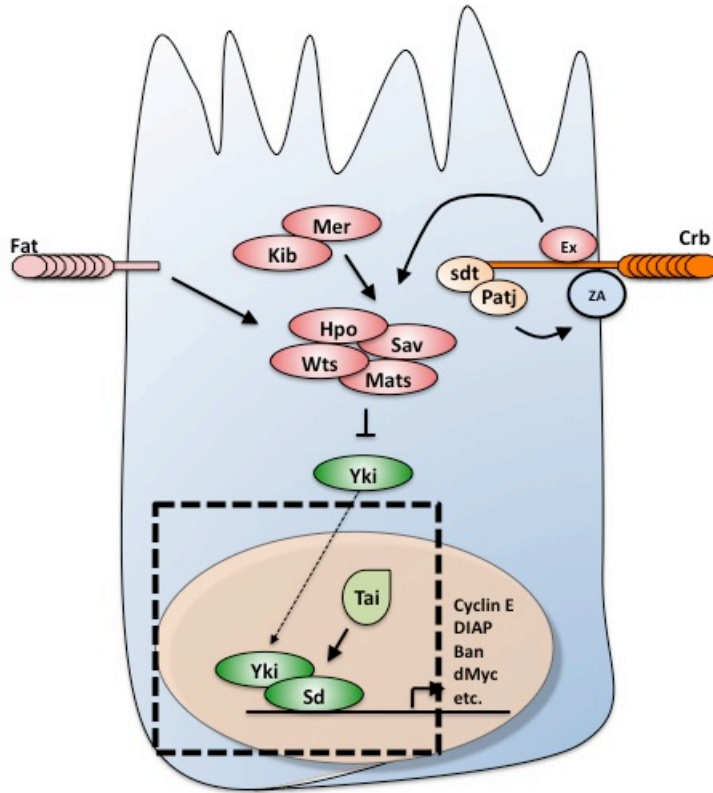


Figure 6.4. Model of SWH-control by *taiman*. In the nucleus, *tai* promotes the co-activation of Yki-Sd signaling through yet-unknown mechanisms. Whether it acts through direct or indirect mechanisms remains to be determined (see Figure 5.13). See text for detailed explanations.

CONCLUDING REMARKS

We have known for sometime that organs contain intrinsic information that dictates their eventual size. Ablation studies in mice have shown that the mouse liver can completely regenerate in 5-7 days after being reduced by over two-thirds its original mass [237]. Similarly, studies of *Drosophila* imaginal discs have shown that normal organs can be produced despite being reduced by 60% during development [238]. Likewise, studies in crickets and salamanders have shown a capacity to regenerate entire limbs upon amputation [239, 240]. And yet, despite knowledge of these observations for years, characterization of the underlying mechanisms detailing the intrinsic program regulating these effects has remained elusive.

The identification that loss of two kinases, Hippo and Warts, and their scaffolding partners could deregulate the ability of *Drosophila* organs achieve proper size has provided considerable insight the molecular machinery required for organ size control. Since their initial discovery, studies have placed these kinases into a linear network that function in a series to regulate proliferation by controlling the pro-growth transcription factor Yki [214]. Feeding into Hippo and Warts kinase activation are signals from a wide-variety of inputs including planar cell polarity, apicobasal polarity, morphogen gradients, actin polymerization, and endocytosis [146, 161, 162, 241-244]. These inputs appear to act in combinatorial fashion, as suggested by the relative minor growth defects observed in individual mutants compared to core pathway members (i.e, Hippo and Warts). Downstream of Yki/Yap are several factors, including DNA binding the partners Scalloped, Teashirt,

Homthorax, and SMAD [86-89]. As discussed in the sections above, the data presented in this thesis provides considerable insight into both of these inputs.

Future studies in *Drosophila* should focus on further clarifying how SWH-signaling operates in cells. What other extrinsic and/or intrinsic signals act to modulate Yki-activity in cells? Moreover, as many of the identified 'upstream regulators' show both a predilection for membrane localization and a network of protein:protein interactions with one another indicative of a large complex, one important question is whether SWH-components exist in cells as a multimeric complex that associates with the cytoplasmic tail of a membrane-bound receptor. Future studies should also focus on how Yki operates in the nucleus. What other factors does Yki co-opt to bind to DNA? Similarly, what factors does Yki recruit to promoters to enhance transcriptional co-activation? What promoters does Yki target? Which of these, if any, are critical to organ size deregulation?

A relatively exciting feature of studies involving the SWH-pathway has been the degree with which its composition and function remains conserved across metazoans [85]. Studies in mice have shown that Mst1/2 and Lats1/2, the orthologs of *hippo* and *warts* respectively, act in concert to restrict the activities of Yap, the vertebrate ortholog of Yki, to restrict the growth of multiple epithelia [85, 96, 245, 246]. Moreover, studies analyzing tumor formation in humans have shown that SWH-components are frequently targeted (reviewed in [197]). An intriguing finding comes from a recent study examining the role of SWH-signaling in NF2-driven (e.g., *Drosophila* Ex/Mer) in oncogenesis that indicate simple heterozygosity for YAP could suppress NF2-driven tumor formation in the liver [96]. These studies not only

provide pathophysiologic insight in a major cancer syndrome, but also indicate that even a mild reduction in YAP activity may be sufficient to restrain SWH-driven tumorigenesis. Thus, future studies examining small molecules that act to suppress Yap-activity may provide therapeutic value in treating human disease.

REFERENCES

1. Virchow, R., *Cellular Pathology: As Based Upon Physiological and Pathological Histology*. 1860, London: John Churchill.
2. Morgan, *Nobel Lectures, Physiology or Medicine 1922-1941*. 1965, Amsterdam: Elsevier Publishing Company.
3. Reiter, L.T., et al., *A systematic analysis of human disease-associated gene sequences in Drosophila melanogaster*. *Genome Res*, 2001. **11**(6): p. 1114-25.
4. Tweedie, S., et al., *FlyBase: enhancing Drosophila Gene Ontology annotations*. *Nucleic Acids Res*, 2009. **37**(Database issue): p. D555-9.
5. Huang, J., et al., *From the Cover: Directed, efficient, and versatile modifications of the Drosophila genome by genomic engineering*. *Proc Natl Acad Sci U S A*, 2009. **106**(20): p. 8284-9.
6. Brand, A.H. and N. Perrimon, *Targeted gene expression as a means of altering cell fates and generating dominant phenotypes*. *Development*, 1993. **118**(2): p. 401-15.
7. Golic, K.G. and S. Lindquist, *The FLP recombinase of yeast catalyzes site-specific recombination in the Drosophila genome*. *Cell*, 1989. **59**(3): p. 499-509.
8. Rorth, P., *A modular misexpression screen in Drosophila detecting tissue-specific phenotypes*. *Proc Natl Acad Sci U S A*, 1996. **93**(22): p. 12418-22.
9. Dietzl, G., et al., *A genome-wide transgenic RNAi library for conditional gene inactivation in Drosophila*. *Nature*, 2007. **448**(7150): p. 151-6.
10. Ni, J.Q., et al., *A Drosophila resource of transgenic RNAi lines for neurogenetics*. *Genetics*, 2009. **182**(4): p. 1089-100.
11. Pignoni, F., et al., *The eye-specification proteins So and Eya form a complex and regulate multiple steps in Drosophila eye development*. *Cell*, 1997. **91**(7): p. 881-91.
12. Xu, T., et al., *Identifying tumor suppressors in genetic mosaics: the Drosophila *lats* gene encodes a putative protein kinase*. *Development*, 1995. **121**(4): p. 1053-63.
13. St Johnston, D., *The art and design of genetic screens: Drosophila melanogaster*. *Nat Rev Genet*, 2002. **3**(3): p. 176-88.
14. Bennett, F.C. and K.F. Harvey, *Fat cadherin modulates organ size in Drosophila via the Salvador/Warts/Hippo signaling pathway*. *Curr Biol*, 2006. **16**(21): p. 2101-10.
15. Harvey, K.F., C.M. Pflieger, and I.K. Hariharan, *The Drosophila *Mst* ortholog, *hippo*, restricts growth and cell proliferation and promotes apoptosis*. *Cell*, 2003. **114**(4): p. 457-67.
16. Moberg, K.H., et al., *Archipelago regulates Cyclin E levels in Drosophila and is mutated in human cancer cell lines*. *Nature*, 2001. **413**(6853): p. 311-6.
17. Pantalacci, S., N. Tapon, and P. Leopold, *The Salvador partner Hippo promotes apoptosis and cell-cycle exit in Drosophila*. *Nat Cell Biol*, 2003. **5**(10): p. 921-7.

18. Emery, G., et al., *Asymmetric Rab 11 endosomes regulate delta recycling and specify cell fate in the Drosophila nervous system*. Cell, 2005. **122**(5): p. 763-73.
19. Janody, F., et al., *A mosaic genetic screen reveals distinct roles for trithorax and polycomb group genes in Drosophila eye development*. Genetics, 2004. **166**(1): p. 187-200.
20. Savant-Bhonsale, S., et al., *A Drosophila derailed homolog, doughnut, expressed in invaginating cells during embryogenesis*. Gene, 1999. **231**(1-2): p. 155-61.
21. Newsome, T.P., B. Asling, and B.J. Dickson, *Analysis of Drosophila photoreceptor axon guidance in eye-specific mosaics*. Development, 2000. **127**(4): p. 851-60.
22. Menut, L., et al., *A mosaic genetic screen for Drosophila neoplastic tumor suppressor genes based on defective pupation*. Genetics, 2007. **177**(3): p. 1667-77.
23. Tepass, U., et al., *Epithelial cell polarity and cell junctions in Drosophila*. Annu Rev Genet, 2001. **35**: p. 747-84.
24. Cohen, S.M., *Imaginal disc development*, in *The Development of Drosophila*, A.A. Martinez and M. Bate, Editors. 1993, Cold Spring Harbor Laboratory Press: New York. p. 747-841.
25. Assemat, E., et al., *Polarity complex proteins*. Biochim Biophys Acta, 2008. **1778**(3): p. 614-30.
26. Grawe, F., et al., *The Drosophila genes crumbs and stardust are involved in the biogenesis of adherens junctions*. Development, 1996. **122**(3): p. 951-9.
27. Muller, H.A. and E. Wieschaus, *armadillo, bazooka, and stardust are critical for early stages in formation of the zonula adherens and maintenance of the polarized blastoderm epithelium in Drosophila*. J Cell Biol, 1996. **134**(1): p. 149-63.
28. Tepass, U., *Crumbs, a component of the apical membrane, is required for zonula adherens formation in primary epithelia of Drosophila*. Dev Biol, 1996. **177**(1): p. 217-25.
29. Bilder, D., M. Li, and N. Perrimon, *Cooperative regulation of cell polarity and growth by Drosophila tumor suppressors*. Science, 2000. **289**(5476): p. 113-6.
30. Tanentzapf, G. and U. Tepass, *Interactions between the crumbs, lethal giant larvae and bazooka pathways in epithelial polarization*. Nat Cell Biol, 2003. **5**(1): p. 46-52.
31. Lu, H. and D. Bilder, *Endocytic control of epithelial polarity and proliferation in Drosophila*. Nat Cell Biol, 2005. **7**(12): p. 1232-9.
32. Wodarz, A., et al., *Expression of crumbs confers apical character on plasma membrane domains of ectodermal epithelia of Drosophila*. Cell, 1995. **82**(1): p. 67-76.
33. Tepass, U., C. Theres, and E. Knust, *crumbs encodes an EGF-like protein expressed on apical membranes of Drosophila epithelial cells and required for organization of epithelia*. Cell, 1990. **61**(5): p. 787-99.
34. Bulgakova, N.A. and E. Knust, *The Crumbs complex: from epithelial-cell polarity to retinal degeneration*. J Cell Sci, 2009. **122**(Pt 15): p. 2587-96.

35. Anderson, K.V. and P.W. Ingham, *The transformation of the model organism: a decade of developmental genetics*. Nat Genet, 2003. **33 Suppl**: p. 285-93.
36. Stark, M.B., *A Benign Tumor that is Hereditary in Drosophila*. Proc Natl Acad Sci U S A, 1919. **5**(12): p. 573-80.
37. Wassarman, D.A., M. Therrien, and G.M. Rubin, *The Ras signaling pathway in Drosophila*. Curr Opin Genet Dev, 1995. **5**(1): p. 44-50.
38. Tapon, N., et al., *The Drosophila tuberous sclerosis complex gene homologs restrict cell growth and cell proliferation*. Cell, 2001. **105**(3): p. 345-55.
39. Xu, T. and G.M. Rubin, *Analysis of genetic mosaics in developing and adult Drosophila tissues*. Development, 1993. **117**(4): p. 1223-37.
40. Justice, R.W., et al., *The Drosophila tumor suppressor gene warts encodes a homolog of human myotonic dystrophy kinase and is required for the control of cell shape and proliferation*. Genes Dev, 1995. **9**(5): p. 534-46.
41. Pasca di Magliano, M. and M. Hebrok, *Hedgehog signalling in cancer formation and maintenance*. Nat Rev Cancer, 2003. **3**(12): p. 903-11.
42. Taipale, J. and P.A. Beachy, *The Hedgehog and Wnt signalling pathways in cancer*. Nature, 2001. **411**(6835): p. 349-54.
43. Hariharan, I.K. and D. Bilder, *Regulation of imaginal disc growth by tumor-suppressor genes in Drosophila*. Annu Rev Genet, 2006. **40**: p. 335-61.
44. Dulic, V., E. Lees, and S.I. Reed, *Association of human cyclin E with a periodic G1-S phase protein kinase*. Science, 1992. **257**(5078): p. 1958-61.
45. Hinds, P.W., et al., *Regulation of retinoblastoma protein functions by ectopic expression of human cyclins*. Cell, 1992. **70**(6): p. 993-1006.
46. Lees, E., et al., *Cyclin E/cdk2 and cyclin A/cdk2 kinases associate with p107 and E2F in a temporally distinct manner*. Genes Dev, 1992. **6**(10): p. 1874-85.
47. Frolov, M.V., et al., *Functional antagonism between E2F family members*. Genes Dev, 2001. **15**(16): p. 2146-60.
48. Tapon, N., et al., *salvador Promotes both cell cycle exit and apoptosis in Drosophila and is mutated in human cancer cell lines*. Cell, 2002. **110**(4): p. 467-78.
49. Winston, J.T., et al., *Regulation of the cell cycle machinery by oncogenic ras*. Oncogene, 1996. **12**(1): p. 127-34.
50. Hunt, K.K. and K. Keyomarsi, *Cyclin E as a prognostic and predictive marker in breast cancer*. Semin Cancer Biol, 2005. **15**(4): p. 319-26.
51. Hsiung, F. and K. Moses, *Retinal development in Drosophila: specifying the first neuron*. Hum Mol Genet, 2002. **11**(10): p. 1207-14.
52. Scott, R.C., G. Juhasz, and T.P. Neufeld, *Direct induction of autophagy by Atg1 inhibits cell growth and induces apoptotic cell death*. Curr Biol, 2007. **17**(1): p. 1-11.
53. Grewal, S.S., et al., *Myc-dependent regulation of ribosomal RNA synthesis during Drosophila development*. Nat Cell Biol, 2005. **7**(3): p. 295-302.
54. Orian, A., et al., *Genomic binding and transcriptional regulation by the Drosophila Myc and Mnt transcription factors*. Cold Spring Harb Symp Quant Biol, 2005. **70**: p. 299-307.
55. Nesbit, C.E., J.M. Tersak, and E.V. Prochownik, *MYC oncogenes and human neoplastic disease*. Oncogene, 1999. **18**(19): p. 3004-16.

56. Montagne, J., et al., *Drosophila S6 kinase: a regulator of cell size*. Science, 1999. **285**(5436): p. 2126-9.
57. Flynn, A. and C.G. Proud, *The role of eIF4 in cell proliferation*. Cancer Surv, 1996. **27**: p. 293-310.
58. Cohen, G.M., *Caspases: the executioners of apoptosis*. Biochem J, 1997. **326 (Pt 1)**: p. 1-16.
59. Hay, B.A., J.R. Huh, and M. Guo, *The genetics of cell death: approaches, insights and opportunities in Drosophila*. Nat Rev Genet, 2004. **5**(12): p. 911-22.
60. Tait, S.W. and D.R. Green, *Caspase-independent cell death: leaving the set without the final cut*. Oncogene, 2008. **27**(50): p. 6452-61.
61. Pearson, G., et al., *Mitogen-activated protein (MAP) kinase pathways: regulation and physiological functions*. Endocr Rev, 2001. **22**(2): p. 153-83.
62. Rossomando, A.J., et al., *Evidence that pp42, a major tyrosine kinase target protein, is a mitogen-activated serine/threonine protein kinase*. Proc Natl Acad Sci U S A, 1989. **86**(18): p. 6940-3.
63. Boulton, T.G., et al., *An insulin-stimulated protein kinase similar to yeast kinases involved in cell cycle control*. Science, 1990. **249**(4964): p. 64-7.
64. Courchesne, W.E., R. Kunisawa, and J. Thorner, *A putative protein kinase overcomes pheromone-induced arrest of cell cycling in S. cerevisiae*. Cell, 1989. **58**(6): p. 1107-19.
65. Elion, E.A., P.L. Grisafi, and G.R. Fink, *FUS3 encodes a cdc2+/CDC28-related kinase required for the transition from mitosis into conjugation*. Cell, 1990. **60**(4): p. 649-64.
66. Boulton, T.G., et al., *ERKs: a family of protein-serine/threonine kinases that are activated and tyrosine phosphorylated in response to insulin and NGF*. Cell, 1991. **65**(4): p. 663-75.
67. Toda, T., M. Shimanuki, and M. Yanagida, *Fission yeast genes that confer resistance to staurosporine encode an AP-1-like transcription factor and a protein kinase related to the mammalian ERK1/MAP2 and budding yeast FUS3 and KSS1 kinases*. Genes Dev, 1991. **5**(1): p. 60-73.
68. Sternberg, P.W. and M. Han, *Genetics of RAS signaling in C. elegans*. Trends Genet, 1998. **14**(11): p. 466-72.
69. Prober, D.A. and B.A. Edgar, *Ras1 promotes cellular growth in the Drosophila wing*. Cell, 2000. **100**(4): p. 435-46.
70. Luo, X., et al., *Foxo and Fos regulate the decision between cell death and survival in response to UV irradiation*. EMBO J, 2007. **26**(2): p. 380-90.
71. Takatsu, Y., et al., *TAK1 participates in c-Jun N-terminal kinase signaling during Drosophila development*. Mol Cell Biol, 2000. **20**(9): p. 3015-26.
72. Gabay, L., R. Seger, and B.Z. Shilo, *MAP kinase in situ activation atlas during Drosophila embryogenesis*. Development, 1997. **124**(18): p. 3535-41.
73. Hsu, J.C. and N. Perrimon, *A temperature-sensitive MEK mutation demonstrates the conservation of the signaling pathways activated by receptor tyrosine kinases*. Genes Dev, 1994. **8**(18): p. 2176-87.
74. Tsuda, L., et al., *A protein kinase similar to MAP kinase activator acts downstream of the raf kinase in Drosophila*. Cell, 1993. **72**(3): p. 407-14.

75. Biggs, W.H., 3rd, et al., *The Drosophila rolled locus encodes a MAP kinase required in the sevenless signal transduction pathway*. EMBO J, 1994. **13**(7): p. 1628-35.
76. Bier, E., *Localized activation of RTK/MAPK pathways during Drosophila development*. Bioessays, 1998. **20**(3): p. 189-94.
77. Igaki, T., *Correcting developmental errors by apoptosis: lessons from Drosophila JNK signaling*. Apoptosis, 2009. **14**(8): p. 1021-8.
78. Teramoto, H., et al., *Signaling from the small GTP-binding proteins Rac1 and Cdc42 to the c-Jun N-terminal kinase/stress-activated protein kinase pathway. A role for mixed lineage kinase 3/protein-tyrosine kinase 1, a novel member of the mixed lineage kinase family*. J Biol Chem, 1996. **271**(44): p. 27225-8.
79. Igaki, T., R.A. Pagliarini, and T. Xu, *Loss of cell polarity drives tumor growth and invasion through JNK activation in Drosophila*. Curr Biol, 2006. **16**(11): p. 1139-46.
80. Sun, G. and K.D. Irvine, *Regulation of Hippo signaling by Jun kinase signaling during compensatory cell proliferation and regeneration, and in neoplastic tumors*. Dev Biol, 2011. **350**(1): p. 139-51.
81. Wu, M., J.C. Pastor-Pareja, and T. Xu, *Interaction between Ras(V12) and scribbled clones induces tumour growth and invasion*. Nature, 2010. **463**(7280): p. 545-8.
82. Pan, D., *The hippo signaling pathway in development and cancer*. Dev Cell, 2010. **19**(4): p. 491-505.
83. Harvey, K. and N. Tapon, *The Salvador-Warts-Hippo pathway - an emerging tumour-suppressor network*. Nat Rev Cancer, 2007. **7**(3): p. 182-91.
84. Lai, Z.C., et al., *Control of cell proliferation and apoptosis by mob as tumor suppressor, mats*. Cell, 2005. **120**(5): p. 675-85.
85. Dong, J., et al., *Elucidation of a universal size-control mechanism in Drosophila and mammals*. Cell, 2007. **130**(6): p. 1120-33.
86. Goulev, Y., et al., *SCALLOPED interacts with YORKIE, the nuclear effector of the hippo tumor-suppressor pathway in Drosophila*. Curr Biol, 2008. **18**(6): p. 435-41.
87. Peng, H.W., M. Slattery, and R.S. Mann, *Transcription factor choice in the Hippo signaling pathway: homothorax and yorkie regulation of the microRNA bantam in the progenitor domain of the Drosophila eye imaginal disc*. Genes Dev, 2009. **23**(19): p. 2307-19.
88. Wu, S., et al., *The TEAD/TEF family protein Scalloped mediates transcriptional output of the Hippo growth-regulatory pathway*. Dev Cell, 2008. **14**(3): p. 388-98.
89. Zhang, L., et al., *The TEAD/TEF family of transcription factor Scalloped mediates Hippo signaling in organ size control*. Dev Cell, 2008. **14**(3): p. 377-87.
90. Grusche, F.A., H.E. Richardson, and K.F. Harvey, *Upstream regulation of the hippo size control pathway*. Curr Biol, 2010. **20**(13): p. R574-82.
91. Lian, I., et al., *The role of YAP transcription coactivator in regulating stem cell self-renewal and differentiation*. Genes Dev, 2010. **24**(11): p. 1106-18.

92. Zhao, B., et al., *Inactivation of YAP oncoprotein by the Hippo pathway is involved in cell contact inhibition and tissue growth control*. *Genes Dev*, 2007. **21**(21): p. 2747-61.
93. Overholtzer, M., et al., *Transforming properties of YAP, a candidate oncogene on the chromosome 11q22 amplicon*. *Proc Natl Acad Sci U S A*, 2006. **103**(33): p. 12405-10.
94. St John, M.A., et al., *Mice deficient of Lats1 develop soft-tissue sarcomas, ovarian tumours and pituitary dysfunction*. *Nat Genet*, 1999. **21**(2): p. 182-6.
95. Takahashi, Y., et al., *Down-regulation of LATS1 and LATS2 mRNA expression by promoter hypermethylation and its association with biologically aggressive phenotype in human breast cancers*. *Clin Cancer Res*, 2005. **11**(4): p. 1380-5.
96. Zhang, N., et al., *The Merlin/NF2 tumor suppressor functions through the YAP oncoprotein to regulate tissue homeostasis in mammals*. *Dev Cell*, 2010. **19**(1): p. 27-38.
97. Li, W.X., *Canonical and non-canonical JAK-STAT signaling*. *Trends Cell Biol*, 2008. **18**(11): p. 545-51.
98. Betz, A., et al., *STAT92E is a positive regulator of Drosophila inhibitor of apoptosis 1 (DIAP/1) and protects against radiation-induced apoptosis*. *Proc Natl Acad Sci U S A*, 2008. **105**(37): p. 13805-10.
99. Gutierrez-Avino, F.J., D. Ferres-Marco, and M. Dominguez, *The position and function of the Notch-mediated eye growth organizer: the roles of JAK/STAT and four-jointed*. *EMBO Rep*, 2009. **10**(9): p. 1051-8.
100. Mukherjee, T., J.C. Hombria, and M.P. Zeidler, *Opposing roles for Drosophila JAK/STAT signalling during cellular proliferation*. *Oncogene*, 2005. **24**(15): p. 2503-11.
101. Tsai, Y.C. and Y.H. Sun, *Long-range effect of upd, a ligand for Jak/STAT pathway, on cell cycle in Drosophila eye development*. *Genesis*, 2004. **39**(2): p. 141-53.
102. Shi, S., et al., *JAK signaling globally counteracts heterochromatic gene silencing*. *Nat Genet*, 2006. **38**(9): p. 1071-6.
103. Artavanis-Tsakonas, S., M.D. Rand, and R.J. Lake, *Notch signaling: cell fate control and signal integration in development*. *Science*, 1999. **284**(5415): p. 770-6.
104. Hansson, E.M., U. Lendahl, and G. Chapman, *Notch signaling in development and disease*. *Semin Cancer Biol*, 2004. **14**(5): p. 320-8.
105. Vaccari, T., et al., *Endosomal entry regulates Notch receptor activation in Drosophila melanogaster*. *J Cell Biol*, 2008. **180**(4): p. 755-62.
106. Deng, W.M., C. Althausen, and H. Ruohola-Baker, *Notch-Delta signaling induces a transition from mitotic cell cycle to endocycle in Drosophila follicle cells*. *Development*, 2001. **128**(23): p. 4737-46.
107. Schaeffer, V., et al., *Notch-dependent Fizzy-related/Hec1/Cdh1 expression is required for the mitotic-to-endocycle transition in Drosophila follicle cells*. *Curr Biol*, 2004. **14**(7): p. 630-6.
108. Baonza, A. and M. Freeman, *Control of cell proliferation in the Drosophila eye by Notch signaling*. *Dev Cell*, 2005. **8**(4): p. 529-39.

109. Nicholson, S.C., et al., *Notch-dependent expression of the archipelago ubiquitin ligase subunit in the Drosophila eye*. Development, 2011. **138**(2): p. 251-60.
110. Ranganathan, P., K.L. Weaver, and A.J. Capobianco, *Notch signalling in solid tumours: a little bit of everything but not all the time*. Nat Rev Cancer, 2011. **11**(5): p. 338-51.
111. Thummel, C.S., *Flies on steroids--Drosophila metamorphosis and the mechanisms of steroid hormone action*. Trends Genet, 1996. **12**(8): p. 306-10.
112. Delanoue, R., M. Slaidina, and P. Leopold, *The steroid hormone ecdysone controls systemic growth by repressing dMyc function in Drosophila fat cells*. Dev Cell, 2010. **18**(6): p. 1012-21.
113. Bai, J., Y. Uehara, and D.J. Montell, *Regulation of invasive cell behavior by taiman, a Drosophila protein related to AIB1, a steroid receptor coactivator amplified in breast cancer*. Cell, 2000. **103**(7): p. 1047-58.
114. Kumar, M.B., et al., *Highly flexible ligand binding pocket of ecdysone receptor: a single amino acid change leads to discrimination between two groups of nonsteroidal ecdysone agonists*. J Biol Chem, 2004. **279**(26): p. 27211-8.
115. Gojis, O., et al., *The role of steroid receptor coactivator-3 (SRC-3) in human malignant disease*. Eur J Surg Oncol, 2010. **36**(3): p. 224-9.
116. Bilder, D., *Epithelial polarity and proliferation control: links from the Drosophila neoplastic tumor suppressors*. Genes Dev, 2004. **18**(16): p. 1909-25.
117. Vaccari, T. and D. Bilder, *At the crossroads of polarity, proliferation and apoptosis: the use of Drosophila to unravel the multifaceted role of endocytosis in tumor suppression*. Mol Oncol, 2009. **3**(4): p. 354-65.
118. Moberg, K.H., et al., *Mutations in erupted, the Drosophila ortholog of mammalian tumor susceptibility gene 101, elicit non-cell-autonomous overgrowth*. Dev Cell, 2005. **9**(5): p. 699-710.
119. Thompson, B.J., et al., *Tumor suppressor properties of the ESCRT-II complex component Vps25 in Drosophila*. Dev Cell, 2005. **9**(5): p. 711-20.
120. Vaccari, T. and D. Bilder, *The Drosophila tumor suppressor vps25 prevents nonautonomous overproliferation by regulating notch trafficking*. Dev Cell, 2005. **9**(5): p. 687-98.
121. Feng, S., J. Huang, and J. Wang, *Loss of the Polycomb group gene polyhomeotic induces non-autonomous cell overproliferation*. EMBO Rep, 2011. **12**(2): p. 157-63.
122. Pellikka, M., et al., *Crumbs, the Drosophila homologue of human CRB1/RP12, is essential for photoreceptor morphogenesis*. Nature, 2002. **416**(6877): p. 143-9.
123. Vaccari, T., et al., *Comparative analysis of ESCRT-I, ESCRT-II and ESCRT-III function in Drosophila by efficient isolation of ESCRT mutants*. J Cell Sci, 2009. **122**(Pt 14): p. 2413-23.
124. Bilder, D. and N. Perrimon, *Localization of apical epithelial determinants by the basolateral PDZ protein Scribble*. Nature, 2000. **403**(6770): p. 676-80.
125. Gateff, E., *Malignant neoplasms of genetic origin in Drosophila melanogaster*. Science, 1978. **200**(4349): p. 1448-59.

126. Stewart, M., C. Murphy, and J.W. Fristrom, *The recovery and preliminary characterization of X chromosome mutants affecting imaginal discs of Drosophila melanogaster*. Dev Biol, 1972. **27**(1): p. 71-83.
127. Humbert, P.O., et al., *Control of tumorigenesis by the Scribble/Dlg/Lgl polarity module*. Oncogene, 2008. **27**(55): p. 6888-907.
128. Hugo, H., et al., *Epithelial--mesenchymal and mesenchymal--epithelial transitions in carcinoma progression*. J Cell Physiol, 2007. **213**(2): p. 374-83.
129. Lee, M. and V. Vasioukhin, *Cell polarity and cancer--cell and tissue polarity as a non-canonical tumor suppressor*. J Cell Sci, 2008. **121**(Pt 8): p. 1141-50.
130. Humbert, P., S. Russell, and H. Richardson, *Dlg, Scribble and Lgl in cell polarity, cell proliferation and cancer*. Bioessays, 2003. **25**(6): p. 542-53.
131. Nolo, R., et al., *The bantam microRNA is a target of the hippo tumor-suppressor pathway*. Curr Biol, 2006. **16**(19): p. 1895-904.
132. Thompson, B.J. and S.M. Cohen, *The Hippo pathway regulates the bantam microRNA to control cell proliferation and apoptosis in Drosophila*. Cell, 2006. **126**(4): p. 767-74.
133. Neto-Silva, R.M., S. de Beco, and L.A. Johnston, *Evidence for a growth-stabilizing regulatory feedback mechanism between Myc and Yorkie, the Drosophila homolog of Yap*. Dev Cell, 2010. **19**(4): p. 507-20.
134. Nicolay, B.N., et al., *Cooperation between dE2F1 and Yki/Sd defines a distinct transcriptional program necessary to bypass cell cycle exit*. Genes Dev, 2011. **25**(4): p. 323-35.
135. Helms, W., et al., *Engineered truncations in the Drosophila mastermind protein disrupt Notch pathway function*. Dev Biol, 1999. **215**(2): p. 358-74.
136. Struhl, G. and I. Greenwald, *Presenilin is required for activity and nuclear access of Notch in Drosophila*. Nature, 1999. **398**(6727): p. 522-5.
137. Ye, Y., N. Lukinova, and M.E. Fortini, *Neurogenic phenotypes and altered Notch processing in Drosophila Presenilin mutants*. Nature, 1999. **398**(6727): p. 525-9.
138. Petcherski, A.G. and J. Kimble, *Mastermind is a putative activator for Notch*. Curr Biol, 2000. **10**(13): p. R471-3.
139. Ng, M., F.J. Diaz-Benjumea, and S.M. Cohen, *Nubbin encodes a POU-domain protein required for proximal-distal patterning in the Drosophila wing*. Development, 1995. **121**(2): p. 589-99.
140. Richardson, E.C. and F. Pichaud, *Crumbs is required to achieve proper organ size control during Drosophila head development*. Development, 2010. **137**(4): p. 641-50.
141. Herranz, H., et al., *Self-refinement of Notch activity through the transmembrane protein Crumbs: modulation of gamma-secretase activity*. EMBO Rep, 2006. **7**(3): p. 297-302.
142. Mitsuishi, Y., et al., *Human CRB2 inhibits gamma-secretase cleavage of amyloid precursor protein by binding to the presenilin complex*. J Biol Chem, 2010. **285**(20): p. 14920-31.
143. Ling, C., et al., *The apical transmembrane protein Crumbs functions as a tumor suppressor that regulates Hippo signaling by binding to Expanded*. Proc Natl Acad Sci U S A, 2010. **107**(23): p. 10532-7.

144. Chen, C.L., et al., *The apical-basal cell polarity determinant Crumbs regulates Hippo signaling in Drosophila*. Proc Natl Acad Sci U S A, 2010. **107**(36): p. 15810-5.
145. Grzeschik, N.A., et al., *Lgl, aPKC, and Crumbs regulate the Salvador/Warts/Hippo pathway through two distinct mechanisms*. Curr Biol, 2010. **20**(7): p. 573-81.
146. Maitra, S., et al., *The tumor suppressors Merlin and Expanded function cooperatively to modulate receptor endocytosis and signaling*. Curr Biol, 2006. **16**(7): p. 702-9.
147. Yu, J., et al., *The hippo pathway promotes Notch signaling in regulation of cell differentiation, proliferation, and oocyte polarity*. PLoS One, 2008. **3**(3): p. e1761.
148. Bowman, A.B., et al., *Drosophila roadblock and Chlamydomonas LC7: a conserved family of dynein-associated proteins involved in axonal transport, flagellar motility, and mitosis*. J Cell Biol, 1999. **146**(1): p. 165-80.
149. Staley, B.K. and K.D. Irvine, *Warts and Yorkie mediate intestinal regeneration by influencing stem cell proliferation*. Curr Biol, 2010. **20**(17): p. 1580-7.
150. Karpowicz, P., J. Perez, and N. Perrimon, *The Hippo tumor suppressor pathway regulates intestinal stem cell regeneration*. Development, 2010. **137**(24): p. 4135-45.
151. Grusche, F.A., et al., *The Salvador/Warts/Hippo pathway controls regenerative tissue growth in Drosophila melanogaster*. Dev Biol, 2011. **350**(2): p. 255-66.
152. Warner, S.J., H. Yashiro, and G.D. Longmore, *The Cdc42/Par6/aPKC Polarity Complex Regulates Apoptosis-Induced Compensatory Proliferation in Epithelia*. Curr Biol, 2010.
153. Cha, G.H., et al., *Discrete functions of TRAF1 and TRAF2 in Drosophila melanogaster mediated by c-Jun N-terminal kinase and NF-kappaB-dependent signaling pathways*. Mol Cell Biol, 2003. **23**(22): p. 7982-91.
154. Liu, H., et al., *A Drosophila TNF-receptor-associated factor (TRAF) binds the ste20 kinase Misshapen and activates Jun kinase*. Curr Biol, 1999. **9**(2): p. 101-4.
155. Badouel, C., et al., *The FERM-domain protein Expanded regulates Hippo pathway activity via direct interactions with the transcriptional activator Yorkie*. Dev Cell, 2009. **16**(3): p. 411-20.
156. Boedigheimer, M. and A. Laughon, *Expanded: a gene involved in the control of cell proliferation in imaginal discs*. Development, 1993. **118**(4): p. 1291-301.
157. Hamaratoglu, F., et al., *The tumour-suppressor genes NF2/Merlin and Expanded act through Hippo signalling to regulate cell proliferation and apoptosis*. Nat Cell Biol, 2006. **8**(1): p. 27-36.
158. Polesello, C. and N. Tapon, *Salvador-warts-hippo signaling promotes Drosophila posterior follicle cell maturation downstream of notch*. Curr Biol, 2007. **17**(21): p. 1864-70.
159. Meignin, C., et al., *The salvador-warts-hippo pathway is required for epithelial proliferation and axis specification in Drosophila*. Curr Biol, 2007. **17**(21): p. 1871-8.

160. de Celis, J.F., et al., *Notch signalling mediates segmentation of the Drosophila leg.* Development, 1998. **125**(23): p. 4617-26.
161. Rogulja, D., C. Rauskolb, and K.D. Irvine, *Morphogen control of wing growth through the Fat signaling pathway.* Dev Cell, 2008. **15**(2): p. 309-21.
162. Matakatsu, H. and S.S. Blair, *The DHHC palmitoyltransferase approximated regulates Fat signaling and Dachs localization and activity.* Curr Biol, 2008. **18**(18): p. 1390-5.
163. Medina, E., et al., *Crumbs interacts with moesin and beta(Heavy)-spectrin in the apical membrane skeleton of Drosophila.* J Cell Biol, 2002. **158**(5): p. 941-51.
164. McCartney, B.M., et al., *The neurofibromatosis-2 homologue, Merlin, and the tumor suppressor expanded function together in Drosophila to regulate cell proliferation and differentiation.* Development, 2000. **127**(6): p. 1315-24.
165. Grzeschik, N.A. and E. Knust, *IrreC/rst-mediated cell sorting during Drosophila pupal eye development depends on proper localisation of DE-cadherin.* Development, 2005. **132**(9): p. 2035-45.
166. Klebes, A. and E. Knust, *A conserved motif in Crumbs is required for E-cadherin localisation and zonula adherens formation in Drosophila.* Curr Biol, 2000. **10**(2): p. 76-85.
167. Belote, J.M. and E. Fortier, *Targeted expression of dominant negative proteasome mutants in Drosophila melanogaster.* Genesis, 2002. **34**(1-2): p. 80-2.
168. Izaddoost, S., et al., *Drosophila Crumbs is a positional cue in photoreceptor adherens junctions and rhabdomeres.* Nature, 2002. **416**(6877): p. 178-83.
169. Jurgens, G., et al., *Mutations affecting the pattern of larval cuticle in Drosophila melanogaster.* Roux's Arch of Dev Biol, 1984. **II**: p. 283-295.
170. Wodarz, A., F. Grawe, and E. Knust, *CRUMBS is involved in the control of apical protein targeting during Drosophila epithelial development.* Mech Dev, 1993. **44**(2-3): p. 175-87.
171. Laprise, P., et al., *The FERM protein Yurt is a negative regulatory component of the Crumbs complex that controls epithelial polarity and apical membrane size.* Dev Cell, 2006. **11**(3): p. 363-74.
172. Karagiosis, S.A. and D.F. Ready, *Moesin contributes an essential structural role in Drosophila photoreceptor morphogenesis.* Development, 2004. **131**(4): p. 725-32.
173. Luo, L., et al., *Distinct morphogenetic functions of similar small GTPases: Drosophila Drac1 is involved in axonal outgrowth and myoblast fusion.* Genes Dev, 1994. **8**(15): p. 1787-802.
174. Harris, K.P. and U. Tepass, *Cdc42 and Par proteins stabilize dynamic adherens junctions in the Drosophila neuroectoderm through regulation of apical endocytosis.* J Cell Biol, 2008. **183**(6): p. 1129-43.
175. Boedigheimer, M.J., K.P. Nguyen, and P.J. Bryant, *Expanded functions in the apical cell domain to regulate the growth rate of imaginal discs.* Dev Genet, 1997. **20**(2): p. 103-10.

176. Zhang, X., et al., *Transcriptional output of the Salvador/warts/hippo pathway is controlled in distinct fashions in Drosophila melanogaster and mammalian cell lines*. Cancer Res, 2009. **69**(15): p. 6033-41.
177. Badouel, C. and H. McNeill, *Apical junctions and growth control in Drosophila*. Biochim Biophys Acta, 2009. **1788**(4): p. 755-60.
178. Herz, H.M., et al., *vps25 mosaics display non-autonomous cell survival and overgrowth, and autonomous apoptosis*. Development, 2006. **133**(10): p. 1871-80.
179. Silva, E., et al., *The tumor-suppressor gene fat controls tissue growth upstream of expanded in the hippo signaling pathway*. Curr Biol, 2006. **16**(21): p. 2081-9.
180. Feng, Y. and K.D. Irvine, *Fat and expanded act in parallel to regulate growth through warts*. Proc Natl Acad Sci U S A, 2007. **104**(51): p. 20362-7.
181. Tyler, D.M., et al., *Genes affecting cell competition in Drosophila*. Genetics, 2007. **175**(2): p. 643-57.
182. Karp, C.M., et al., *Role of the polarity determinant crumbs in suppressing mammalian epithelial tumor progression*. Cancer Res, 2008. **68**(11): p. 4105-15.
183. Hamaratoglu, F., et al., *The Hippo tumor-suppressor pathway regulates apical-domain size in parallel to tissue growth*. J Cell Sci, 2009. **122**(Pt 14): p. 2351-9.
184. Genevet, A., et al., *The Hippo pathway regulates apical-domain size independently of its growth-control function*. J Cell Sci, 2009. **122**(Pt 14): p. 2360-70.
185. Pellock, B.J., et al., *The Drosophila tumor suppressors Expanded and Merlin differentially regulate cell cycle exit, apoptosis, and Wingless signaling*. Dev Biol, 2007. **304**(1): p. 102-15.
186. Zhao, M., et al., *Basolateral junctions utilize warts signaling to control epithelial-mesenchymal transition and proliferation crucial for migration and invasion of Drosophila ovarian epithelial cells*. Genetics, 2008. **178**(4): p. 1947-71.
187. Skouloudaki, K., et al., *Scribble participates in Hippo signaling and is required for normal zebrafish pronephros development*. Proc Natl Acad Sci U S A, 2009. **106**(21): p. 8579-84.
188. Rives, A.F., et al., *Endocytic trafficking of Wingless and its receptors, Arrow and DFrizzled-2, in the Drosophila wing*. Dev Biol, 2006. **293**(1): p. 268-83.
189. Moberg, K.H., et al., *The Drosophila F box protein archipelago regulates dMyc protein levels in vivo*. Curr Biol, 2004. **14**(11): p. 965-74.
190. Javier, R.T., *Cell polarity proteins: common targets for tumorigenic human viruses*. Oncogene, 2008. **27**(55): p. 7031-46.
191. Fischer, J.A., S.H. Eun, and B.T. Doolan, *Endocytosis, endosome trafficking, and the regulation of Drosophila development*. Annu Rev Cell Dev Biol, 2006. **22**: p. 181-206.
192. Katzmann, D.J., M. Babst, and S.D. Emr, *Ubiquitin-dependent sorting into the multivesicular body pathway requires the function of a conserved endosomal protein sorting complex, ESCRT-I*. Cell, 2001. **106**(2): p. 145-55.

193. Bishop, N. and P. Woodman, *TSG101/mammalian VPS23 and mammalian VPS28 interact directly and are recruited to VPS4-induced endosomes*. J Biol Chem, 2001. **276**(15): p. 11735-42.
194. Gilbert, M.M., B.S. Robinson, and K.H. Moberg, *Functional interactions between the erupted/tsg101 growth suppressor gene and the DaPKC and rbf1 genes in Drosophila imaginal disc tumors*. PLoS One, 2009. **4**(9): p. e7039.
195. Gilbert, M.M., et al., *Genetic interactions between the Drosophila tumor suppressor gene ept and the stat92E transcription factor*. PLoS One, 2009. **4**(9): p. e7083.
196. Shaw, R.L., et al., *The Hippo pathway regulates intestinal stem cell proliferation during Drosophila adult midgut regeneration*. Development, 2010. **137**(24): p. 4147-58.
197. Zeng, Q. and W. Hong, *The emerging role of the hippo pathway in cell contact inhibition, organ size control, and cancer development in mammals*. Cancer Cell, 2008. **13**(3): p. 188-92.
198. White, K., et al., *Genetic control of programmed cell death in Drosophila*. Science, 1994. **264**(5159): p. 677-83.
199. Bonifacino, J.S. and L.M. Traub, *Signals for sorting of transmembrane proteins to endosomes and lysosomes*. Annu Rev Biochem, 2003. **72**: p. 395-447.
200. Gilbert, M.M., et al., *A Screen for Conditional Growth Suppressor Genes Identifies the Drosophila Homolog of HD-PTP as a Regulator of the Oncoprotein Yorkie*. Dev Cell, 2011. **20**(5): p. 700-12.
201. Robinson, B.S., et al., *Crumbs regulates Salvador/Warts/Hippo signaling in Drosophila via the FERM-domain protein Expanded*. Curr Biol, 2010. **20**(7): p. 582-90.
202. Adachi-Yamada, T., et al., *Distortion of proximodistal information causes JNK-dependent apoptosis in Drosophila wing*. Nature, 1999. **400**(6740): p. 166-9.
203. Uhlirova, M. and D. Bohmann, *JNK- and Fos-regulated Mmp1 expression cooperates with Ras to induce invasive tumors in Drosophila*. EMBO J, 2006. **25**(22): p. 5294-304.
204. Brumby, A.M. and H.E. Richardson, *scribble mutants cooperate with oncogenic Ras or Notch to cause neoplastic overgrowth in Drosophila*. EMBO J, 2003. **22**(21): p. 5769-79.
205. Shivas, J.M., et al., *Polarity and endocytosis: reciprocal regulation*. Trends Cell Biol, 2010. **20**(8): p. 445-52.
206. Igaki, T., et al., *Intrinsic tumor suppression and epithelial maintenance by endocytic activation of Eiger/TNF signaling in Drosophila*. Dev Cell, 2009. **16**(3): p. 458-65.
207. Rodahl, L.M., et al., *Disruption of Vps4 and JNK function in Drosophila causes tumour growth*. PLoS One, 2009. **4**(2): p. e4354.
208. Lee, M.P. and A.P. Feinberg, *Aberrant splicing but not mutations of TSG101 in human breast cancer*. Cancer Res, 1997. **57**(15): p. 3131-4.
209. Li, L. and S.N. Cohen, *Tsg101: a novel tumor susceptibility gene isolated by controlled homozygous functional knockout of allelic loci in mammalian cells*. Cell, 1996. **85**(3): p. 319-29.

210. Wagner, K.U., et al., *Genomic architecture and transcriptional activation of the mouse and human tumor susceptibility gene TSG101: common types of shorter transcripts are true alternative splice variants*. *Oncogene*, 1998. **17**(21): p. 2761-70.
211. Wang, Q., et al., *Low frequency of TSG101/CC2 gene alterations in invasive human breast cancers*. *Oncogene*, 1998. **16**(5): p. 677-9.
212. Zhong, Q., et al., *Identification of cellular TSG101 protein in multiple human breast cancer cell lines*. *Cancer Res*, 1997. **57**(19): p. 4225-8.
213. Oh, H. and K.D. Irvine, *Cooperative regulation of growth by Yorkie and Mad through bantam*. *Dev Cell*, 2011. **20**(1): p. 109-22.
214. Huang, J., et al., *The Hippo signaling pathway coordinately regulates cell proliferation and apoptosis by inactivating Yorkie, the Drosophila Homolog of YAP*. *Cell*, 2005. **122**(3): p. 421-34.
215. Jang, A.C., et al., *Border-cell migration requires integration of spatial and temporal signals by the BTB protein Abrupt*. *Nat Cell Biol*, 2009. **11**(5): p. 569-79.
216. Pignoni, F. and S.L. Zipursky, *Induction of Drosophila eye development by decapentaplegic*. *Development*, 1997. **124**(2): p. 271-8.
217. Brennecke, J., et al., *bantam encodes a developmentally regulated microRNA that controls cell proliferation and regulates the proapoptotic gene hid in Drosophila*. *Cell*, 2003. **113**(1): p. 25-36.
218. Xu, J. and Q. Li, *Review of the in vivo functions of the p160 steroid receptor coactivator family*. *Mol Endocrinol*, 2003. **17**(9): p. 1681-92.
219. Colombani, J., et al., *Antagonistic actions of ecdysone and insulins determine final size in Drosophila*. *Science*, 2005. **310**(5748): p. 667-70.
220. Zhao, B., et al., *The Hippo-YAP pathway in organ size control and tumorigenesis: an updated version*. *Genes Dev*, 2010. **24**(9): p. 862-74.
221. Louie, M.C., et al., *ACTR/AIB1 functions as an E2F1 coactivator to promote breast cancer cell proliferation and antiestrogen resistance*. *Mol Cell Biol*, 2004. **24**(12): p. 5157-71.
222. Belandia, B. and M.G. Parker, *Functional interaction between the p160 coactivator proteins and the transcriptional enhancer factor family of transcription factors*. *J Biol Chem*, 2000. **275**(40): p. 30801-5.
223. Yoshida, H., et al., *Steroid receptor coactivator-3, a homolog of Taiman that controls cell migration in the Drosophila ovary, regulates migration of human ovarian cancer cells*. *Mol Cell Endocrinol*, 2005. **245**(1-2): p. 77-85.
224. Lonard, D.M. and W. O'Malley B, *Nuclear receptor coregulators: judges, juries, and executioners of cellular regulation*. *Mol Cell*, 2007. **27**(5): p. 691-700.
225. Gupta, T. and T. Schupbach, *Cct1, a phosphatidylcholine biosynthesis enzyme, is required for Drosophila oogenesis and ovarian morphogenesis*. *Development*, 2003. **130**(24): p. 6075-87.
226. Weber, U., C. Eroglu, and M. Mlodzik, *Phospholipid membrane composition affects EGF receptor and Notch signaling through effects on endocytosis during Drosophila development*. *Dev Cell*, 2003. **5**(4): p. 559-70.
227. Yan, Y., et al., *Drosophila PI4KIIIalpha is required in follicle cells for oocyte polarization and Hippo signaling*. *Development*, 2011. **138**(9): p. 1697-703.

228. Jou, T.S. and W.J. Nelson, *Effects of regulated expression of mutant RhoA and Rac1 small GTPases on the development of epithelial (MDCK) cell polarity.* J Cell Biol, 1998. **142**(1): p. 85-100.
229. Neisch, A.L., et al., *Rho1 regulates apoptosis via activation of the JNK signaling pathway at the plasma membrane.* J Cell Biol, 2010. **189**(2): p. 311-23.
230. Anderson, M.G., et al., *drifter, a Drosophila POU-domain transcription factor, is required for correct differentiation and migration of tracheal cells and midline glia.* Genes Dev, 1995. **9**(1): p. 123-37.
231. Chung, S., et al., *The balance between the novel protein target of wingless and the Drosophila Rho-associated kinase pathway regulates planar cell polarity in the Drosophila wing.* Genetics, 2007. **176**(2): p. 891-903.
232. Cho, E., et al., *Delineation of a Fat tumor suppressor pathway.* Nat Genet, 2006. **38**(10): p. 1142-50.
233. Shaw, R.J., et al., *RhoA-dependent phosphorylation and relocalization of ERM proteins into apical membrane/actin protrusions in fibroblasts.* Mol Biol Cell, 1998. **9**(2): p. 403-19.
234. Matsui, T., et al., *Rho-kinase phosphorylates COOH-terminal threonines of ezrin/radixin/moesin (ERM) proteins and regulates their head-to-tail association.* J Cell Biol, 1998. **140**(3): p. 647-57.
235. King-Jones, K. and C.S. Thummel, *Nuclear receptors--a perspective from Drosophila.* Nat Rev Genet, 2005. **6**(4): p. 311-23.
236. Lei, Q.Y., et al., *TAZ promotes cell proliferation and epithelial-mesenchymal transition and is inhibited by the hippo pathway.* Mol Cell Biol, 2008. **28**(7): p. 2426-36.
237. Michalopoulos, G.K. and M.C. DeFrances, *Liver regeneration.* Science, 1997. **276**(5309): p. 60-6.
238. Haynie, J.L. and P.J. Bryant, *The effects of X-rays on the proliferation dynamics of cells in the imaginal wing disc of Drosophila melanogaster.* Roux Arch. Dev. Biol, 1977(183): p. 85-100.
239. Bryant, P.J., S.V. Bryant, and V. French, *Biological regeneration and pattern formation.* Sci Am, 1977. **237**(1): p. 66-76, 81.
240. French, V., P.J. Bryant, and S.V. Bryant, *Pattern regulation in epimorphic fields.* Science, 1976. **193**(4257): p. 969-81.
241. Sansores-Garcia, L., et al., *Modulating F-actin organization induces organ growth by affecting the Hippo pathway.* EMBO J, 2011.
242. Fernandez, B.G., et al., *Actin-Capping Protein and the Hippo pathway regulate F-actin and tissue growth in Drosophila.* Development, 2011. **138**(11): p. 2337-46.
243. Shimizu, T., L.L. Ho, and Z.C. Lai, *The mob as tumor suppressor gene is essential for early development and regulates tissue growth in Drosophila.* Genetics, 2008. **178**(2): p. 957-65.
244. Fanto, M., et al., *The tumor-suppressor and cell adhesion molecule Fat controls planar polarity via physical interactions with Atrophin, a transcriptional co-repressor.* Development, 2003. **130**(4): p. 763-74.

245. Song, H., et al., *Mammalian Mst1 and Mst2 kinases play essential roles in organ size control and tumor suppression*. Proc Natl Acad Sci U S A, 2010. **107**(4): p. 1431-6.
246. Lee, J.H., et al., *A crucial role of WW45 in developing epithelial tissues in the mouse*. EMBO J, 2008. **27**(8): p. 1231-42.

Appendix

Table A.1. Mapping of Df(2R)H3C1

Df tested	Cytologic Region	Breakpoints	BL #	PCR	p-value
Df(2R)Exel6054	43E9;43E18	2R:3553300;3699977	7536	0.70	1.5E-01
Df(2R)Exel6055	43F1;44A4	2R:3773849;3948670	7537	0.70	6.2E-01
Df(2R)Exel6056	44A4;44C2	2R:3948670;4119961	7538	0.70	6.2E-01
Df(2R)Exel6057	44B8;44C4	2R:4062156;4214936	7539	0.70	5.3E-01
Df(2R)Exel6058	44C4;44D1	2R:4215033;4332249	7540	0.71	7.8E-01
Df(2R)Exel7094	44A4;44B3	2R:3948670;4019248	7859	0.71	2.1E-02
Df(2R)Exel7095	44B3;44C2	2R:4012164;4119968	7860	0.69	5.1E-03
Df(2R)Exel7096	44C6;44D3	2R:4321177;4460278	7862	0.70	1.5E-01
Df(2R)Exel8047	44D4;44D5	2R:4487805;4536994	7863	0.71	2.2E-01
Df(2R)Exel7098	44D5;44E3	2R:4536987;4621135	7864	0.69	4.8E-02
Df(2R)ED1770	44D5;45B4	2R:4543134;5095046	9157	-	-
Df(2R)ED1735	43F8;44D4	2R:3849654;4487956	9275	0.70	9.6E-01
Df(2R)ED1742	44B8;44E3	2R:4061673;4611634	9276	0.69	9.2E-03
Df(2R)BSC265	43E16;43F4	2R:3670332;3826552	23164	0.70	6.8E-01
Df(2R)BSC267	44A4;44F1	2R:3970399;4732831	24335	0.69	3.3E-03

Table A.2. Mapping of Df(2L)sc19-8

Df tested	Cytologic Region	Breakpoints	BL #	PCR	p-value
Df(2L)Exel7018	24A1;24C2	2L:3602642;3730180	7789	0.69	3.3E-03
Df(2L)ED247	24A2;24C3	2L:3632218;3771177	24123	0.70	4.4E-01
Df(2L)BSC171	24C1;24C6	2L:3713827;3825535	9604	0.69	9.0E-02
Df(2L)Exel6009	24C3;24C8	2L:3771368;3888977	7495	0.71	3.4E-01
Df(2L)Exel8010	24C8;24D4	2L:3887981;4031325	7790	0.69	7.1E-02
Df(2L)BSC166	24D4;24D7	2L:4031318;4162968	9601	0.70	5.3E-01
Df(2L)BSC165	24D4;24D8	2L:4031318;4195308	9600	0.71	5.8E-01
Df(2L)BSC295	24D4;24F3	2L:4031318;4455780	23680	0.69	3.9E-02
Df(2L)BSC218	24D8;24E1	2L:4197800;4361214	9695	0.70	4.0E-01
Df(2L)BSC217	24D8;24F1	2L:4197800;4403405	9694	0.67	5.3E-07
Df(2L)ED250	24F4;25A7	2L:4477085;4821294	9270	0.70	1.5E-01
Df(2L)BSC52	25A1--3;25B6--8	-	8471	0.69	3.8E-03
Df(2L)BSC51	25A2--3;25C2--5	-	8470	0.70	2.5E-01
Df(2L)BSC225	25A3;25A7	2L:4721280;4821108	9702	0.71	4.2E-01
Df(2L)ED7853	25A3;25B10	2L:4701129;5000402	24124	0.72	-
Df(2L)Exel6010	25A7;25B1	2L:4820718;4887766	7496	0.67	3.4E-07
Df(2L)Exel9062	25B1;25B1	2L:4846961;4887766	7792	0.69	2.3E-01
Df(2L)BSC182	25B1;25B4	2L:4892286;4945300	9673	0.70	7.4E-01
Df(2L)BSC811	25B1;25B4	2L:4892286;4955471	27382	0.70	2.8E-01
Df(2L)Exel8012	25B1;25B5	2L:4846961;4977638	7793	0.70	5.6E-01
Df(2L)BSC172	25B10;25C1	2L:5000838;5037253	9605	0.69	3.5E-03
Df(2L)Exel7022	25B10;25C3	2L:5000837;5058522	7794	0.69	1.9E-02
Df(2L)Exel7021	25B3;25B5	2L:4915628;4979299	7795	0.70	2.2E-01
Df(2L)Exel8013	25B5;25B10	2L:4975605;5000943	7796	0.69	1.6E-03
Df(2L)BSC110	25C1;25C4	2L:5029595;5064620	8835	0.69	4.9E-04
Df(2L)BSC693	25C10;25D5	2L:5209495;5305646	26545	0.69	5.8E-03
Df(2L)BSC109	25C4;25C8	2L:5073453;5145500	8674	0.69	4.5E-03
Df(2L)Exel6011	25C8;25D5	2L:5147258;5305646	7497	-	-

Table A.3. Mapping of Df(2R)ST1

Df tested	Cytologic Region	Breakpoints	BL #	PCR	p-value
Df(2L)Exel6049	40A5;40D3	2L:21828252;22019296	7531	0.70	2.5E-01
Df(2R)BSC326	42A14;42C7	2R:2123567;2633535	24351	0.71	2.0E-01
Df(2R)BSC260	42C4;42E1	2R:2567171-- 2567597;2873193	23160	0.70	6.6E-01
Df(2R)ED1618	42C4;43A1	2R:2556592;3074730	8939	0.70	2.2E-01
Df(2R)Exel6050	42C7;42D6	2R:2628314;2760146	7532	0.70	6.0E-01
Df(2R)BSC261	42D1;42E5	2R:2670129;2912551	23161	0.70	2.0E-01
Df(2R)Exel6051	42D6;42E4	2R:2760146;2880531	7533	0.69	4.1E-01
Df(2R)BSC262	42D6;42F1	2R:2789579;2994138	23297	0.70	8.1E-01
Df(2R)ED1673	42E1;43D3	2R:2873307;3421058	9062	0.70	8.7E-01
Df(2R)Exel6283	42E5;42F2	2R:2927526;3034554	7748	0.71	1.5E-03
Df(2R)BSC263	42F2;43C1	2R:3034369;3334915	23162	0.69	6.7E-02
Df(2R)Exel7092	42F3;43E12	2R:2683473;3220520	7858	0.69	1.2E-04
Df(2R)ED1715	43A4;43F1	2R:3214456;3804428	8931	0.70	9.9E-01
Df(2R)BSC264	43B2;43C5	2R:3283390;3377339	23163	0.71	2.1E-02
Df(2R)Exel6052	43C5;43E5	2R:3380702;3510588	7534	0.71	6.8E-03
Df(2R)Exel6053	43D3;43E9	2R:3421058;3553300	7535	0.70	3.1E-01
Df(2R)ED1725	43E4;44B5	2R:3501429;4043550	8941	0.69	1.3E-01

Table A.4. Mapping of Df(2L)N22-14

Df tested	Cytologic Region	Breakpoints		BL #	PCR	p-value
grk ⁰⁰⁰⁰⁷	-	-	-	10002	0.69	5.90E-01
numb ¹	-	-	-	4096	0.69	9.11E-01
Df(2L)ED611	29B4--29C3	8382851	8419818	9298	0.70	1.35E-02
Df(2L)ED623	29C1;29E4	8403564	8700124	8930	0.69	6.15E-01
Df(2L)Exel7038	29C4;29D5	8438123	8528528	7809	0.69	2.64E-01
Df(2L)Exel7039	29D5--29F1	8529000	PBac{WH}f05176	7810	0.68	1.24E-01
Df(2L)ED647	29E1;29F5	8543972	8958148	8678	0.69	6.52E-01
Df(2L)Exel7040	29F1--29F6	8798000	8985000	7811	0.69	2.56E-01
Df(2L)Exel6021	29F7--30A2	P{XP}d05178	P{XP}d04273	7505	0.68	4.65E-02
Df(2L)ED680	30A4--30B12	9205076	9581740	9342	0.67	2.31E-07
Df(2L)Exel7042	30B10--30C1	9623000	P{XP}d02198	7812	0.69	8.82E-01
Df(2L)Exel6022	30B5--30B11	9560000	P{XP}d03590	7506	0.70	7.36E-03
Df(2L)BSC17	30C3--30F1	970600	9967500	6478	0.70	6.11E-03

Table A.5. Mapping of Df(2L)ast2

Df tested	Cytologic Region	Breakpoints	BL #	PCR	p-value
Df(2L)BSC107	21C2;21E2	2L:431096;574741	8673	0.69	8.3E-04
Df(2L)BSC16	21C3--4;21C6--8	-	6608	0.69	3.1E-04
Df(2L)ED33	21D1;21D2	2L:480873;490448	9184	0.71	5.5E-01
Df(2L)ED40	21D1;21D2	2L:480873;490853	9188	0.69	1.1E-01
Df(2L)ED62	21D1;21E2	2L:480873;826788	8937	0.70	2.1E-01
Df(2L)BSC456	21D1;21E2	2L:479689;816226	24960	0.70	9.9E-01
Df(2L)Exel6002	21E2;21E2	2L:715084;826285	7489	0.69	6.4E-02
Df(2L)Exel8003	21E2;21E2	2L:559139;715085	7774	0.70	6.5E-01
Df(2L)Exel7005	21E2;21E2	2L:777148;868373	7775	0.69	1.5E-03
Df(2L)ED87	21E2;21E2	2L:568095;852827	8677	0.69	1.0E-02
Df(2L)ED49	21E2;21E2	2L:568095;587983	9190	0.70	8.9E-01
Df(2L)ED80	21E2;21E2	2L:568095;850645	9191	0.70	1.9E-01
Df(2L)ED94	21E2;21E3	2L:568095;1036969	8908	0.70	-
Df(2L)Exel6003	21E2;21E4	2L:826173;1074079	7490	0.70	9.5E-01
Df(2L)ED105	21E2;22A1	2L:852854;1420528	24118	0.71	2.9E-01
Df(2L)Exel6004	21E4;21F1	2L:1074079;1158137	7491	0.69	4.6E-02
Df(2L)BSC481	21F1;21F2	2L:1151484;1185905	24985	0.70	6.5E-01
Df(2L)Exel7006	21F1;21F4	2L:1158197;1311170--1311516	7776	0.70	5.0E-01
Df(2L)ED108	21F1;22A1	2L:1119134;1420528	24629	0.69	1.7E-01
Df(2L)Exel6005	22A3;22B1	2L:1555098;1737249	7492	0.71	5.6E-02
Df(2L)BSC521	22A5;22B3	2L:1650856;1849437	25025	0.70	7.1E-01
Df(2L)BSC480	22A5;22C3	2L:1650856;2110387	24984	0.69	6.4E-03
Df(2L)ED7762	22A6;22D3	2L:1657408;2197121	24119	0.69	7.0E-02
Df(2L)Exel7007	22B1;22B5	2L:1716977;1909976	7778	0.70	3.2E-01
Df(2L)BSC688	22B1;22D6	2L:1736964;2273384--2273572	26540	0.70	6.7E-01
Df(2L)Exel8005	22B2;22B8	2L:1737960;2010136	7779	0.67	-
Df(2L)ED125	22B2;22D4	2L:1737465;2222091	24120	0.68	1.8E-05
Df(2L)BSC37	22D2--3;22F1--2	-	7144	-	-
Df(2L)BSC455	22D5;22E1	2L:2242285;2374023	24959	0.67	3.2E-06
Df(2L)BSC156	23A1;23A3	2L:2621016;2753261	9543	0.70	7.8E-01
Df(2L)BSC692	23B3;23B7	2L:2830265--2830267;2868633	26544	0.70	9.5E-01

Table A.6. Mapping of Df(2R)AA21

Df tested	Cytologic Region	Breakpoints	BL #	PCR	p-value
Df(2R)ED3728	56D10;56E2	2R:15349955;15614252	9067	0.70	5.7E-01
Df(2R)BSC22	56D7--E3;56F9--12	-	6647	0.69	1.2E-02
Df(2R)BSC594	56E1;56F9	2R:15519529;16086540--16086559	25678	0.70	2.0E-01
Df(2R)Exel7162	56F11;56F16	2R:16132691--16132995;16201140	7896	0.70	7.4E-01
Df(2R)BSC19	56F12--14;57A4	-	6609	0.70	1.9E-01
Df(2R)BSC701	56F15;57A9	2R:16166339;16554778	26553	0.71	8.4E-01
Df(2R)BSC400	56F16;57B1	2R:16171733;16585801	24424	0.70	4.3E-01
Df(2R)BSC702	57A2;57B3	2R:16311622;16758360	26554	0.70	2.2E-01
Df(2R)BSC430	57A4;57A6	2R:16418478;16471969	24934	0.70	2.0E-01
Df(2R)Exel7164	57A6;57A9	2R:16469676;16554355	7898	0.69	4.0E-03
Df(2R)Exel6070	57A6;57B3	2R:16470285;16723538	7552	0.69	3.3E-02
Df(2R)BSC402	57A8;57B1	2R:16510729;16585801	24426	0.70	6.1E-02
Df(2R)BSC403	57A8;57B1	2R:16518066;16585801	24427	0.70	7.1E-01
Df(2R)BSC404	57A9;57B4	2R:16554779;16770204	24428	0.69	4.3E-02
Df(2R)ED3791	57B1;57D4	2R:16585916;17138486	9267	0.71	5.2E-01
Df(2R)Exel6072	57B16;57D4	2R:16944303;17138350	7554	0.64	-
Df(2R)Exel6071	57B3;57B16	2R:16723538;16944303	7553	-	-
Df(2R)Exel7166	57B3;57B5	2R:16758362;16887668	7998	0.71	4.2E-01
Df(2R)BSC814	57B5;57B19	2R:16862884;16975752	27385	0.71	8.8E-01
Df(2R)BSC462	57B5;57C8	2R:16862884;17068495	24966	0.71	4.4E-01
Df(2R)BSC484	57C3;57C7	2R:17031082;17064815	24988	0.69	2.5E-03
Df(2R)BSC821	57D10;57E6	2R:17189303;17384714	27582	0.71	8.1E-01
Df(2R)BSC664	57D12;58A3	2R:17229152;17759533	26516	0.70	9.3E-01

Table A.7. Mapping of Df(2R)Jp1

Df tested	Cytologic Region	Breakpoints	BL #	PCR	p-value
Df(2R)Exel6284	51B1;51C2	2R:10462255;10653073--10653275	7749	0.70	3.3E-01
Df(2R)BSC429	51C2;51D1	2R:10657714;10761429	24933	0.69	1.5E-03
Df(2R)BSC651	51C5;51E2	2R:10740461;11022806	25741	0.71	3.1E-01
Df(2R)BSC330	51D3;51F9	2R:10818780;11237187	24335	0.69	3.3E-03
Df(2R)Exel7135	51E2;51E11	2R:11017461;11150447	7879	0.69	1.5E-03
Df(2R)ED2426	51E2;52B1	2R:11016313;11498329	9064	0.67	5.8E-05
Df(2R)BSC346	51E7;52C2	2R:11105513;11622949	24370	0.68	1.5E-04
Df(2R)Exel9015	51F11;51F12	2R:11262681;11273829	7880	0.71	2.5E-01
Df(2R)ED2436	51F11;52D11	2R:11260565;11887804	8914	0.69	2.2E-03
Df(2R)BSC427	52A10;52D2	2R:11422223;11809624	24931	0.68	3.1E-05
Df(2R)Exel7137	52A13-- 14;52C8	2R:11463390--11466117;11746753	7882	0.69	1.5E-01
Df(2R)Exel9026	52A13;52A13	2R:11456133;11463121--11463338	7881	0.70	8.9E-01
Df(2R)BSC398	52A13;52D2	2R:11456134;11809625	24422	0.61*	-
Df(2R)Exel6285	52A4;52B5	2R:11371023;11563707	7750	0.70	3.6E-01
Df(2R)BSC308	52B5;52D15	2R:11567721;11918784	23691	0.71	5.4E-01
Df(2R)BSC482	52C8;52D5	2R:11748787;11838157	24986	0.68	2.7E-04
Df(2R)Exel7138	52D1;52D12	2R:11805928;11895238	7883	0.69	1.2E-03
Df(2R)ED2457	52D11;52E7	2R:11887814;12017662	8915	0.68	1.2E-05
Df(2R)Exel9060	52E11;52F1	2R:12030362--12030372;12046356	7885	0.70	4.1E-01
Df(2R)BSC434	52F6;53A1	2R:12075259;12128184	24938	0.71	6.5E-02
Df(2R)BSC609	52F6;53A5	2R:12075259;12169783	25442	0.69	5.8E-03
Df(2R)Exel6063	52F6;53C4	2R:12075393;12274020	7545	0.71	5.1E-01

Table A.8. Mapping of Df(3R)ea

Df/allele tested	Cytologic Region	Breakpoints		BL #	PCR	p-value
Df(3R)ED5664	88D1;88E3	10523031	11054571	24137	0.70	2.6E-02
Df(3R)ED5705	88E12;89A5	11117380	11619518	9152	0.71	7.5E-04
Df(3R)Exel6174	88F1;88F7	11154444	11363188	7653	0.69	2.5E-01
Df(3R)Exel7326	88F7--89A5	11619000	P{XP}d02119	7980	0.70	2.1E-02
UAS-DN-Hsc70	-			5845	-	-
atx2	-			11688	0.68	1.0E-02
srp	-			11538	0.69	3.9E-01

Table A.9. Mapping of Df(3R)3450

Df tested	Cytologic Region	Breakpoints	BL #	3/15/09		2/9/09	
				PCR	p-value	PCR	p-value
Df(3R)BSC567	98B6;98E5	3R:23763552 ;24627253	25390	0.73	7.0E-05	-	-
Df(3R)Exel6210	98E1;98F5	3R:24500683 ;24816740	7688	0.70	2.4E-01	0.69	1.3E-03
Df(3R)BSC789	98E5;98F6	3R:24645856 ;24866229	27361	0.69	4.9E-02	-	-
Df(3R)BSC806	98F1;98F10	3R:24696033 ;24938249	27378	0.71	3.3E-01	-	-
Df(3R)BSC500	98F10;99B7	3R:24938249 ;25501422	25004	0.70	2.2E-01	0.69	3.5E-05
Df(3R)BSC501	98F10;99B9	3R:24938249 ;25550407	25005	0.67	1.2E-04	-	-
Df(3R)ED6310	98F12;99B2	3R:24964617 ;25337875	8961	0.71	4.3E-02	0.69	2.7E-03
Df(3R)Exel6211	98F5;98F6	3R:24816740 ;24889986	7689	0.69	1.8E-03	0.70	1.5E-01
Df(3R)Exel6212	99A1;99A5	3R:25040897 ;25113953	7690	0.71	1.4E-01	0.70	6.3E-01
Df(3R)BSC846	99A1;99B10	3R:25017393 ;25589319	27919	0.67	2.9E-04	-	-
Df(3R)ED6316	99A5;99C1	3R:25081045 ;25608389	8925	-	-	-	-

Table A.10. Mapping of Df(3R)ME15

Df tested	Cytologic Region	Breakpoints		BL #	PCR	p-value
		Left	Right			
Df(3R)ED5021	81F6;82A5	3R:22995	216113	9196	0.74	2.1E-04
Df(3R)ED5046	81F6;82D2	3R:22995	564853	9197	0.71	3.1E-01
Df(3R)ED5071	81F6;82E4	3R:22995	778404	9224	0.73	1.0E-02
Df(3R)ED5100	81F6;82E7	3R:22995	912807	9226	0.70	2.7E-01
Df(3R)Exel6140	82A1;82A4	3R:107401	186686	7619	0.69	2.0E-02
Df(3R)BSC421	82A1;82A4	3R:77491	186784	24925	0.70	1.2E-01
Df(3R)ED5020	82A1;82A5	3R:107408	216113	9075	0.72	1.3E-01
Df(3R)ED5092	82A1;82E7	3R:107408	912807	8091	0.72	7.6E-04
Df(3R)BSC173	82A3;82A4	3R:144838--145197	186784	9606	0.70	5.2E-01
Df(3R)BSC146	82A5;82A5	3R:206616	226208--226217	9538	0.72	8.9E-03
Df(3R)BSC316	82A5;82B2	3R:213288--213333	279012	24342	0.70	8.7E-01
Df(3R)BSC246	82B1;82B3	3R:254982	301892	9720	0.72	9.8E-02
Df(3R)Exel6141	82B2;82C3	3R:288185	425532	7620	0.70	7.6E-01
Df(3R)ED5142	82B2;82F8	3R:279018	1090605	9198	0.71	5.4E-01
Df(3R)BSC174	82C1;82D1	3R:337662	485651	9607	0.71	1.3E-01
Df(3R)ED5066	82C5;82E4	3R:475607	778404	8092	0.73	1.8E-04
Df(3R)ED5095	82C5;82E7	3R:475607	912807	8093	0.73	5.0E-06
Df(3R)Exel6142	82D2;82D6	3R:540173	632615	7621	0.71	7.9E-01
Df(3R)ED5138	82D5;82F8	3R:606794	1090605	8680		
Df(3R)BSC175	82D6;82E5	3R:632615	844642	9608	0.70	2.5E-01
Df(3R)Exel6143	82E3;82E7	3R:776726	912504	7622	0.71	7.9E-01
Df(3R)ED5147	82E7;83A1	3R:912842	1193526	8967	0.70	3.7E-01
Df(3R)BSC176	82F6;82F8	3R:1057000	1090181	24334	0.70	2.2E-01

Table A.11. Mapping of Df(3R)by10

Df tested	Cytologic Region	Breakpoints	BL #	PCR	p-value
Df(3R)BSC666	85C2;85D11	3R:4839488;5181129	26518	0.70	2.6E-01
Df(3R)BSC24	85C4--9;85D12--14	-	6756	0.69	9.7E-03
Df(3R)ED5339	85D1;85D11	3R:5052798;5178097	9204	0.70	9.1E-01
Df(3R)Exel9036	85D11;85D11	3R:5152997;5165728	7955	0.69	9.7E-02
Df(3R)BSC476	85D16;85D24	3R:5243395;5380704	24980	0.69	1.4E-03
Df(3R)Exel6153	85D19;85E1	3R:5338742;5457646	7632	0.70	9.4E-01
Df(3R)ED5429	85D19;85F8	3R:5336031;5874333	8919	-	-
Df(3R)Exel6264	85D24;85E5	3R:5376427;5530672	7731	0.71	5.5E-01
Df(3R)BSC507	85D6;85D15	3R:5084968;5220302	25011	0.70	6.7E-01
Df(3R)BSC528	85E1;85E1	3R:5426220;5457407	25056	0.71	8.6E-01
Df(3R)BSC468	85E1;85E4	3R:5457646;5509008	24972	0.70	9.0E-01
Df(3R)ED5428	85E1;85F8	3R:5456513;5874333	9227	0.70	7.8E-01
Df(3R)ED5454	85E5;85F12	3R:5552399;5937180	9080	0.70	6.6E-01
Df(3R)ED5438	85E5;85F8	3R:5552399;5874333	9078	0.70	9.1E-01
Df(3R)BSC526	85E8;85F14	3R:5604266;5970476	25054	0.70	3.9E-01
Df(3R)Exel6154	85E9;85F1	3R:5619087;5754513	7633	0.67	3.8E-04

Table A.12. Mapping of Df(3R)p712

Df tested	Cytologic Region	Breakpoints	BL #	PCR	p-value
Df(3R)ED5221	84C4;84E11	3R:2954004;3919805	9201	0.70	8.6E-01
Df(3R)Exel6146	84C8;84D9	3R:2988409;3317319	7625	0.69	3.7E-02
Df(3R)BSC423	84D1;84D5	3R:3012954;3222044	24927	0.68	6.3E-04
Df(3R)BSC729	84D14;84F5	3R:3575809;4069851	26581	-	-
Df(3R)BSC465	84D3;84F9	3R:3132512;4127907	24969	0.68	2.2E-04
Df(3R)ED5223	84D9;84E11	3R:3317426;3919805	9076	0.71	7.8E-01
Df(3R)BSC747	84D9;84E5	3R:3356396;3737470	26845	0.70	1.2E-01
Df(3R)BSC513	84D9;84F6	3R:3356396;4076143	25017	0.70	9.8E-01
Df(3R)BSC466	84E1;85A10	3R:3657392;4573406	24970	0.70	9.7E-01
Df(3R)ED5220	84E6;84E11	3R:3803496;3919805	9200	0.70	8.9E-01
Df(3R)Exel6263	84E6;84E13	3R:3792892--3792893;3945737	7630	0.68	1.4E-03
Df(3R)BSC196	84E6;84E8	3R:3799845;3852982	9622	0.71	8.2E-01
Df(3R)ED5230	84E6;85A5	3R:3803496;4478856	8682	0.70	9.9E-01
Df(3R)BSC222	84E8;84F6	3R:3837757;4076143	9699	0.69	2.3E-02
Df(3R)Exel6148	84F12;85A2	3R:4159500;4303404--4303405	7627	-	-
Df(3R)BSC198	84F13;85A2	3R:4162088;4303405	9624	0.72	6.0E-02
Df(3R)BSC248	84F13;85A5	3R:4173193;4495310	23148	0.69	1.9E-01
Df(3R)Exel6147	84F6;84F13	3R:4076136;4166717	7626	0.69	6.6E-02
Df(3R)ED5296	84F6;85C3	3R:4076143;4882413	9338	0.70	8.7E-01
Df(3R)Exel6149	85A2;85A2	3R:4303405;4495198	7628	0.68	2.2E-04
Df(3R)BSC195	85A2;85A5	3R:4303341;4468737	9621	0.69	2.3E-02
Df(3R)BSC477	85A3;85A10	3R:4379821;4573406	24981	0.71	4.0E-01
Df(3R)BSC197	85A5;85A9	3R:4484617;4555205	9623	0.69	5.0E-03
Df(3R)Exel8143	85A5;85B2--3	3R:4495303;4631087--4659772	7954	0.69	3.7E-03
Df(3R)Exel6150	85A5;85B6	3R:4495354;4753483	7629	0.69	5.6E-02
Df(3R)BSC478	85A5;85B8	3R:4512363;4781368	24982	0.71	5.6E-01
Df(3R)ED5330	85A5;85D1	3R:4495308;5055517	9077	0.69	7.0E-02
Df(3R)BSC506	85B1;85C2	3R:4617076;4845745	25010	0.70	8.9E-01

Table A.13. Mapping of Df(3L)fz-GF3b

Df tested	Cytologic Region	Breakpoints	BL #	PCR	p-value
Df(3L)ED4502	70A3;70C10	3L:13220865;13986651	8097	0.72	2.7E-01
Df(3L)Exel6119	70B2;70C2	3L:13470335;13659905	7598	0.71	4.9E-01
Df(3L)ED4536	70C11;70D3	3L:13995861;14198424	9214	0.71	9.9E-01
Df(3L)ED4528	70C15;70D2	3L:14030141;14070123	9072	0.69	1.1E-04
Df(3L)ED4534	70C15;70D3	3L:14030141;14186794	9074	0.70	2.1E-01
Df(3L)ED4515	70C6;70C15	3L:13932272;14030132	9071	0.69	1.8E-03
Df(3L)ED4529	70C6;70D2	3L:13932272;14070123	9073	0.70	8.3E-01
Df(3L)ED4543	70C6;70F4	3L:13928325;14751140	8073	0.70	8.7E-01
Df(3L)Exel6120	70D1;70D3	3L:14052761;14183963	7599	0.70	6.0E-01
Df(3L)Exel6121	70D3;70D4	3L:14183963;14266263	7600	0.68	1.1E-04
Df(3L)Exel6122	70D4;70D4	3L:14266160;14402934	7601	0.70	8.8E-02

Table A.14. Mapping of Df(3L)XDI98

Df tested	Cytologic Region	Breakpoints	BL #	PCR	p-value
Df(3L)Exel7210	65A1;65A5	3L:5919748;6058752	7927	0.69	2.1E-02
Df(3L)BSC551	65A2;65A6	3L:5969060;6118140	25115	0.72	1.3E-01
Df(3L)BSC411	65A2;65C1	3L:5969060;6618729	24915	0.71	7.2E-01
Df(3L)Exel8101	65A3;65A9	3L:6035939;6211152	7928	0.69	6.9E-02
Df(3L)BSC373	65A7;65A10	3L:6166678;6249842	24397	0.71	8.6E-01
Df(3L)Exel6108	65A9;65A11	3L:6211261;6256974	7587	-	-
Df(3L)ED211	65A9;65B4	3L:6211235;6545859	8063	0.71	1.4E-01
Df(3L)Exel6109	65C3;65D3	3L:6736213;6936639	7588	0.67	1.8E-05
Df(3L)BSC27	65D4--5;65E4--6	-	6867	0.70	4.1E-01
Df(3L)BSC374	65D5;65E2	3L:6957558;7032145	24398	0.71	3.4E-01
Df(3L)BSC224	65D5;65E6	3L:6957557;7150109	9701	0.71	4.6E-01

Table A.15. Mapping of Df(3L)BSC21

Gene	Cytologic Location	Breakpoints	Stock Tested	BL #	PCR	p-value
<i>eg</i>	78F2	3L:21801898..21801898	<i>eg</i> ^{EY00149}	15285	0.71	1.6E-01
<i>I(3)0083</i>	79A2	3L:21872674..21872674	<i>I(3)00836</i> ⁰⁰⁸³⁶	11512	0.68	2.5E-05
<i>mub</i>	79A2	3L:21873158..21873158	<i>mub</i> ⁰⁴⁰⁹³	11624	0.70	6.1E-01
<i>RpLP0</i>	79B2	3L:22069233..22069233	<i>RpLP0</i> ⁰¹⁵⁴⁴	11537	0.70	2.0E-02
<i>olf413</i>	79C2--D2	-	<i>olf413</i> ⁰²⁵⁵³	18561	0.70	6.5E-02
<i>I(3)09070</i>	79D3	3L:22260911..22260911	<i>I(3)09070</i> ⁰⁹⁰⁷⁰	11734	0.69	1.3E-04
<i>Aats-ile</i>	79D4	3L:22281801..22281801	<i>Aats-ile</i> ⁰⁰⁸²⁷	11510	0.69	1.6E-03
<i>Aats-ile</i>	79D4	3L:22281795..22281795	<i>Aats-ile</i> ^{EY03542}	19905	0.71	1.3E-01
<i>Hem</i>	79D4	3L:22281244..22281244	<i>Hem</i> ⁰³³³⁵	11584	0.69	1.8E-02
<i>Ten-m</i> , <i>CG10496</i>	79D4--E3	3L:22286132..22400987	<i>Ten-m</i> ⁰⁵³⁰⁹ , <i>CG10496</i> ^{05309b}	11657	0.68	1.4E-06
<i>Ten-m</i>	79E3	3L:22400924..22400924	<i>Ten-m</i> ^{KG00101}	13039	0.70	2.1E-01
<i>CG11426</i>	79E4	3L:22465126..22465126	<i>CG11426</i> ⁰⁰⁵⁸⁴⁶	19222	0.68	8.3E-05
<i>I(3)00506</i>	79F1--2	-	<i>I(3)00506</i> ⁰⁰⁵⁰⁶	11498	0.68	1.7E-04
<i>I(3)04053</i>	80A1	3L:22734300..22734300	<i>I(3)04053</i> ⁰⁴⁰⁵³	11620	0.70	1.9E-01
<i>mael</i>	80A1	3L:22731811..22731811	<i>mael</i> ^{KG03309a}	13015	-	-
<i>CG11241</i>	80A1	3L:22731588..22731588	<i>CG11241</i> ⁰⁰⁶⁷⁸⁶	19249	0.70	5.9E-02
<i>CG14451</i> , <i>mael</i>	80A1	3L:22715250..22715250	<i>PjKG03309b</i> , <i>mael</i> ^{KG03309a}	13015	0.69	3.1E-03
<i>CG11367</i>	80A1	3L:22721251..22721251	<i>CG11367</i> ^{KG07420}	14919	0.71	6.5E-01
<i>Df(3L)BSC5</i> <i>54</i>	80A1;80C1	3L:22716011;22953565	<i>Df(3L)BSC54</i>	25669	0.70	1.8E-01
<i>I(3)L7251</i>	80A2	3L:22766543..22766543	<i>I(3)L7251</i> ^{L7251}	10205	0.71	9.5E-01

Table A.16. Mapping of Df(3L)Exel6087

Df tested	Cytologic Region	Breakpoints	BL #	PCR	p-value
Df(3L)ED4191	61C3;62A	3L:544273;1478937	8049	0.70	9.7E-01
Df(3L)ED4196	61C7;62A2	3L:639583;1478937	8050	0.70	6.4E-02
Df(3L)ED4238	61C9;62A4	3L:738739;1546931	8052	0.71	5.2E-01
Df(3L)ED207	61C9;62A6	3L:738739;1568108	8053	0.72	4.3E-02
Df(3L)BSC289	61F6;62A9	3L:1332329;1628100	23647	0.70	9.4E-01
Df(3L)BSC178	61F8;62A3	3L:1368841;1534423	9609	0.71	5.7E-01
Df(3L)ED4256	62A3;62A6	3L:1546104;1586663	8054	0.72	7.1E-03
Df(3L)BSC670	62A3;62A9	3L:1534423;1637053	26522	0.71	1.7E-01

Table A.17. Mapping of Df(3R)BSC56

Df tested	Cytologic Region	Breakpoints	BL #	PCR	p-value
Df(3R)ED6091	94B5;94C4	3R:18413403;18552029	9092	0.69	9.6E-02
Df(3R)ED6096	94B5;94E7	3R:18413403;19047691	8684	0.72	6.0E-03
Df(3R)BSC618	94C4;94E3	3R:18577855;18999345	25693	0.70	7.8E-01
Df(3R)BSC619	94D10;94E13	3R:18887281;19172138	25694	0.71	5.5E-02
Df(3R)BSC55	94D2--10;94E1--6	-	8491	0.69	4.7E-02
Df(3R)Exel6193	94D3;94E4	3R:18724953;19001169	7672	-	-
Df(3R)ED6103	94D3;94E9	3R:18724275;19084137	8963	0.73	1.1E-03
Df(3R)BSC803	94D9;94E8	3R:18845384;19074727	27375	0.71	3.0E-01
Df(3R)Exel6274	94E4;94E11	3R:19001169;19121235-- 19121356	7741	-	-
Df(3R)Exel6280	94E5;94E11	3R:19017039;19121235-- 19121356	7746	0.69	8.2E-04
Df(3R)Exel9012	94E9;94E13	3R:19105480;19172109	7990	0.70	7.7E-01
Df(3R)Exel6194	94F1;95A4	3R:19210900;19467128	7673	0.67	2.0E-06
Df(3R)BSC137	94F1;95A4	3R:19195438;19431394	9497	0.70	7.3E-01